CHARACTERIZATION OF THE NON-PROTEOLYTIC MECHANISM AND CELLULAR SITE OF ACTION OF PCSK9-MEDIATED DEGRADATION OF THE LOW-DENSITY LIPOPROTEIN RECEPTOR

APPROVED BY SUPERVISORY COMMITTEE

Jay D. Horton, M.D.

Joachim Herz, M.D.

Keith L.Parker, M.D., Ph.D.

Joyce J. Repa, Ph.D.

DEDICATION

For Mark, Kathy, Morine, Annah and Connor.

For their endless love and support.

CHARACTERIZATION OF THE NON-PROTEOLYTIC MECHANISM AND CELLULAR SITE OF ACTION OF PCSK9-MEDIATED DEGRADATION OF THE LOW-DENSITY LIPOPROTEIN RECEPTOR

by

MARKEY CARDEN MCNUTT II

DISSERTATION

Presented to the Faculty of the Graduate School of Biomedical Sciences

The University of Texas Southwestern Medical Center at Dallas

In Partial Fulfillment of the Requirements

For the Degree of

DOCTOR OF PHILOSOPHY

The University of Texas Southwestern Medical Center at Dallas

Dallas, Texas

October, 2008

ACKNOWLEDGMENTS

Although a dissertation is meant to embody the work of an individual, it also reflects the work, help, and support of a family, a group of friends, and a scientific community. I would like to briefly bring these people to the forefront and place credit where credit is due.

I would like to begin with my parents, Mark and Kathy McNutt who have contributed a lifetime of encouragement and continual emotional, spiritual, and financial support. You are both the foundation on which I stand and the roof that covers me.
To my wife, Annah, and son, Connor: Thank you for you patience and love. Everything I accomplish is for you. You have provided balance in my life and continually remind me of the priorities that are most important. My paternal grandmother, Morine McNutt, deserves a huge thanks. She has been continually interested in what I am doing and has been a great encouragement. She has also provided significant financial support that has allowed us things like a house and vehicle. Gran, thank you for believing and investing in me.

It has become cliché in our society to publicly thank god, but I would be remiss if I did thank Him. It seems almost taboo in science to talk about religion, but I can say that the more I learn, the more I see the incredible design of an awesome and loving God. In all honesty, it is by the grace of God alone that everything that I have accomplished has been done. Thanks be to God through my personal Lord and Savior, Jesus Christ.

There are so many people within the UT Southwestern community that have not only been a great help to me; they have also become great friends. I would like to thank

all my friends in the MST program for sharing your lives with me and allowing me to share my life with you over these tough years. I'd like to give special thanks to Rodney Infante for the many scientific and life discussions; and for being a role model of scientific enthusiasm, rigor, and work ethic.

The molecular genetics department is a great place to work, thanks to everyone for creating a great scientific community. I want to especially thank the cell culture techs, Lisa Beatty, Shomanike Head, and Angela Carroll, for all their hard work. Thanks to Michael Brown and Joseph Goldstein for their leadership. They were integral to my learning in the first two years of my research when I attended their lab meeting. There was always something to be learned from them and they taught me to really be critical of my work. Their suggestions and criticisms were always useful. It was an honor to be under their mentorship.

Hyock Kwon has been integral in all of my recent work. He did a tremendous amount of work on the crystal structures and protein purification projects that we undertook. More than that, he was a mentor to me in the field of structural biology. Thanks for all your hard work and answering all my questions.

Thanks to the best MST program in the world. Robin Downing and Stephanie Robertson are the heart of the program. Thanks for all your hard work and making sure I always got paid.

It has been my great pleasure to get to work in the best lab at UT Southwestern, the Horton Lab. You could not hope for a better group of people to work around. To Tuyet Dang and Norma Anderson, you are the backbone of the lab. You have both helped me so much in learning to navigate the treacherous terrain of the lab. The person I owe

the most to in the lab is Tom Lagace. I simply could not say enough here to express my gratitude. You have taught me everything I know about lab work. You are a mentor and friend. Thanks. Of course none of this would be possible without our leader, Jay Horton. Thank you for the opportunity to work in your lab under your mentorship. You have allowed me every opportunity to learn and grow and have provided constant encouragement and been a role model of what a physician scientist should be.

Last, but not least, thanks to my committee, Joachim Herz, Keith Parker, and Joyce Repa. You have all been role models of professionalism and collegiate spirit. Thank you for always making time to come to my presentations, for guiding my research and for providing constructive feedback.

CHARACTERIZATION OF THE NON-PROTEOLYTIC MECHANISM AND CELLULAR SITE OF ACTION OF PCSK9-MEDIATED DEGRADATION OF THE LOW-DENSITY LIPOPROTEIN RECEPTOR

Markey Carden McNutt II, Ph.D.

The University of Texas Southwestern Medical Center at Dallas, 2008

Supervising Professor: Jay D. Horton, M.D.

Proprotein Convertase Subtilisin/Kexin Type 9 (PCSK9) is a serine protease that has emerged as a central regulator of plasma low-density lipoprotein cholesterol levels. Here, it is demonstrated that PCSK9 is secreted into the blood and that the secreted PCSK9 binds and degrades LDLRs in liver. To determine if PCSK9 catalytic activity was involved in the degradation of the LDLR, a mutant PCSK9 was engineered that is catalytically inactive. Studies with catalytically inactive PCSK9 demonstrated that the protein degraded LDLRs in a manner that was indistinguishable from wild-type PCSK9, suggesting that proteolytic activity is not required for PCSK9-mediated degradation of the LDLR. Crystallographic analysis of a PCSK9:LDLR complex supported the

experimental findings that PCSK9 does not catalytically cleave LDLRs. These studies also suggested that one therapeutic approach for treating hypercholesterolemia might be to disrupt the PCSK9:LDLR interaction at the cell surface. Recombinant LDLR sub-fragments were synthesized and added to the medium of cells that overexpressed PCSK9. These sub-fragments restored LDLRs to levels found in the control cells. These experiments confirmed that the disruption of PCSK9:LDLR at the cell surface can inhibit PCSK9 activity and suggested that the majority of PCSK9 activity is extracellular. Further structural analysis of the PCSK9:LDLR co-crystal predicted that an *LDLR* mutation (His306Tyr) might increase the affinity of PCSK9 for the LDLR, and thus could be associated with familial hypercholesterolemia (FH). A search of the LDLR mutation database revealed that the *LDLR* mutation (His306Tyr) had been reported in a kindred with FH. Structure/function studies with the mutant LDLR(H306Y) protein showed that this mutation mimics a conformation change in the wild-type LDLR that occurs at low pH, which results in increased binding. The increased affinity between PCSK9 and LDLR(H306Y) promoted enhanced LDLR degradation. Thus, this mutation represents a previously unrecognized class (Class VI) of FH mutants. Finally, two high-throughput assays were developed to discover new small molecule inhibitors of intracellular PCSK9 autocleavage and to identify previously unrecognized protein activators of PCSK9 action. Use of these assays could provide additional avenues for modulating PCSK9 activity and lead to new therapeutic options for the treatment of hypercholesterolemia.

TABLE OF CONTENTS

PRIOR PUBLICATIONS

McNutt, M.C., Kwon, H.J., Chen, C., Chen, J.R., Lagace, T.A., and Horton, J.D. (2008). Increased binding of a mutant LDL receptor by PCSK9: a novel molecular phenotype of familial hypercholesterolemia. (*In preparation*)

Grefhorst, A., **McNutt, M.C.**, Lagace, T.A., and Horton, J.D. (2008). Plasma PCSK9 preferentially reduces liver LDL receptors in mice. *Journal of lipid research* 49(6): 1303-1311.

Kwon, H.J., Lagace, T.A., **McNutt, M.C.**, Horton, J.D., and Deisenhofer, J. (2008). Molecular basis for LDL receptor recognition by PCSK9. *Proceedings of the National Academy of Sciences of the United States of America* 105(6): 1820-1825.

McNutt, M.C., Lagace, T.A., and Horton, J.D. (2007). Catalytic activity is not required for secreted PCSK9 to reduce low density lipoprotein receptors in HepG2 cells. *The Journal of biological chemistry* 282(29): 20799-20803.

Lagace, T.A., Curtis, D.E., Garuti, R., **McNutt, M.C.**, Park, S.W., Prather, H.B., Anderson, N.N., Ho, Y.K., Hammer, R.E., and Horton, J.D. (2006). Secreted PCSK9 decreases the number of LDL receptors in hepatocytes and in livers of parabiotic mice. *The journal of clinical investigation* 116(11): 2995-3005.

McNutt, M.C., Tongbai, R., Cui, W., Collins, I., Freebern, W.J., Montano, I., Haggerty, C.M., Chandramouli, G., and Gardner, K. (2005). Human promoter genomic composition demonstrates non-random groupings that reflect general cellular function. *BMC bioinformatics* 6, 259.

Freebern, W.J., Haggerty, C.M., Montano, I., **McNutt, M.C.**, Collins, I., Graham, A., Chandramouli, G.V., Stewart, D.H., Biebuyck, H.A., Taub, D.D., and Gardner, K. (2005). Pharmacologic profiling of transcriptional targets deciphers promoter logic. *The pharmacogenomics journal* 5(5): 305-323.

Smith, J.L., Freebern, W.J., Collins, I., De Siervi, A., Montano, I., Haggerty, C.M., **McNutt, M.C.**, Butscher, W.G., Dzekunova, I., Petersen, D.W.*, et al.* (2004). Kinetic profiles of p300 occupancy in vivo predict common features of promoter structure and coactivator recruitment. *Proceedings of the National Academy of Sciences of the United States of America* 101(32): 11554-11559.

LIST OF FIGURES

LIST OF TABLES

LIST OF APPENDICES

LIST OF DEFINITIONS

ADH – Autosomal dominant hypercholesterolemia

ApoB – Apolipoprotein B

ARH – Autosomal dominant hypercholesterolemia

CHD – Coronary heart disease

CI-MPR – Cation-independent mannose-6-phosphate receptor

ECD – Extracellular domain

EGF – Epidermal growth factor

ER – Endoplasmic reticulum

FH – Familial hypercholesterolemia

GFP – Green fluorescent protein

HEK – Human embryonic kidney

LDL – Low-density lipoprotein

LDL-C – LDL cholesterol

LDLR – Low-density lipoprotein receptor

MEF – Mouse embryonic fibroblast

NARC1 – Neural apoptosis regulated convertase 1

PC – Proprotein convertase

PCSK9 – Proprotein convertase Subtilisin/Kexin type 9

RAP – Receptor-associated protein

SREBP – Sterol regulatory element-binding protein

TFR– Transferrin receptor

WT – Wild-type

CHAPTER ONE
Introduction

The Proprotein Convertase Subtilisin/Kexin type 9 (PCSK9) protein is a recently discovered serine protease that plays an important role in the regulation of plasma LDL cholesterol levels and has emerged as a very promising drug target for the treatment of hypercholesterolemia. PCSK9 was first identified and cloned by Millennium Pharmaceuticals as a gene that was induced in response to serum depletion; culture conditions that induce apoptosis in cultured primary neuronal cells. At this time, the protein was designated neural apoptosis regulated convertase 1 (NARC1), but no functional studies were published. In 2003 Seidah, *et al*. (108) published the first information on NARC1 when they cloned the cDNA after identifying it through a homology search using the sequence of the catalytic fragment of a subtilisin-like protease (SKI-1 or site 1 protease), another proprotein convertase subtilisin/kexin type protein family member (108). Subsequently, the *NARC1* gene was re-named *PCSK9* by the Hugo Gene Nomenclature Committee as there has been no convincing data to suggest that PCSK9 has any role in apoptosis.

The first insight into the function of PCSK9 came from a genetics study that identified three mutations in *PCSK9* that were associated with a rare autosomal dominant form of hypercholesterolemia (1). The studies described in this dissertation have focused on elucidating the mechanism by which PCSK9 regulates plasma LDL cholesterol levels.

Proprotein Convertases and PCSK9 structure

The proprotein convertase (PC) family to which PCSK9 belongs includes nine mammalian subtilisin-like serine proteases: PCSK1/PC1/3; PCSK2/PC2; PCSK3/furin; PCSK4/PC4; PCSK5/PC5/6; PCSK6/PACE4; PCSK7/PC7; PCSK8/SKI-1/site 1 protease; and PCSK9. The proprotein convertases are responsible for the proteolytic cleavage of a wide variety of substrates within the secretory pathway, including pro-growth factors, pro-receptors, pro-transcription factors, pro-hormones, and pro-neuropeptides (110). PC family members process substrates in the endoplasmic reticulum/early Golgi, late in the secretory pathway, within secretory granules, at the cell surface, or in endosomes (110). It is unclear where PCSK9 may act along the secretory pathway, but it is secreted from cells and found in detectable amounts in plasma (72).

The PCs share a number of structural and functional similarities. The generic PC structure is compared to PCSK9 in Figure 1-1. All PCs are synthesized as pro-enzymes, with a signal sequence that targets them to the lumen of the ER. Once localized to the ER, the PCs undergo auto-catalytic cleavage of an N-terminal prodomain that remains non-covalently associated with the mature enzyme and is thought to act as both an intermolecular chaperone and an inhibitor of protease action (14, 115). With all members of the PC family except PCSK9, the enzyme is activated when a secondary cleavage event occurs within the prodomain, which relieves the inhibition of catalytic function by exposing the catalytic domain. A similar secondary cleavage event has yet to be reported for PCSK9 and three independent crystal structures of PCSK9 suggest that such an event is unlikely (28, 47, 91).

The first 7 members of the PC family cleave protein substrates after a dibasic motif (R/K) – $(X)_n$ – R ↓ where n = 0,2,4, or 6 (13, 41). The eighth member of the family, site 1 protease (S1P), recognizes a variant cleavage motif, and cleaves substrate proteins after a non-basic residue, (R/K) – X – X – (L/T) ↓ (110). The cleavage motif of PCSK9 varies significantly from other PC family members. Currently, there are no known substrates for PCSK9, besides its own auto-catalytic cleavage, which occurs at SSVFAQ ↓ SIP (10, 86), a site containing no basic residues. Obtaining a robust *in vitro* assay for PCSK9 activity has proved difficult and little is known about the requirements for catalytic activity. Mutagenesis studies have revealed that the sequence required for autocatalytic cleavage is degenerate, which has further complicated efforts to identify the natural substrate(s) of PCSK9 (86). PCSK1-8 also contain a P-domain, which lies C-terminal to the catalytic domain and spans approximately 150 amino acids. The P-domain is a regulatory domain that has been shown to modulate the catalytic activity with respect to sensitivity to pH and calcium in some of the family members (131). PCSK9 lacks this canonical P-domain and has not been shown to require calcium, magnesium, manganese, or zinc and has little pH dependence (86). The functional significance of the C-terminus of PCSK9 remains to be elucidated.

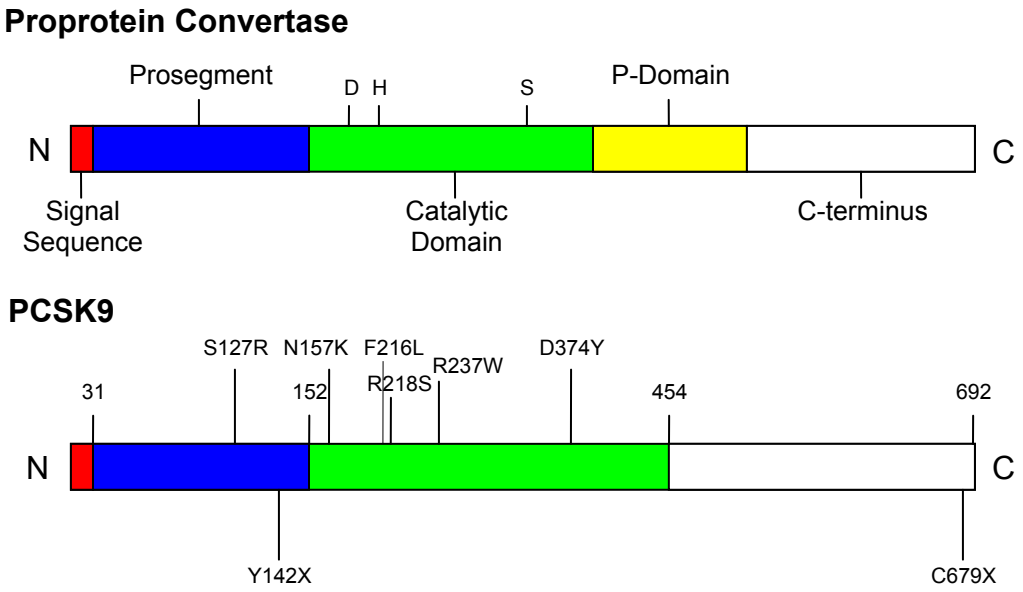

FIGURE 1-1. **General PC Structure and *PCSK9* mutations.**
The generic structure of the proprotein convertases is shown. The catalytic site is a conserved triad of aspartate, histidine, and serine. An asparagine within the oxyanion hole is also conserved in all members of the family. PCSK9 lacks the P-domain found in the other family members. The residues highlighted above PCSK9 indicate mutations associated with familial high cholesterol in pedigrees from Utah, France, French-Canada, Norway, Britain, and Japan (1, 74, 84, 113, 119). The residues highlighted below PCSK9 indicate mutations associated with familial low cholesterol in African American populations (24).

PCSK9 and Hypercholesterolemia

High cholesterol or hypercholesterolemia is a major problem in Western society. Heart disease and cerebrovascular events are the number 1 and 3 causes, respectively, of mortality in the U.S., and plasma levels of LDL-cholesterol directly correlate with the incidence of coronary heart disease and cardiovascular events (52). While as much as 50% of plasma LDL-cholesterol levels can be attributed to environmental factors, the other half is contributed by genetic variations in individuals (50). Of these familial forms, a large proportion is contributed by polygenic traits, but the most severe phenotypes are

due to monogenic, Mendelian mutations (95). There are several forms of monogenic familial hypercholesterolemia that are inherited as autosomal recessive traits and include Autosomal Recessive Hypercholesterolemia (ARH gene mutations) and Sitosterolemia (ABCG 5 and 8 genes), but these are rare, occurring in less than 1 in a million in the population. Much more common are the autosomal dominant hypercholesterolemias (ADH), due to mutations in either the LDL-receptor (LDLR) or apolipoprotein B (APOB) genes. The frequency of mutations in these two genes is as high as 1:500 and 1:1000, respectively, in the heterozygous state (95). In 1999, a group in France identified 13 families with a severe, autosomal dominant form of hypercholesterolemia that did not have mutations in either the LDLR or APOB genes. They were able to map the mutation to 1p34.1-p32 (122), and this site was later identified in a large Utah pedigree (61). In 2003, after PCSK9 was cloned and mapped to chromosome 1 (77, 108), this third locus of ADH was shown to be due to mutations in *PCSK9* (1). Subsequent studies have elucidated many families and other mutations in PCSK9 responsible for ADH (Figure 1-1) (2, 21, 74, 84, 113, 119). The frequency of mutations in PCSK9 appears to be less than the other forms of ADH, and current data suggests a prevalence of less than 1:2500 for the heterozygous state (24).

Inasmuch as these mutations in *PCSK9* led to an autosomal dominant phenotype, it was hypothesized that these resulted in a gain-of-function of the protein (see discussion of PCSK9 function below), Cohen *et al*. (24) hypothesized that loss-of-function mutations in *PSCK9* might also exist and be responsible for low plasma LDL cholesterol levels. Using a large multiethnic population, the Dallas Heart Study (123), they found that nearly 2% of the African Americans harbor loss-of-functions mutations in *PCSK9*,

leading to a greater than 40% reduction in plasma LDL-cholesterol levels (Figure 1-1). Similar mutations were also found in the Caucasian population, but at a frequency of less than 0.1%.

PCSK9 Regulation and Function

Sterol regulated element-binding proteins (SREBPs) are a group of three isoforms of membrane bound transcription factors that are proteolytically cleaved and activate transcription when cells become sterol deficient (58). SREBPs transcriptionally activate all of the cholesterol biosynthetic enzymes as well as the LDL receptor (LDLR), which is responsible for clearing plasma LDL-cholesterol from the blood. Thus, SREBPs are key regulators of cholesterol homeostasis. Data by two separate groups that was obtained shortly after PCSK9 was cloned supported the notion that PCSK9 may be involved in cholesterol metabolism. Maxwell *et al.* (77) found by both microarray and real-time PCR measurements that PCSK9 was down-regulated in the livers of mice that were fed high cholesterol diets. In addition, in transgenic mice overexpressing the transactivation domain of both SREBP-1a and SREBP-2, PCSK9 was found to be upregulated, indicating PCSK9 might be a target of SREBPs (77). At the same time, Horton *et al.* (60) found that PCSK9 was upregulated in SREBP-1a and 2 transgenic mice and downregulated in mice lacking SCAP, a membrane protein necessary for the processing and activation of all three SREBPs, further evidence that PCSK9 is a direct target of SREBPs. Expression studies done by Seidah, *et al*. (108) showed that adult rats had high expression of PCSK9 in both the liver and small intestine, consistent with a role for PCSK9 in cholesterol metabolism.

PCSK9 Regulates the LDLR

To determine the function of PCSK9, mice were infected with an adenovirus expressing wild-type PCSK9. When PCSK9 was overexpressed, LDLR protein levels in the liver were markedly reduced and total plasma cholesterol and LDL levels became markedly elevated (75, 90). The reduction in LDLR protein was not due to an effect on LDLR mRNA levels or from alterations in SREBP mRNA or protein. No changes in plasma cholesterol levels were measured in LDLR null mice when PCSK9 was overexpressed (75, 90), indicating that PCSK9's ability to affect LDL cholesterol was through the LDLR. To confirm that the biological function of PCSK9 was to regulate LDLR protein levels, *Pcsk9* was deleted in mice. The PCSK9-null mice were phenotypically normal, except the LDLR protein levels in liver were significantly increased and total and LDL cholesterol plasma levels were reduced (97). These data confirmed that one normal function of PCSK9 is to regulate LDLR protein levels in liver.

The SREBP-mediated up-regulation of PCSK9 creates a potential problem for therapy with HMG-CoA reductase inhibitors like lovastatin and other statins. These inhibitors block cholesterol synthesis and thereby cause an increase in cleaved SREBP-2 (Figure 1-2). Nuclear SREBP-2 enhances the transcription of the *LDLR* gene leading to increased LDLRs and a fall in plasma LDL. The elevated nuclear SREBP-2 also increases the mRNA for PCSK9, and this would lead to a reduction in LDLR protein. If this scenario is correct, lovastatin should increase LDLRs to a greater extent in *Pcsk9*$^{-/-}$ mice than in wild-type mice.

This hypothesis was tested by administering wild-type and PCSK9-null mice lovastatin. The administration of lovastatin to wild-type mice increased nuclear SREBP-2

protein and the mRNAs of both the LDLR and PCSK9. Despite the transcriptional activation of the *Ldlr*, total hepatic LDLR protein was slightly lower than in wild-type mice fed chow and the plasma cholesterol levels were not statistically reduced. One reason for the apparent paradoxical response appears to be the simultaneous induction of PCSK9, which post-transcriptionally reduces LDLR protein levels. This interpretation is supported by the findings that *Pcsk9*$^{-/-}$ mice administered lovastatin had higher LDLR protein levels, increased LDL clearance from plasma, and lower plasma cholesterol levels than *Pcsk9*$^{-/-}$ mice fed chow. These results suggest that inhibitors of PCSK9 may have beneficial effects on plasma cholesterol levels, especially when combined with statins.

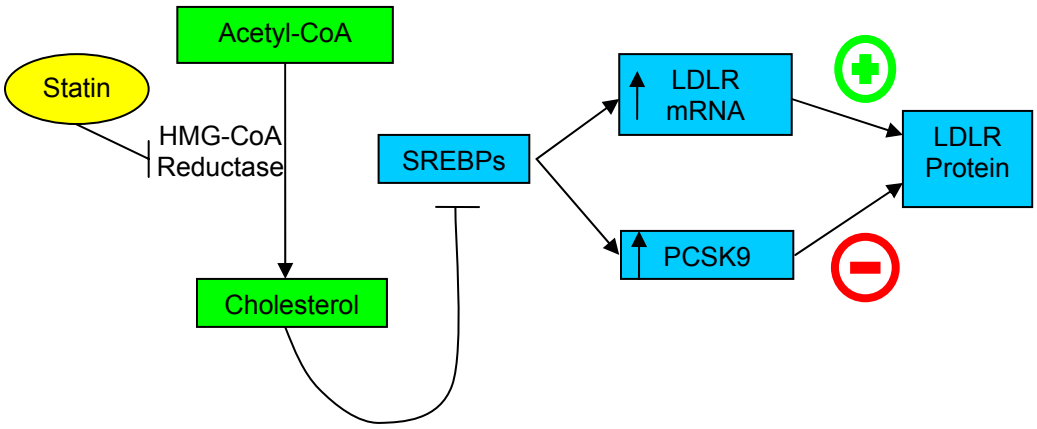

Figure 1-2. Schema of PCSK9 regulation.
The regulation and role of PCSK9 in cholesterol metabolism. The action of SREBPs appears to both negatively and positively affect LDLR protein levels. The addition of a PCSK9 inhibitor to statin treatment blocks the negative arm of this regulation, leading to increased LDLR protein expression and lowered plasma LDL.

PCSK9: A Validated Drug Target for the Treatment of Hypercholesterolemia

The low plasma LDL-C levels associated with loss-of-function mutations in *PCSK9* indicate that inhibition of PCSK9 either through small molecules, antibodies, or RNAi should be effective in lowering cholesterol independent of statins. The validation of PCSK9 as a promising drug target to treat hypercholesterolemia has been revealed in outcome studies that included individuals who are heterozygous for inactivating mutations in *PCSK9*. In a large, bi-racial 15-year prospective study (ARIC), nonsense mutations in *PCSK9* that reduced LDL-cholesterol levels by 28% decreased the frequency of coronary heart disease (defined as myocardial infarction, coronary death, or coronary revascularization) by 88% (25). In the same study, Caucasians with a R46L allele manifest a 50% reduction in coronary heart disease despite having a mean reduction in LDL-cholesterol levels of only 15%.

This study strongly suggested that inhibitors of PCSK9 could have a positive impact on the development of atherosclerosis, but would inhibiting PCSK9 be safe in humans? PCSK9 is expressed in the kidney and cerebellum of adult mice, in addition to the liver and small intestine (108). Although inactivation of PCSK9 in embryos of zebrafish results in disordered neuronal development and death (93), mice lacking PCSK9 develop normally and have no gross neurological defects (97). Humans heterozygous for loss-of-function mutations in PCSK9 appear to be healthy (24) and have a normal life-span (25). In addition, a compound heterozygote with two inactivating mutations in PCSK9 and plasma levels of LDL-cholesterol of 14 mg/dL was recently identified (130). This 31-year-old African-American has grossly normal renal, hepatic,

and neuronal function (unpublished observations). Combined, the available data suggest that inhibiting PCSK9 should be safe in humans.

Summary

PCSK9 has emerged as an important new drug target for the treatment of hypercholesterolemia. The studies presented herein focused on elucidating the site of PCSK9 action and the mechanism by which it functions to degrade LDLRs. The following questions about PCSK9 will be addressed here:

1) Is the LDLR a physiological substrate of PCSK9 proteolytic activity? It will be shown in Chapter 3 that the effect of PCSK9 is not due to cleavage of the LDLR, but that proteolytic activity of PCSK9 is required for a mature PCSK9 protein to be formed. An unanswered question will remain as to whether any natural substrates for PCSK9 exist. Data presented in Chapter 4 will suggest that PCSK9 is unlikely to function as a protease at any time other than during the initial maturation of the protein. These studies suggest that a possible therapeutic intervention is the pharmacologic intracellular inhibition of PCSK9 proteolysis. Chapter 6 presents an assay that was developed to specifically identify these agents in a high-throughput manner.

2) Where does PCSK9 action occur? While studies show that PCSK9 can affect the LDLR after secretion from the ER (76) and when added exogenously (Chapter 2), it is still unclear if physiologically PCSK9 acts intracellularly or at the cell surface. ARH knockout mice, which are incapable of LDLR-mediated endocytosis of LDL, are affected the same as wild-type mice after adenovirus expression of PCSK9 (90). This would seem to indicate that PCSK9 acts before endocytosis, but does not exclude the possibility that

PCSK9 acts on LDLR that has been endocytosed by ARH-independent mechanisms. Additionally, these are the only data presented to suggest an intercellular pathway and it is the result of high levels of overexpression that could represent a physiologically irrelevant mechanism. Chapter 5 presents data to indicate that the effect of PCSK9 is mediated via an intracellular pathway. By understanding the location of PCSK9 action, it now allows one to specifically target PCSK9 for therapeutic intervention by targeting the LDLR:PCSK9 interaction extracellularly. This approach is demonstrated in Chapter 5.

3) What other proteins are involved in PCSK9-mediated LDLR regulation? PCSK9's effects on LDLR levels appear to be cell-type dependent. While PCSK9 decreases LDLR receptors in HepG2 cells (72, 76), it has no effect on Chinese hamster ovary cells (90). *In vivo*, PCSK9 reduced LDLR in the liver, while leaving the LDLRs of the adrenal gland unchanged (45). This indicates that there may be a PCSK9 interacting factor that is not present in all cells. This would explain the observation that although patients with PCSK9 mutations have lower LDLR levels in their lymphoblasts (10), LDLR activity was found to be normal in the fibroblasts of these patients (122). Elucidation of such a factor would help to understand the PCSK9-mediated LDLR regulatory pathway and provide a new drug target(s) for the treatment of hypercholesterolemia. Chapter 6 presents a high-throughput assay for cDNA or siRNA screening that could identify either positive or negative effectors of PCSK9 action, respectively. As a whole, the data presented here provide important insights into the site and mode of PCSK9 action and as a result provide a clear framework for the development of inhibitors of PCSK9 function for the treatment of hypercholesterolemia, which could have a positive impact on the health of millions of patients who suffer from high cholesterol and atherosclerosis.

CHAPTER TWO
Secreted PCSK9 Decreases LDL Receptors [f]

Summary

Proprotein Convertase Subtilisin/kexin Type 9 (PCSK9) is a member of the proteinase K subfamily of subtilases that reduces LDL receptors (LDLR) in liver through an undefined post-transcriptional mechanism. Here, it is show that purified PCSK9 added to the medium of HepG2 cells reduces cell-surface LDLRs in dose- and time-dependent manners. This activity was ~10-fold greater for a gain-of-function mutant PCSK9(D374Y) that causes hypercholesterolemia. Binding and uptake of PCSK9 is largely dependent on the presence of LDLRs. Co-immunoprecipitation and ligand blotting studies indicate that PCSK9 and LDLR directly associate; both proteins co-localize to late endocytic compartments. Purified PCSK9 has no effect on cell-surface LDLRs in hepatocytes lacking ARH, an adaptor protein required for endocytosis of the receptor. Transgenic mice overexpressing human PCSK9 in liver secreted large amounts (~180-400 μg/ml) of the protein into plasma, which increased plasma LDL-cholesterol concentrations to levels similar to those of LDLR knockout mice. To determine if PCSK9 was active in plasma, transgenic PCSK9 mice were parabiosed with wild-type littermates. After parabiosis, secreted PCSK9 was transferred to the circulation of wild-type mice and reduced hepatic LDLRs to nearly undetectable levels. These data show that secreted PCSK9 associates with the LDLR and reduces hepatic LDLR protein levels.

[f] This chapter is adapted from (72). Used with permission.

Introduction

The genetic data from humans and the *in vivo* studies in mice demonstrate that one function of PCSK9 is to reduce the number of the LDLRs. The mechanism by which PCSK9 reduces LDLRs is still undetermined. For example, it is unclear whether PCSK9 acts to destroy LDLRs in the secretory pathway, or whether it acts outside of the cell. In the current studies, evidence is provided that extracellular PCSK9 can be internalized by cultured liver cells and fibroblasts in a manner that is largely dependent on LDLRs. Incubation with extracellular PCSK9 leads to loss of LDLRs from the cell surface and accelerated destruction of LDLRs in liver-derived cells. Finally, it is demonstrated that increased PCSK9 levels in the circulation of mice leads to diminished liver LDLR protein and increased plasma cholesterol levels.

Results

PCSK9, like other subtilisin family proteases, is synthesized with a prodomain (10, 108). In the other subtilisin family proteases, the cleaved prodomain remains associated with the protein and acts as an inhibitor of the cognate enzyme activity. The prosegment often undergoes secondary proteolytic processing, which relieves this inhibition and unmasks enzymatic activity (5). When PCSK9 is overexpressed in cultured cells, the protein is secreted with the prodomain still attached (10, 108). This result raised the possibility that cellular PCSK9 remains inactive within the secretory pathway and that PCSK9 may act on LDLRs after secretion, either at the cell surface or after the LDLR is internalized into the endosomal/lysosomal system.

To test this possibility, the rate and extent of secretion of endogenous PCSK9 expressed at physiological levels in cultured human hepatoma HepG2 cells was assessed. This study was made possible by the development of antibodies against the catalytic domain of PCSK9. Synthesis and secretion of PCSK9 was quantified by pulse-labeling the cells with [^{35}S]methionine/cysteine, followed by a chase period in isotope-free medium. Radiolabeled PCSK9 was immunoprecipitated from cells and the medium at different times. Figure 2-1 shows a representative pulse/chase experiment. Two forms of the protein, corresponding to the uncleaved precursor (~74-kDa) and the cleaved mature catalytic fragment (~60-kDa), were detected in cells at 0.5 and 1 hour of chase. After 2 hours, none of the labeled uncleaved PCSK9 was detected in the cells. After 4 hours, nearly all of the radiolabeled PCSK9 was recovered in the medium, demonstrating that the cleaved form of PCSK9 is rapidly and efficiently secreted from these cells.

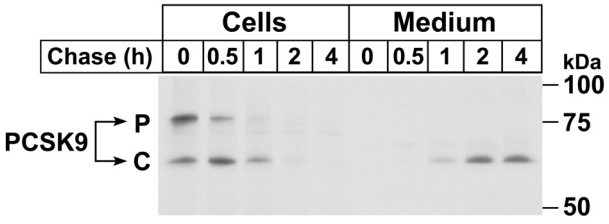

FIGURE 2-1. **Pulse/chase analysis of endogenous PCSK9 secretion from HepG2 cells.** Cells were cultured in sterol-depleting Medium C for 18 hours prior to labeling for 30 min with [^{35}S]methionine/cysteine. After washing, cells were incubated in chase medium containing unlabeled methionine and cysteine for the indicated times. Cells were lysed and PCSK9 was immunoprecipitated from the medium and cell lysates as described in Methods. Samples were subjected to 8% SDS-PAGE and the gel was treated with Amplify™ fluorogenic reagent prior to drying and exposure to film. P and C denote the proprotein and cleaved forms of PCSK9, respectively. Similar results were obtained in four independent experiments.

We recently reported that PCSK9 can be detected in human plasma by immunoprecipitation (130). To quantify the concentration and determine the physiological range of PCSK9 in human plasma, an ELISA was developed that used an anti-human PCSK9 monoclonal antibody to capture PCSK9 and a polyclonal anti-human PCSK9 antibody for detection. The linear range of the ELISA was determined to be 3-100 ng/ml for purified PCSK9 protein. Plasma levels of PCSK9 were quantified in 72 volunteers. The range of plasma levels varied from ~50 to ~600 ng/ml (Figure 2-2). These measurements demonstrate that significant amounts of PCSK9 circulate in plasma and provided a range of physiologically relevant PCSK9 concentrations.

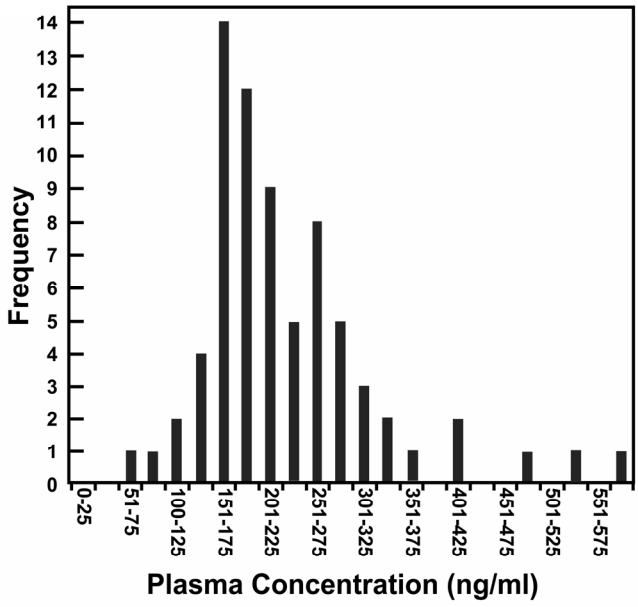

FIGURE 2-2. **PCSK9 concentrations in plasma from 72 individuals.**
The cohort consisted of 35 males and 37 females ranging from 21-56 years of age. Plasma was collected in an EDTA tube following an overnight fast. PCSK9 concentrations were measured by ELISA as described in Materials and Methods.

We next determined whether the secreted form of PCSK9 can reduce LDLRs when added to the medium of HepG2 cells cultured in sterol-depleted medium to induce LDLR expression. Recombinant PCSK9 that contained a FLAG tag at the carboxyl terminus was purified from HEK 293S cells as described in Methods. SDS-PAGE and Coomassie blue staining analysis showed that purified FLAG-tagged PCSK9 consisted of the catalytic fragment and the cleaved prodomain that migrated with apparent molecular masses of ~60 kDa and ~17 kDa, respectively (Figure 2-3*A*). Gel filtration analysis revealed that the protein elutes at a single peak volume corresponding to an apparent molecular mass of ~70 kDa (Figure 2-3*B*). After incubation with purified PCSK9, the surface proteins of HepG2 cells were covalently modified with a cell-impermeable biotinylation reagent and isolated using streptavadin beads. The amounts of total cellular LDLRs in whole cell extracts and cell surface LDLRs were measured by SDS-PAGE immunoblotting using a monoclonal antibody. The amounts of total cell PCSK9 accumulation and cell surface PCSK9 were also measured by SDS-PAGE and immunoblotting, but with anti-FLAG antibody.

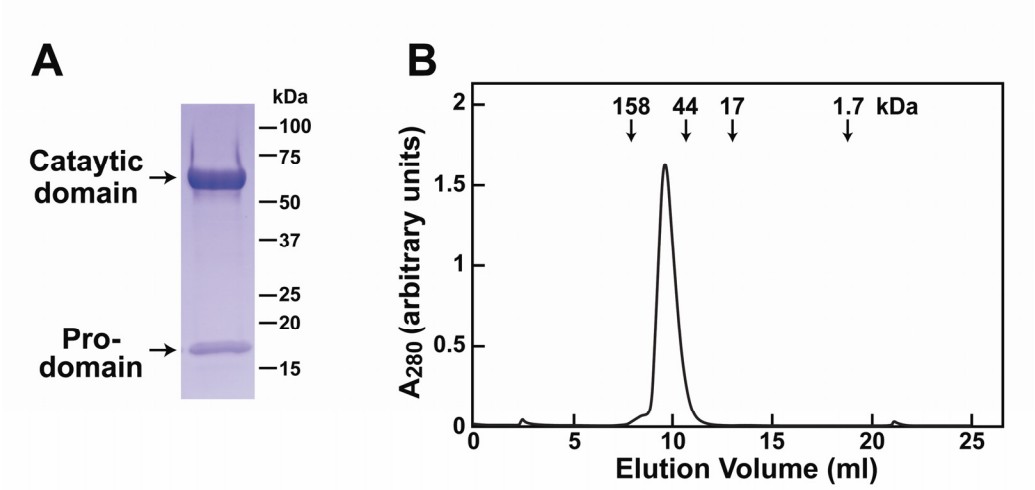

FIGURE 2-3. **Purification of secreted PCSK9.**
A, Coomassie blue staining of purified PCSK9. FLAG-tagged human PCSK9 secreted from HEK 293S cells was purified as described in Methods. Ten μg of purified protein was subjected to SDS-PAGE on a 4-15% gradient gel and protein bands were detected with Coomassie brilliant blue R-250 stain. Arrows indicate the catalytic and prodomains of secreted PCSK9. *B,* gel filtration chromatography of purified secreted PCSK9. Protein (100 μg) was loaded onto a Superdex 75 10/300 GL column and chromatographed at a flow rate of 0.4 ml/min. Absorbance at 280 nm was monitored continuously to identify the position of eluted FLAG-tagged PCSK9. Standard molecular weight markers (γ globulin, M_r 158,000; ovalbumin, M_r 44,000; myoglobin, M_r 17,000; vitamin B_{12}, M_r 1,700) were chromatographed on the same column under identical conditions (arrows).

As shown in Figure 2-4*A*, cell surface LDLRs declined by 50% after incubation with the physiologically relevant concentration of 0.5 μg/ml PCSK9 (lane 2) and they became nearly undetectable after exposure to 2.5 μg/ml PCSK9 (lane 4). Incubation of HepG2 cells for 4 hours with 5 or 10 μg/ml PCSK9 decreased whole-cell LDLR protein levels by ~50% (lanes 11 and 12). FLAG-tagged PCSK9 was detected in whole-cell extracts in a concentration-dependent manner (lanes 7-12) but it was not detected among the biotin-labeled cell surface proteins (lanes 1-6), suggesting that most of the cell-associated PCSK9 had been internalized.

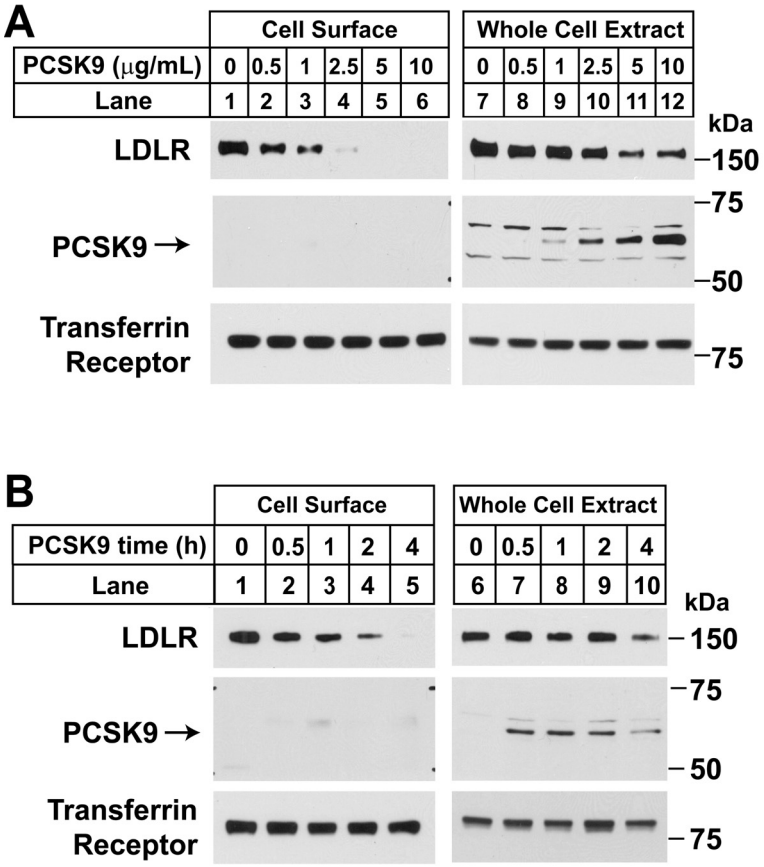

FIGURE 2-4. **Reduction of endogenous LDLRs in HepG2 cells following the addition of recombinant purified PCSK9 to the culture medium.**
A, dose response of exogenous PCSK9-mediated LDLR degradation in HepG2 cells. Cells were cultured for 18 hours in Medium C prior to treatment for 4 hours with the indicated amounts of purified human PCSK9. *B,* time course of exogenous PCSK9-mediated LDLR degradation. HepG2 cells cultured as described above were treated with 5 μg/ml of purified PCSK9 for the indicated times. For all studies, cell lysates were prepared following cell surface biotinylation as described in Methods. Proteins were subjected to SDS-PAGE for immunoblot analysis of the LDLR using IgG-HL1 and anti-FLAG M2 monoclonal antibody to detect purified PCSK9. The transferrin receptor protein was detected as described in Methods and used as a control for loading and non-specific protein degradation. Similar results were obtained in three independent experiments.

To determine the time-course of PCSK9 action, the HepG2 cells were incubated in the presence of 5 μg/ml of PCSK9 and then harvested at different intervals over a 4 hour period (Figure 2-4*B*). Cell surface LDLR declined noticeably at 2 hours (lane 4) and was undetectable at 4 hours (lane 5). The amount of cell-associated FLAG-tagged PCSK9 was maximal after 30 min (lane 7) and decreased slightly at 4 hours (lane 10). PCSK9 had no effect on whole cell or cell surface transferrin receptors (Figures 2-4*A* and 2-4*B*).

As discussed in the Introduction, certain point mutations in PCSK9 cause hypercholesterolemia. To determine if one such mutation increases the activity of PCSK9 in a cell-based assay, varying amounts of wild-type PCSK9 and the PCSK9 mutant, D374Y (1) were added to HepG2 cells, after which LDLR protein levels were measured (Figure 2-5). The D374Y mutation was chosen for study because individuals who harbor this mutation have been shown to manifest severe hypercholesterolemia (84). PCSK9(D374Y) was at least 10-fold more active that wild-type PCSK9 in reducing cell surface LDLRs. Thus, PCSK9(D374Y) at 0.25 μg/ml was at least as effective as 2.5 μg/ml (compare lanes 5 and 11). After incubation with wild-type PCSK9, LDLRs were significantly reduced in whole-cell extracts, and similar results were found with 10-fold lower concentrations of PCSK9(D374Y) (lanes 13-24). Despite the different concentrations employed, the amounts of wild-type and mutant PCSK9 measured in the cell extracts were similar, indicating that the mutant protein was taken up by the cell ~10-fold more efficiently than the wild-type protein.

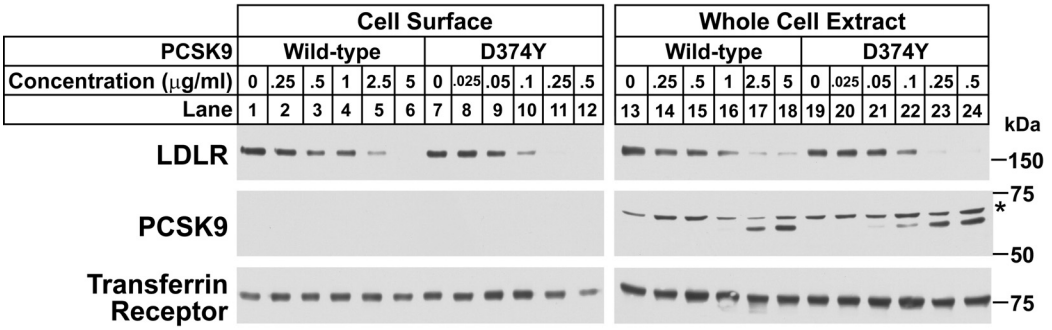

FIGURE 2-5. **Increased cell association and LDLR degradation by addition of purified mutant PCSK9(D374Y) to the medium of HepG2 cells.** Cells were cultured for 18 hours in Medium C and then incubated for 4 hours with the indicated amounts of purified human PCSK9 or PCSK9(D374Y). Immunoblot analysis of LDLR, FLAG-tagged PCSK9 and transferrin receptor was carried out as described in the legend to Figure 2-4. Asterisk indicates a non-specific band. Similar results were obtained in three independent experiments.

To determine whether cellular association/uptake of PCSK9 is dependent upon LDLRs, mouse embryonic fibroblasts (MEFs) were used in order to exploit the availability of cells from gene knockout mice that lack the LDLR and the closely related receptor, the LDL receptor-related protein (LRP). MEFs derived from wild-type, *Ldlr*$^{-/-}$, *Lrp*$^{-/-}$, and *Ldlr*$^{-/-}$;*Lrp*$^{-/-}$ mice were incubated with varying amounts of PCSK9 (Figure 2-6*A*). Immunoblots revealed that abundant PCSK9 was associated with the wild-type (lanes 1-4) and *Lrp*$^{-/-}$ cells (lanes 9-12). PCSK9 cellular association was markedly reduced in *Ldlr*$^{-/-}$ MEFs (lanes 5-8); however, a small, but reproducible, amount of PCSK9 was detectable in cells incubated with the highest concentration of PCSK9 (lane 8). This small amount of association was abolished in cells that lacked both LDLR and LRP (lane 16). These data suggest that exogenous PCSK9 associates with MEFs in a manner that is almost totally dependent upon the LDLR and that LRP may play a small role in uptake at high concentrations of PCSK9.

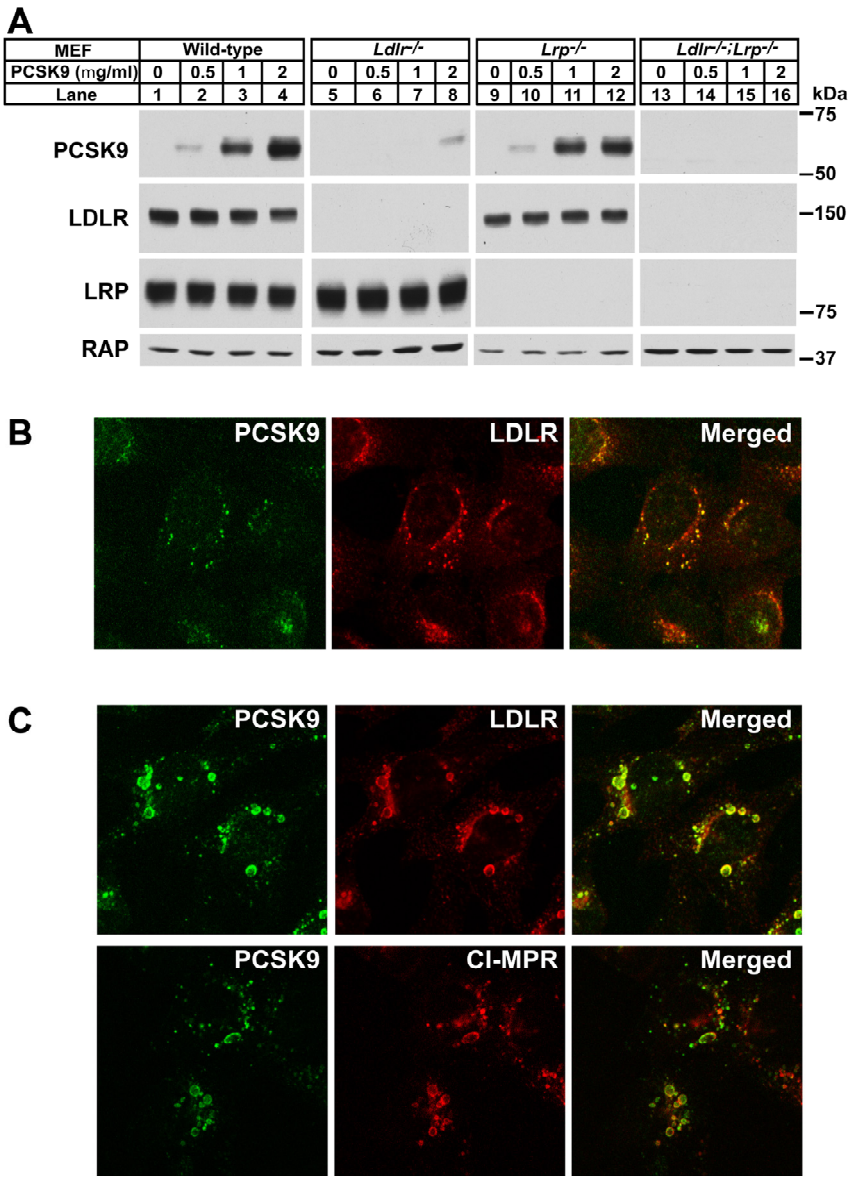

FIGURE 2-6. **LDLR-dependent endocytosis of PCSK9 in MEF cells.**
A, immunoblot analysis of PCSK9 association with MEF cells. Immortalized MEFs derived from wild-type, *Ldlr*$^{-/-}$, *Lrp*$^{-/-}$, and *Ldlr*$^{-/-}$;*Lrp*$^{-/-}$ mice were cultured for 18 hours in Medium F prior to treatment for 4 hours with the indicated amounts of purified human PCSK9. Cell lysates (30 μg) were subjected to SDS-PAGE and immunoblot analysis to detect PCSK9 or the LDLR. Immunoblots of RAP were used as a loading control. *B,* indirect immunofluorescence localization of PCSK9 and the LDLR in wild-type MEFs. MEF cells were incubated for 4 hours with 5 μg/ml purified human PCSK9 and processed for double immunofluorescence of PCSK9 (green) and the LDLR (red). *C,*

indirect immunofluorescence localization of PCSK9, LDLR, and the late-endosomal marker cation-independent mannose 6-phosphate receptor (CI-MPR) in MEF cells cultured in the presence of chloroquine. Wild-type MEF cells were incubated for 4 hours with 5 μg/ml purified human PCSK9 in presence of 0.1 mM chloroquine, and processed for double immunofluorescence of PCSK9 (green) and the LDLR (red) or CI-MPR (red). The merged image shows areas of co-localization of PCSK9 with the LDLR and CI-MPR. Magnification, 630X.

The uptake of PCSK9 was characterized morphologically using indirect immunofluorescence of wild-type MEF cells. Double immunofluorescence labeling of cells incubated with PCSK9 for 4 hours showed diffuse localization of the protein in small punctate structures, possibly representing endocytic vesicles, which partially overlapped with the LDLR staining pattern (Figure 2-6*B*). To determine whether these structures were endosomal and whether PCSK9 co-localized intracellularly with the LDLR, MEFs were incubated in the presence of chloroquine, which raises the pH of acidic cellular compartments and inhibits lysosomal hydrolases. In the presence of chloroquine, the cation-independent mannose-6-phosphate receptor (CI-MPR) accumulates in late endosomes and was used as a marker of these structures (17). As shown in Figure 2-6*C*, PCSK9 became concentrated in large perinuclear vacuoles of MEFs in the presence of chloroquine. These vacuoles were also labeled with the anti-LDLR and with anti-CI-MRP antibodies. Considered together, the data indicate that exogenous PCSK9 is taken up by fibroblasts in a manner that is dependent upon the LDLR and that the PCSK9 travels with the LDLR to the endosome/lysosome. Despite this uptake, PCSK9 does not destroy the LDLR in fibroblasts at the concentrations tested, either in the absence or presence of chloroquine. A similar lack of destruction was

observed earlier when PCSK9 was overexpressed in fibroblasts and Chinese hamster ovary cells by transfection (90).

The requirement of LDLRs for PCSK9 internalization suggests that PCSK9 may bind to the LDLR. Moreover, PCSK9(D374Y) is taken up with higher efficiency than wild-type PCSK9, suggesting that the mutant protein may bind to the LDLR more avidly than the wild-type protein. To test this possibility, co-immunoprecipitation studies with wild-type PCSK9 or mutant PCSK9(D374Y) and the LDLR were carried out in HepG2 cells. The cells were incubated with wild-type and mutant PCSK9 proteins containing FLAG epitope tags. After incubation for 1 hour in the presence of chloroquine, the cells were solubilized and exogenously added PCSK9 was precipitated with an anti-FLAG antibody. As shown in Figure 2-7*A* (lanes 1 and 5), the FLAG antibody efficiently pulled down the wild-type and mutant PCSK9 from cell extracts and the immunoprecipitation was reduced in the presence of competing FLAG octapeptide (lanes 2 and 6). In cells that were incubated with wild-type PCSK9, no detectable LDLR was co-immunoprecipitated with PCSK9. In contrast, a significant amount of LDLR was pulled down from cells incubated with PCSK9(D374Y) (lanes 1 and 5). When the LDL receptor antibody was used for the immunoprecipitation, a small, but consistently detectable amount of wild-type PCSK9 was co-immunoprecipitated. The LDLR antibody pulled down much larger amounts of PCSK9(D374Y) (lanes 3 and 7).

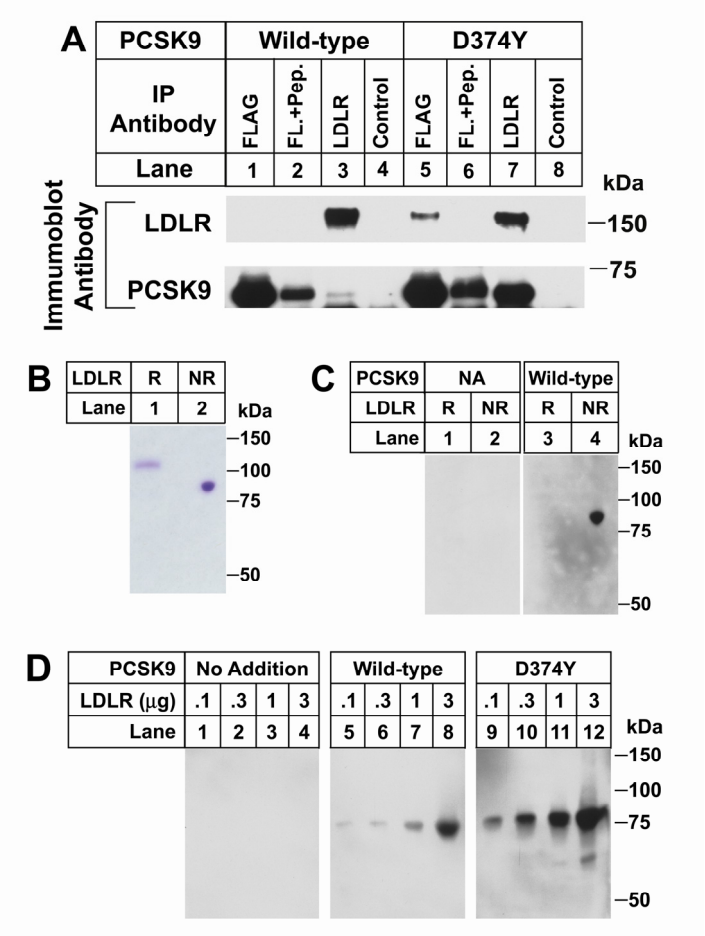

FIGURE 2-7. **Association of PCSK9 and mutant PCSK9(D374Y) with the LDLR.** *A,* co-immunoprecipitation of the LDLR and exogenously added purified wild-type PCSK9 or PCSK9(D374Y) protein. HepG2 cells were cultured for 18 hours in Medium C prior to treatment for 1 hour in the presence of 0.1 mM chloroquine with 20 μg/ml or 2 μg/ml amounts of purified human PCSK9 or PCSK9(D374Y), respectively. Cells were harvested, lysed, and immunoprecipitated with the indicated antibodies. Pellets of the immunoprecipitation were subjected to SDS-PAGE and immunoblot analysis to detect LDLR and PCSK9. *B,* reduced (R) or non-reduced (NR) LDLR extracellular domain (amino acids 1-699) was resolved by SDS-PAGE. Protein was detected with Coomassie brilliant blue R-250 stain. *C,* binding of PCSK9 to LDLR on ligand blots. LDLR protein (2 μg) resolved on SDS-PAGE as described above was transferred to nitrocellulose and blotted with 5 μg/ml of purified wild-type PCSK9 or no addition (NA). *D,* wild-type and mutant PCSK9(D374Y) binding to the LDLR. The indicated amounts of purified LDLR were subjected to non-reducing SDS-PAGE, transferred to nitrocellulose, and blotted with 5 μg/ml of purified wild-type PCSK9, mutant PCSK9(D374Y) or buffer control (no addition). Abbreviations used: FL, FLAG; Pep, FLAG octapeptide.

To determine whether the interaction of PCSK9 and the LDLR was direct, ligand blotting was performed using purified extracellular domain LDLR protein and PCSK9. First, the migration of the purified LDLR under reducing and non-reducing conditions was determined (Figure 2-7*B*). Next, it was determined whether PCSK9 could bind to the extracellular domain of the LDLR in a specific manner. The reduced and non-reduced LDLR protein was resolved by SDS-PAGE and transferred to nitrocellulose. The filters were then incubated with 5 μg/ml of purified PCSK9 protein and bound PCSK9 was visualized using the monoclonal antibody IgG-15A6. As shown in Figure 2-7*C*, PCSK9 bound to non-reduced LDLR protein but not to LDLR protein that had been reduced. The binding of wild-type PCSK9 and PCSK9(D374Y) to increasing amounts of the LDLR protein was then determined by ligand blotting (Figure 2-7*D*). Both forms of purified PCSK9 bound to the extracellular domain of the LDLR protein in a concentration dependent manner. Consistent with the co-immunoprecipitation, the PCSK9(D374Y) mutant appeared to bind to the LDLR protein with a greater affinity. Combined, these studies indicate that PCSK9(D374Y) binds to LDLRs with higher affinity than does wild-type PCSK9, a finding that correlates with the enhanced ability of the mutant PCSK9 to destroy LDLRs.

In hepatocytes, the internalization of LDLRs is dependent upon functional ARH, an adapter protein that binds to the intracellular domain of the LDLR and to clathrin, thereby clustering the receptor in coated vesicles (40, 49). To determine whether ARH was similarly required for removal of LDLR from the cell surface, PCSK9 was added to the medium of primary hepatocytes isolated from two types of genetically engineered mice: those that express only the human LDLR ($LDLR^{h/h}$;$Arh^{+/+}$) (67) and those that

express the human LDLR and lack ARH (*LDLR*$^{h/h}$;*Arh*$^{-/-}$) (66). In *LDLR*$^{h/h}$;*Arh*$^{+/+}$ hepatocytes LDLRs were visualized on the cell surface and in intracellular vesicles concentrated in the cell periphery (Figure 2-8*A*, upper left panel). Incubation with PCSK9 eliminated the surface LDLRs and the remaining LDLRs were concentrated in perinuclear vesicles (Figure 2-8*A*, upper right panel). In *LDLR*$^{h/h}$;*Arh*$^{-/-}$ hepatocytes, the LDLRs were visualized almost entirely on the cell surface (Figure 2-8*A*, lower left panel), and PCSK9 did not reduce the surface LDLRs in these cells (Figure 2-8*A*, lower right panel).

To confirm that PCSK9 still associated with the cell in the absence of ARH, total lysates and cell surface proteins were isolated for immunoblot analysis from *LDLR*$^{h/h}$;*Arh*$^{+/+}$ and *LDLR*$^{h/h}$;*Arh*$^{-/-}$ primary hepatocytes incubated with increasing concentrations of PCSK9 (Figure 2-8*B*). LDLR protein was reduced by exogenously added PCSK9 in a dose dependent manner in both total extracts and on the cell surface in hepatocytes expressing ARH (lanes 1-3 and 9-11). In contrast, incubation of *LDLR*$^{h/h}$/*Arh*$^{-/-}$ hepatocytes with PCSK9 did not alter LDLR protein levels in either fraction (lanes 4-6 and 12-14) despite similar levels of PCSK9 cell association (lanes 1-3 and 4-6). In the absence of ARH, significantly more PCSK9 was detected at the cell surface (lanes 13-14). No PCSK9 was detected in hepatocytes isolated from *Ldlr*$^{-/-}$ mice (lanes 7-8 and 15-16). PCSK9 had no effect on whole cell or cell surface transferrin receptors in hepatocytes, and cellular integrity was maintained during cell surface biotinylation as indicated by a lack of detection of intracellular actin among biotin-labeled proteins. These results demonstrate that PCSK9 can associate with the cell in the absence of ARH, but that internalization is required for PCSK9 to reduce the cell surface expression of

LDLR protein. They also show that PCSK9 binding is largely dependent upon LDLR expression in mouse hepatocytes.

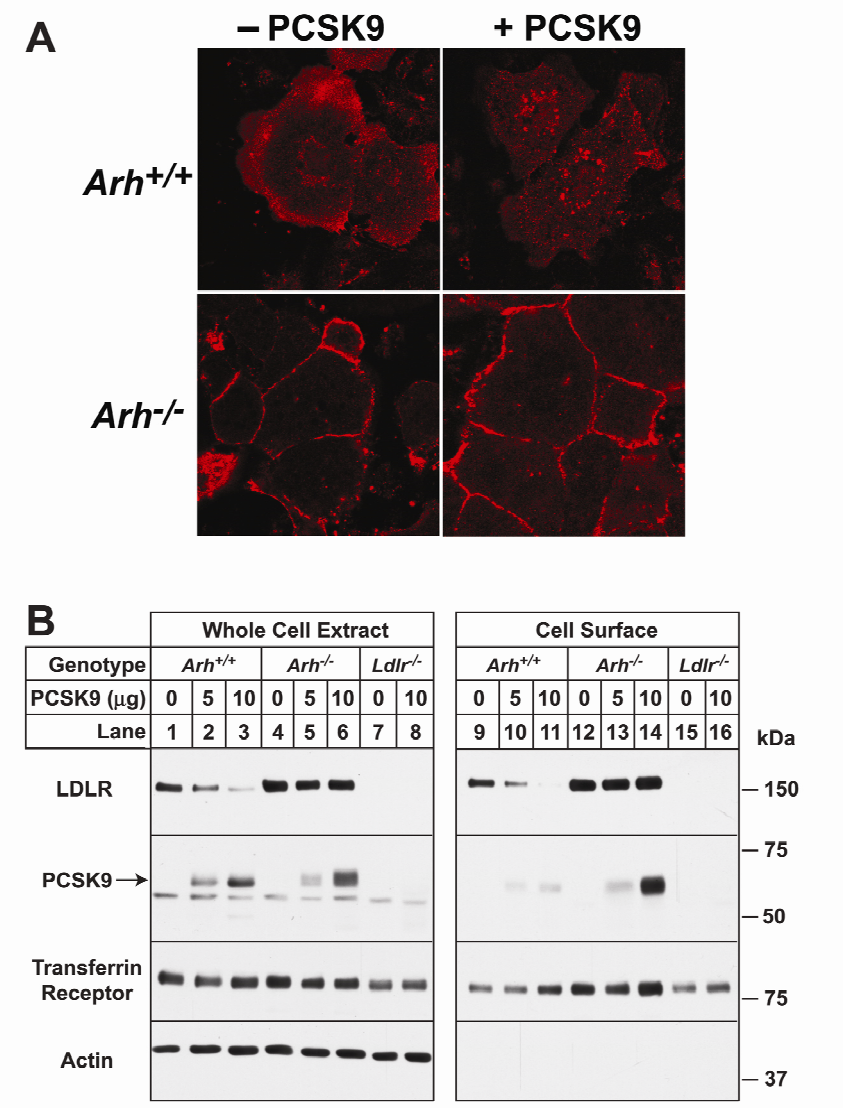

FIGURE 2-8. **PCSK9-mediated degradation of the LDLR is dependent on ARH.** Immunofluorescence, *A,* and immunoblot analyses, *B,* of the PCSK9-mediated changes in LDLR protein in mouse primary hepatocytes derived from $LDLR^{h/h}/Arh^{+/+}$ ($Arh^{+/+}$) or $LDLR^{h/h}/Arh^{-/-}$ ($Arh^{-/-}$) mice. *A,* primary hepatocytes were incubated either in the absence of PCSK9 (-PCSK9) or with 5 μg/ml purified PCSK9 (+PCSK9) for 4 hours and processed for indirect immunofluorescence of LDLR using IgG-C7 and Alexa563-conjugated secondary antibody. Images were taken using a 63 x 1.3 objective using a confocal microscope (Leica TCS_SP). *B,* immunoblot analysis of LDLR, FLAG-tagged PCSK9, and transferrin receptor protein in mouse primary hepatocytes from mice of the indicated genotype incubated with varying amount of PCSK9. Actin was used as a control for cell integrity during cell surface biotinylation.

To test whether PCSK9 could function as a secreted protein *in vivo*, transgenic mice that express human PCSK9 in liver (TgPCSK9) were produced. The transgene was under the control of an apoE promoter with a liver-specific enhancer (114). As shown in Figure 2-9*A*, transgenic overexpression of human PCSK9 eliminated LDLR protein expression in liver and caused a marked increase in plasma LDL-cholesterol levels (Figure 2-9*B*). The increase in plasma LDL-cholesterol was similar to that measured in *Ldlr*$^{-/-}$ mice that lack LDLRs in all tissues. The effects of transgenic PCSK9 overexpression are consistent with previously published experiments that used adenoviral vectors to overexpress PCSK9 in mice (10, 73, 75, 90). The concentration of human PCSK9 in plasma from the transgenic mice as measured using the ELISA assay ranged from ~146-440 μg/ml (Table 2-1, animals 9a, 10a, 11a, and 12a). (This data is post-parabiosis)

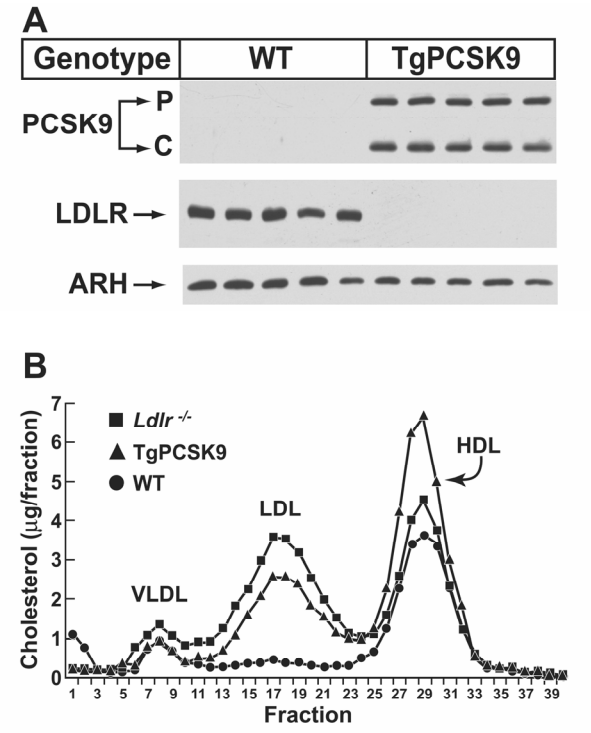

FIGURE 2-9. **Decreased LDLR and increased plasma LDL-C in transgenic PCSK9 mice.**

A, whole cell lysates (30 μg) from the livers from 5 wild-type and 5 TgPCSK9 mice were subjected to SDS-PAGE and immunoblot analyses of human PCSK9, mouse LDLR, and mouse ARH. P and C for PCSK9 denote the proprotein and cleaved forms of PCSK9, respectively. *B,* plasma from the mice of each genotype described in *A* and from 5 age-matched male *Ldlr*$^{-/-}$ mice was pooled and subjected to gel filtration by FPLC. The concentration of total cholesterol in each fraction was measured as described in Materials and Methods.

TABLE 2-1. **Total plasma cholesterol and secreted PCSK9 concentrations in parabiotic mice.**

Parabiotic Pair	Genotype	Pre-parabiosis Cholesterol (mg/dl)	Post-parabiosis Cholesterol (mg/dl)	hPCSK9 (μg/ml)
1a	WT	54	79	0
1b	WT	60	85	0
2a	WT	67	91	0
2b	WT	67	60	0
3a	WT	54	85	0
3b	WT	42	63	0
4a	WT	51	81	0
4b	WT	60	71	0
5a	*Ldlr*$^{-/-}$	178	288	0
5b	WT	56	76	0
6a	*Ldlr*$^{-/-}$	182	270	0
6b	WT	57	64	0
7a	*Ldlr*$^{-/-}$	175	278	0
7b	WT	53	82	0
8a	*Ldlr*$^{-/-}$	179	145	0
8b	WT	68	101	0
9a	Tg	142	365	440
9b	WT	70	775	246
10a	Tg	132	350	198
10b	WT	66	364	148
11a	Tg	180	278	146
11b	WT	61	233	80
12a	Tg	140	171	184
12b	WT	61	131	17

Although an apoE promoter fragment and a liver-specific enhancer were used to express the human PCSK9 cDNA in mice, the transgene mRNA was detected at low levels in other tissues such as the adrenal gland. This expression compromised analysis of the effect of plasma PCSK9 on LDLR protein expression in these extrahepatic tissues. Therefore, TgPCSK9 mice were parabiosed with wild-type mice to determine if secreted PCSK9 derived from the transgenic mouse was able to decrease LDLR protein levels in

liver when transferred via the shared circulation to the recipient wild-type mouse. For these studies, a liver biopsy was performed one week prior to parabiosis to obtain a liver sample for quantifying basal levels of LDLR protein expression. The mice were allowed to recover from the partial hepatectomy and then were parabiosed for two weeks to permit the development of shared circulation. To control for potential changes induced by surgery, wild-type mice were parabiosed with wild-type mice. TgPCSK9 mice manifest elevated plasma LDL-cholesterol levels that could independently alter LDLR protein expression in the recipient wild-type mouse. To control for this effect, wild-type mice were parabiosed with *Ldlr*$^{-/-}$ mice, which have similar lipoprotein profiles as TgPCSK9 mice (Figure 2-9*B*).

As shown in Table 2-1, parabiosis or partial hepatectomy itself slightly increased plasma total cholesterol levels in most mouse pairs. Plasma cholesterol concentrations in wild-type mice parabiosed with *Ldlr*$^{-/-}$ mice (pairs 5-8) were not significantly higher than those measured in the wild-type mouse parabiotic pairs (pairs 1-4). Concentrations of human PCSK9 in parabiotic TgPCSK9:wild-type pairs ranged from ~17-250 μg/ml (pairs 9-12), suggesting that the protein was transferred from the plasma of transgenic mice into the plasma of the parabiosed wild-type mouse with varying efficiencies. There also appeared to be a correlation between the plasma PCSK9 concentration and the degree in plasma cholesterol elevation of the recipient wild-type mouse. The wild-type mouse with the highest PCSK9 concentration (mouse 9b) had an ~10-fold increase in plasma total cholesterol, whereas the wild-type mouse with the lowest PCSK9 level (mouse 12b) had an ~2-fold increase in plasma cholesterol.

To confirm that the observed plasma cholesterol changes were a result of alterations in LDLR protein levels, immunoblots of liver protein were performed in all parabiotic pairs before (-) and 2 weeks after parabiosis (+) (Figure 2-10). LDLR protein levels in livers of wild-type mice parabiosed with wild-type mice were not significantly different before and after parabiosis (panel A). Similarly, the LDLR protein levels in wild-type mice parabiosed with *Ldlr*$^{-/-}$ mice were not different after parabiosis, suggesting that the increased LDL-cholesterol present in the knockout mouse did not alter LDLR expression in the wild-type mouse liver (panel B). In contrast, the LDLR protein was essentially undetectable in livers of wild-type mice after being parabiosed with TgPCSK9 mice (panel C), indicating that PCSK9 was active in mouse plasma.

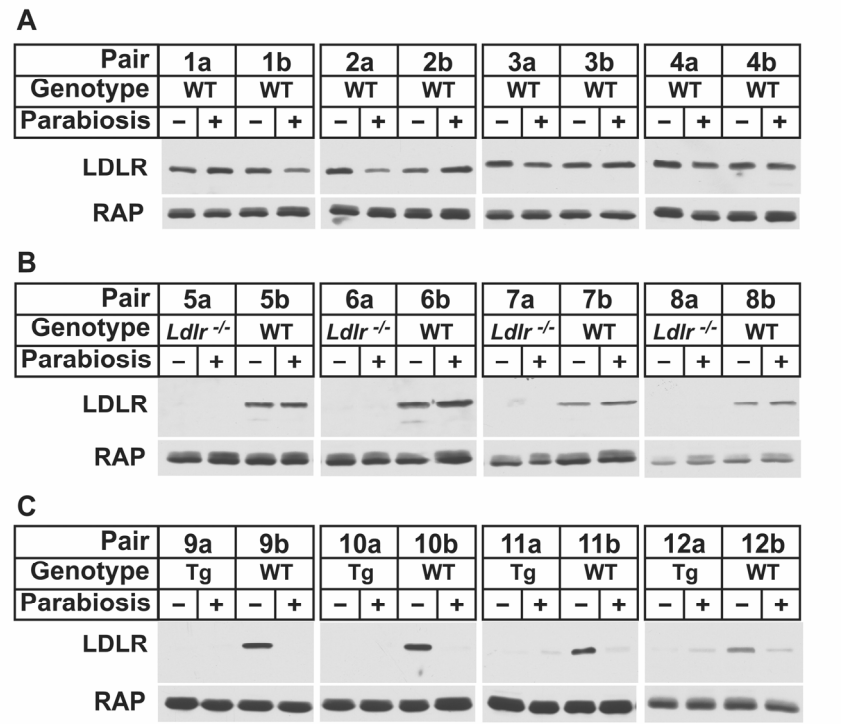

FIGURE 2-10. **Amounts of LDLR protein in livers of parabiosed mice.**
Three combinations of mice were parabiosed for study: *A,* wild-type:wild-type; *B, Ldlr*$^{-/-}$:wild-type; and *C,* TgPCSK9:wild-type. Prior to parabiosis, a liver sample (<100 mg) was obtained from each mouse via a partial hepatectomy and ~50 μl of blood was obtained via the tail vein. After a 7 day recovery period, 12-20 wk-old female mice of the indicated genotype were parabiosed as described in Methods. After 2 weeks of parabiosis, the animals were killed and blood and liver was collected for analysis. Liver membrane protein (40 μg) obtained from each mouse before *(-)* and after *(+)* parabiosis was subjected to SDS-PAGE for immunoblot analyses of LDLR and RAP as a loading control (90).

To ensure that the reduction in LDLR protein measured in livers of the recipient wild-type mice parabiosed to the TgPCSK9 mice was due to post-transcriptional changes, mRNA levels of the LDLR and SREBP-2 were measured using real time RT-PCR (Table 2-2). Although individual mRNAs varied in amount from mouse to mouse, no consistent changes in the mRNAs encoding these genes were measured before and after parabiosis.

Combined, the data suggested that secreted PCSK9 in plasma of mice reduced hepatic LDLR protein independent of changes in mRNA levels.

TABLE 2-2. **Relative hepatic gene expression levels in parabiotic mice.**

Parabiotic Pair	**Genotype**	**SREBP-2**		**LDLR**	
		Pre	Post	Pre	Post
1a	WT	1.0	0.7	1.0	1.2
1b	WT	1.0	1.4	1.0	1.5
2a	WT	1.0	0.8	1.0	0.7
2b	WT	1.0	1.0	1.0	0.7
3a	WT	1.0	1.0	1.0	1.9
3b	WT	1.0	1.1	1.0	0.8
4a	WT	1.0	1.2	1.0	0.9
4b	WT	1.0	1.1	1.0	1.2
5a	*Ldlr*$^{-/-}$	1.0	1.1	-	-
5b	WT	1.0	1.1	1.0	0.8
6a	*Ldlr*$^{-/-}$	1.0	0.8	-	-
6b	WT	1.0	1.3	1.0	1.9
7a	*Ldlr*$^{-/-}$	1.0	1.8	-	-
7b	WT	1.0	1.2	1.0	1.1
8a	*Ldlr*$^{-/-}$	1.0	0.9	-	-
8b	WT	1.0	0.9	1.0	1.0
9a	Tg	1.0	0.9	1.0	0.7
9b	WT	1.0	0.6	1.0	0.8
10a	Tg	1.0	0.9	1.0	0.9
10b	WT	1.0	1.8	1.0	1.7
11a	Tg	1.0	1.5	1.0	1.8
11b	WT	1.0	1.5	1.0	1.1
12a	Tg	1.0	1.6	1.0	1.3
12b	WT	1.0	0.7	1.0	1.9

Discussion

In the current report, it is clearly demonstrated that endogenous PCSK9 is rapidly secreted from cells and that secreted PCSK9 destroys LDLRs when added to the medium of cultured HepG2 cells and mouse primary hepatocytes. The effective concentration of PCSK9 required to reduce LDLRs in cultured cells were within the range of plasma concentrations measured in human plasma. The cell association and uptake of PCSK9 is via binding to the LDLR and both proteins co-localize to a late endocytic/lysosomal compartment. The internalization of PCSK9 with the LDLR into an endosomal/lysosomal compartment is required for PCSK9 to reduce LDLR protein levels since this activity is blocked in the absence of ARH. Finally, it was show that PCSK9 is present in plasma of transgenic mice and that the secreted protein is active in destroying hepatic LDLRs.

Insights into the mechanism of secreted PCSK9's action were derived from studies in MEFs and mouse hepatoctyes, which showed that LDLRs were required for the majority of PCSK9 to associate with the cell surface (Figures 2-6*A* and 2-8*B*). These studies suggested that the LDLR and PCSK9 may directly interact, which was confirmed by co-immunoprecipitation and ligand blotting studies with the LDLR and PCSK9 (Figure 2-7). The co-immunoprecipitation studies with PCSK9(D374Y) and the LDLR suggested that the interaction of the mutant protein with the LDLR was much more avid than wild-type PCSK9 (Figure 2-7*A*). In addition, PCSK9(D374Y) was ~10 times more efficient in destroying cell surface LDLRs when added exogenously to HepG2 cells (Figure 2-5). Previous overexpression studies in McArdle-7777 rat hepatoma cells with PCSK9(D374Y) suggested that the mechanism by which the mutant protein increased plasma LDL-cholesterol was through the overproduction of apoB (118). Similar

conclusions were drawn from *in vivo* kinetic studies in humans that carry a different point mutation in PCSK9 (S127R) (88). The current studies with the D374Y mutant suggest an alternative mechanism that involves enhanced LDLR association and degradation. Whether the S127R and F216L point mutations in PCSK9 behave in a manner similar to PCSK9(D374Y) will be tested in future studies. Our observations that purified PCSK9(D374Y) added to cells reduced LDLRs extend the results from a publication that appeared during the preparation of this manuscript demonstrating that conditioned medium containing PCSK9(D374Y) reduced the uptake of LDL (19).

A small amount of residual PCSK9 binding to LRP was detected in LDLR-deficient MEF cells (Figure 2-6*B*). Previously, it was shown that hepatic LRP protein levels are not altered by the adenoviral overexpression of PCSK9 in mice (90), and LRP protein levels were not significantly different in livers of wild-type mice parabiosed with the TgPCSK9 mice (data not shown). Thus, although a small amount of PCSK9 may associate with LRP *in vitro*, it does not appear to significantly regulate LRP protein levels. The residual LRP-dependent cellular association of PCSK9 might be due to the sequence similarity between LRP and the LDLR. LRP contains four copies of the LDLR extracellular domain with similar charge distributions, which may sufficiently resemble LDLR to support PCSK9 binding (53).

Recent studies by Maxwell and Breslow (76) showed that overexpression of PCSK9 in HpeG2 cells induced the degradation of LDLR intracellularly in a post-ER compartment. These experiments also suggested that PCSK9-mediated reduction in LDLR was not attributable to the proteasome or lysosomal cysteine proteases. In addition, our previous studies using adenoviral overexpression of PCSK9 in mice

demonstrated that high levels of PCSK9 expression in liver eliminated LDLR protein expression in wild-type and *Arh*$^{-/-}$ mice equally, indicating functional ARH was not required for PCSK9 activity (90). These results differ from the data of Figure 2-8 that show functional ARH is required for PCSK9 to destroy LDLRs when added exogenously to primary hepatocytes. Therefore, it is possible that PCSK9 overexpression may result in the association of PCSK9 with the LDLR within the cell and that this binding leads to intracellular LDLR protein degradation through the pathway described by Maxwell and Breslow, whereas PCSK9's action at the cell surface is mediated by a distinct mechanism that is dependent upon ARH-mediated endocytosis.

Considered together, the available data now suggest that PCSK9 can function both extra- and intracellularly, but it is unknown which pathway predominates under normal and/or pathologic conditions. Currently, all studies suggesting that the protein functions intracellularly have been performed using PCSK9 overexpression via a strong CMV promoter. Overexpression may permit the association of PCSK9 and the LDLR in an intracellular compartment that does not occur physiologically. In the current studies, it was demonstrated that physiologically relevant concentrations of PCSK9 could significantly reduce cell surface LDLRs when added to HepG2 cells (Figures 2-4 and 2-5). Additional studies to determine the relative contribution of extracellular PCSK9 in the regulation of LDLR protein levels will require determining whether the infusion of PCSK9 into the circulation of PCSK9 knockout mice will decrease the LDLRs in liver and raise plasma cholesterol levels.

The parabiosis studies shown in Figure 2-10 provide evidence that PCSK9 can function in plasma to destroy LDLRs in liver. The liver is the principal site of PCSK9

expression and *PCSK9* is transcriptionally regulated by SREBP-2 (60). SREBP-2 regulates all genes required for cholesterol synthesis and its activity is modulated by cellular sterol levels (16, 60). If the concentration of PCSK9 in plasma is primarily determined by the liver, then plasma PCSK9 levels may be a reflection of hepatic cholesterol stores since *PCSK9* transcription is reduced under conditions where SREBP-2 is suppressed, i.e. high cellular cholesterol concentrations. Such a regulatory event also raises the possibility that the liver indirectly regulates the amount of LDLRs in peripheral tissues by determining the amount of PCSK9 secreted into plasma. It is currently not known whether PCSK9 in plasma is capable of destroying LDLRs in tissues other than liver. This could not be directly addressed in the current studies, owing to the detection limits of the anti-LDLR antibody in tissues other than liver.

The genetic data from humans with loss-of-function mutations in *PCSK9* combined with the studies in knockout mice that lack PCSK9 clearly indicate that inhibitors of the protease would be of therapeutic benefit for the treatment of hypercholesterolemia. Inasmuch as overexpression of the catalytically inactive form of PCSK9 in mice did not alter LDLR protein levels (90), an inhibitor of PCSK9's protease activity in the ER should be sufficient to block its ability to reduce LDLR protein levels. If PCSK9 functions as a secreted factor as suggested by the current data, then additional approaches to neutralize its activity, including the development of antibodies to block its interaction with the LDLR or inhibitors that block its action in plasma, can be explored for the treatment of hypercholesterolemia.

Materials and Methods

Cholesterol, triglyceride, and protein concentrations in plasma were measured as previously described (112). Reagents were obtained from Sigma-Aldrich Chemicals unless stated otherwise. Real-time reverse transcriptase-PCR was performed as described previously (97). *Ldlr*$^{-/-}$ (63), *Pcsk9*$^{-/-}$ (97), *Arh*$^{-/-}$ (66), and *LDLR*$^{h/h}$ (67) mice were produced as described in the indicated reference. Mice that express only human LDLR (*LDLR*$^{h/h}$) and lack ARH were generated by breeding *LDLR*$^{h/h}$ with *Arh*$^{-/-}$ mice.

Tissue Culture Medium. Medium A contained Dulbecco's Modified Eagle Medium (DMEM) (Cellgro) supplemented with 100 units/ml penicillin, 100 μg/ml streptomycin sulfate and 1 g/L glucose. Medium B contained Medium A supplemented with 10% (v/v) fetal calf serum (FCS). Medium C contained Medium A supplemented with 5% (v/v) newborn calf lipoprotein-deficient serum (NCLPDS), 10 μM sodium compactin, and 50 μM sodium mevalonate. Medium D contained DMEM supplemented with 100 units/ml penicillin, 100 μg/ml streptomycin sulfate, and 4.3 g/L glucose. Medium E contained Medium E supplemented with 10% (v/v) fetal calf serum (FCS). Medium F contained Medium E supplemented with 5% (v/v) NCLPDS, 10 μM sodium compactin, and 50 μM sodium mevalonate.

Cultured Cell Experiments. HepG2 cells (ATCC, HB-8065) were set up at 5 x 10^5 cells/60-mm dish in Medium B on day 0. On day 2, Medium B was replaced with Medium C for 18-24 h before initiating experiments. Immortalized mouse embryonic fibroblasts (MEFs) were a gift from Joachim Herz (UT Southwestern) (124). MEF cells

were set up at 1 x 10^5 cells/60-mm dish in Medium E on day 0. On day 1, medium was replaced with Medium F 18-24 h before initiating the experiments.

Stable Transfection of Human Embryonic Kidney (HEK) 293S cells with Epitope-tagged PCSK9. HEK 293S cells (98) were cultured in Medium B and transfected with 2 μg of expression plasmid pCMV-hPCSK9-FLAG (90) or pCMV-hPCSK9(D374Y)-FLAG using FuGENE 6 transfection reagent according to manufacturer's instructions (Roche). Plasmid pCMV-hPCSK9(D374Y)-FLAG was produced by site-directed mutagenesis (Stratagene) using the oligonucleotide 5'-GGTGCCTCCAGCTACTGCAGCACCTG-3' and pCMV-hPCSK9-FLAG. Colonies expressing the *neo*-containing plasmid were isolated and expression of PCSK9 was assessed by immunoblot analysis using an anti-FLAG M2 antibody.

Purification of Human Wild-type and PCSK9(D374Y)-FLAG Fusion Proteins. HEK 293S cells stably expressing FLAG-tagged human PCSK9 or PCSK9(D374) were cultured in suspension without CO_2 in HI GRO^{TM} complete serum-free medium (Irvine Scientific) supplemented with 10% FCS, 10 mM L-glutamine, 100 units/ml penicillin, and 100 μg/ml streptomycin. PCSK9 was purified by anti-FLAG M2 affinity gel chromatography from 500 ml of medium per the manufacturer's instructions followed by size-exclusion chromatography on a Tricorn Superose 6 10/300 fast-performance liquid chromatography (FPLC) column (Amersham). Fractions containing PCSK9 were concentrated ~5-fold using a Centricon filter (10 kDa MW cut-off, Millipore). Protein purity was monitored by SDS-PAGE and Coomassie Brilliant Blue R-250 staining (Bio-Rad).

Antibodies. For the anti-human PCSK9 polyclonal antibody, the human PCSK9 amino acid sequence was analyzed using Protean software (DNAStar) for immunogenic regions. Amino acids 165-180 (RYRADEYQPPDGGSLV) and 220-240 (ASKCDSHGTHLAGVVSGRDAG) were synthesized, conjugated to KLH using the Imject Maleimide Activated mcKLH Kit (Pierce), and rabbits were injected with a mixture of the peptides (20 μg each) as described (112). IgG fractions from sera were purified using the Immunopure (A/G) IgG purification kit (Pierce). Monoclonal antibodies that recognize human PCSK9 were generated by fusion of Sp2/mIL-6 (ATCC, CRL-2016) mouse myeloma cells with splenic B-lymphocytes derived from a female BALB/c mouse injected with purified human PCSK9 protein (54). The resulting antibodies, 13D3 and 15A6, belong to the IgG subclass 1 and recognize epitopes in the catalytic domain and the C-terminal region of PCSK9, respectively. Additional antibodies used were the following: IgG-HL1 and IgG-C7, mouse monoclonal antibodies that recognize the human LDLR (121); anti-human transferrin receptor (Zymed Laboratories); horseradish peroxidase-conjugated donkey anti-mouse IgG (Jackson ImmunoResearch Laboratories); horseradish peroxidase-conjugated donkey anti-rabbit IgG (Amersham); monoclonal anti-actin mouse ascites (clone AC-10 - Sigma); and Alexa Fluor conjugated goat anti-rabbit and anti-mouse IgGs (Invitrogen). Polyclonal antiserum against the bovine LDLR (Ab 4548), the murine LDLR cytoplasmic tail (Ab 3143), LRP, RAP, ARH, polyclonal antibodies were described previously (90, 103). Rabbit polyclonal IgG recognizing the bovine CI-MPR was the kind gift of Dr. Stuart Kornfeld (Washington University).

Immunoblot Analysis. Whole cell lysate protein extracts were subjected to SDS-PAGE for immunoblot analysis as previously described (90). Biotinylation of cell surface proteins of HepG2 cells was performed as described (48). Following biotinylation, whole cell lysates were prepared (90) and protein concentration was determined. An aliquot of the whole cell lysate was reserved, and the remainder was transferred to a fresh tube containing 50 µl of Ultralink Neutravidin Protein Plus (1:1 slurry). After 12-18 h of incubation with rotation at 4^{o}C, beads were collected by centrifugation at 300 x *g* for 5 min and washed 3 times with lysis buffer. Proteins were eluted from the beads by boiling in SDS-PAGE sample buffer (normalized for protein concentration) and subjected to 8% SDS-PAGE and immunoblot analysis as described (90).

PCSK9 "Sandwich" ELISA. LumiNunc Maxisorp white assay plates (NalgeNunc) were coated with anti-human PCSK9 monoclonal antibody (IgG-13D3) diluted to 5 µg/ml in 100 µl of Buffer A (20 mM sodium phosphate pH 7.5, 100 mM sodium chloride) by incubation overnight at 4°C. The assay plates were then washed with 350 µl of Phosphate Buffered Saline with Tween 20, pH 7.4 (PBSt) and blocked with 150 µl of 0.5% BSA in Buffer A for 1 h at room temperature with shaking. Sample preparation was carried out in a separate polypropylene microtiter sample plate. Standards were prepared in duplicate using dilutions of purified PCSK9 protein in Buffer A + 0.5% BSA. Plasma samples were prepared in triplicate by diluting 6 µl of plasma in 84 µl of Buffer A + 0.5% BSA. Thirty µl of Buffer B (Buffer A, 0.5% BSA, 7.2 M urea, and 0.68% Tween 20) was then added to each well and the sample plate was incubated at 46°C for 30 min. Aliquots (100 µl) were transferred to the assay plate and incubated for 2 h at room temperature with shaking. The plate was then washed with PBSt and incubated

for 1 h at room temperature with 100 µl of rabbit anti-human PCSK9 polyclonal antibody (7.5 µg/ml in Buffer A + 0.5% BSA). After washing with PBSt, 100 µl of donkey anti-rabbit IgG + HRP (GE Healthcare) diluted 1:10,000 was added for 1 h at room temperature. After a final wash with PBSt, 100 µl of SuperSignal ELISA Femto Substrate (Pierce) was added for 1 min and luminescence quantified using a Dynex MLX microtiter plate luminometer (Dynex Technologies). To determine plasma PCSK9 concentrations, luminescence of the sample were compared to those generated in the standard curve with purified PCSK9. Assay validation experiments were conducted in accordance with current bioanalytical recommendations (32). Human plasma was obtained from 72 volunteers (35 men and 37 women) after an overnight fast. The age of the individuals ranged from 21-56 and none were taking lipid altering medications.

Pulse/Chase Analysis of PCSK9. HepG2 cells were cultured in Medium C and the pulse/chase was carried out as described (97). Immunoprecipitation of cell and medium extracts was performed using the polyclonal anti-PCSK9 antibody (105). Immunoprecipitates were eluted in SDS sample buffer, and subjected to 8% SDS-PAGE. The gels were fixed and then immersed for 15 min in Amplify™ fluorogenic reagent (Amersham), dried under vacuum and exposed to film.

Co-immunoprecipitation of PCSK9 and the LDLR. HepG2 cells were cultured for 18 h in Medium C prior to treatment with 20 µg/ml or 2 µg/ml amounts of purified PCSK9 or PCSK9(D374Y) for 1 h in the presence of 0.1 mM chloroquine. Pooled cell pellets from 6 dishes of cells were lysed in 2 ml of Buffer C (20 mM Hepes-KOH at pH 7.4, 150 mM NaCl, 1 mM $MgCl_2$ and protease inhibitors) containing 1% (w/v) digitonin. Cell lysates were subjected to immunoprecipitation using 50 µl anti-FLAG M2 agarose

(Sigma) to immunoprecipitate FLAG-tagged PCSK9 (for competition assays, 0.1 mg/ml of FLAG octapeptide was included), IgG-HL1 to immunoprecipitate LDLR, or IgG-2001 a mouse monoclonal antibody to an irrelevant antigen (9). Immunoprecipitates were washed 3 times with 500 μl Buffer C containing 0.1% (w/v) digitonin, eluted in SDS sample buffer by boiling for 5 min and subjected to 8% SDS-PAGE.

Ligand blotting. Purified human LDLR extracellular domain (amino acids 1-699) was kindly provided by Dr. Johann Deisenhofer (UT Southwestern) and described previously (101). LDLR protein was resolved on non-reducing SDS-PAGE and transferred to nitrocellulose as described (29). In control experiments, LDLR protein was heated for 5 min at 96^{o}C in sample buffer containing 2.5% (v/v) 2-mercaptoethanol (reducing conditions). All subsequent steps were preformed at 20^{o}C. Blots were blocked for 30 min in Buffer D (50 mM Tris-Cl at pH 7.4, 90 mM NaCl, 2 mM $CaCl_2$, 5% (w/v) BSA) and incubated sequentially for 60 min with gentle agitation in Buffer D containing purified PCSK9 (5 μg/ml), the monoclonal anti-PCSK9 antibody IgG-15A6 (5 μg/ml), and horseradish peroxidase-conjugated goat anti-mouse IgG. PCSK9 and antibody incubations were followed by washes in Buffer E (50 mM Tris-Cl at pH 7.4, 90 mM NaCl, 2 mM $CaCl_2$, 0.5% (w/v) BSA). Blots were developed by immunoblotting as described above.

Immunofluorescence Microscopy. Indirect immunofluorescence using antibodies that detect the LDLR, PCSK9, and CI-MPR in MEF cells was performed as follows. MEF cells cultured on glass coverslips to 50% confluence were fixed in 4% (w/v) paraformaldehyde in Buffer F (PBS containing 2 mM $MgCl_2$), quenched with 5 mM NH_4Cl in Buffer F, permeabilized in Buffer F containing 0.05% (w/v) Triton X-100

(Pierce) for 10 min at -20°C and blocked for 30 min in Buffer G (Buffer F containing 1% (w/v) BSA). For double-label staining, cells were incubated sequentially with the monoclonal anti-PCSK9 antibody IgG-15A6 (2.5 μg/ml), Alexa488-conjugated goat anti-mouse IgG (0.6 μg/ml), polyclonal LDLR antiserum Ab 4548 (1:1000) or polyclonal CI-MPR IgG (2 μg/ml), and Alexa555-conjugated goat anti-rabbit IgG (0.6 μg/ml). Primary (16 h at 4^{o}C) and secondary (1 h at 20^{o}C) antibody incubations were followed by three 20 min washes with Buffer G. Coverslips were mounted in Vectashield mounting medium (Vector Laboratories) and images were taken on a Zeiss confocal microscope model LSM510-META. Indirect immunofluorescence for the LDLR in primary hepatocytes derived from *LDLR*$^{h/h}$;*Arh*$^{+/+}$ and *LDLR*$^{h/h}$;*Arh*$^{-/-}$ mice was carried out as described (66, 97).

Generation of Transgenic Mice that Overexpress Human PCSK9 (TgPCSK9). A cDNA encoding human PCSK9 was inserted into a pLiv-11 vector that contains the constitutive human apoE promoter and its hepatic control region (a gift from Dr. John Taylor, Gladstone Institute) (114). The integrity of the construct (pLiv-11-hPCSK9) was verified by sequencing. Transgenic mice were generated by injecting linearized pLiv-11-hPCSK9 into the fertilized eggs as described (112).

Liver Biopsy and Parabiosis. One week prior to parabiosis, a liver biopsy was performed to obtain a liver sample for protein analysis. Mice were anesthetized with Nembutal, hair over the abdomen shaved, and the skin cleaned with chlorhexidine. A 0.5 cm transverse incision was made in the upper abdomen and a small lobe of the liver (~50-100 mg) was tied off with 5-0 silk suture and excised. The liver sample was placed in liquid nitrogen for storage. The incision was closed in two layers using 5-0 silk suture

and wound clips. During sedation, 50 µl of blood was removed from the tail vein for plasma cholesterol and PCSK9 measurements. The mice were allowed to recover from this surgery before performing the parabiosis surgery. For parabiosis, mice were surgically joined following a previously published protocol (125), with slight modifications. Matching skin incisions were made from the shoulder to the hip joint of each mouse, and a 10-mm incision was made in the muscles of the abdominal wall. The muscular incisions were joined using 5-0 silk suture. The scapulae were attached by a 2-0 silk suture, and the skin was approximated using wound clips and 5-0 silk suture. Three genetically disctinct groups of female mice were studied: wild-type mice joined with wild-type mice; *Ldlr*$^{-/-}$ mice joined with wild-type mice; and TgPCSK9 mice joined with wild-type mice. Shared circulation was confirmed by injecting Evans Blue into one of the parabiotic pairs prior to study. Mice were killed by Isoflurane overdose two weeks after the parabiotic surgery and blood and liver were harvested for analysis. All mice were housed in colony cages and maintained on a 12-h light/12-h dark cycle, fed Teklad Mouse/Rat Diet 7002 from Harlan Teklad Premier Laboratory Diets, (Madison WI). Animal experiments were approved by the Institutional Animal Care and Research Advisory Committee at the University of Texas Southwestern Medical Center.

CHAPTER THREE
Catalytic Activity is Not Required for Secreted PCSK9 to Reduce LDLRs[f]

Summary

Proprotein convertase subtilisin/kexin type 9 (PCSK9), a member of the proteinase K subfamily of subtilases, promotes internalization and degradation of LDL receptors (LDLRs) after binding the receptor on the surface of hepatocytes. PCSK9 has autocatalytic activity that releases the prodomain at the N-terminus of the protein. The prodomain remains tightly associated with the catalytic domain as the complex transits the secretory pathway. It is not known if enzymatic activity is required for the LDLR-reducing effects of PCSK9. Here, the prodomain is expressed together with a catalytically inactive protease domain in cells and the protein purified from the medium. The ability of the catalytically inactive PCSK9 to bind and degrade LDLRs when added to culture medium of human hepatoma HepG2 cells at physiological concentrations was similar to that seen using wild-type protein. Similarly, a catalytic-dead version of a gain-of-function mutant PCSK9(D374Y) showed no loss of activity compared to a catalytically active counterpart; both proteins displayed ~10-fold increased activity in degradation of cell surface LDLRs compared to wild-type PCSK9. Thus, it is concluded that the ability of PCSK9 to degrade LDLRs is independent of catalytic activity, suggesting that PCSK9 functions as a chaperone to prevent LDLR recycling and/or to target LDLRs for lysosomal degradation.

[f] This chapter is adapted from (80) and (45). Used with permission.

Introduction

The secretory proprotein convertase (PC) enzymes are structurally related to the bacterial subtilisin-like serine protease kexin found in yeast (39). There are nine subtilisin-like serine proteinases in mammals designated PC1/3, PC2, furin, PC4, PC5/6, PACE4, PC7, S1P (site-1 protease) and PCSK9 (proprotein convertase subtilisin/kexin type 9) (111). PCs share a general structure that consists of a signal sequence, followed by a heterogeneous prodomain, a highly conserved subtilisin-like catalytic domain, and a C-terminal domain that varies in length and sequence among members (108, 109). All family members except PC2 undergo autocatalytic cleavage in the endoplasmic reticulum (ER), releasing the prodomain (12, 81, 83). PC1/3, PC2, furin, PC4, PC5/6, PACE4 and PC7 cleave at single or paired basic amino acids with the general sequence (K/R)-(X_n)-(K/R)↓. S1P and PCSK9 cleave after non-basic amino acids in the motifs RXX(L/K)↓ (23) and (V/I)FAQ↓ (10, 86), respectively.

The prodomain serves a dual chaperone function, assisting in both the proper folding of the protease domain and in the regulation of catalytic activity (3, 4, 83). Autocatalytic cleavage of the zymogen in the ER is a requirement for transport from this compartment (12, 81, 83). The excised prodomain remains non-covalently associated with the protein and inhibits aberrant protease activity (3, 83). In most PCs, the prodomain undergoes a second proteolytic processing event that relieves inhibition and unmasks enzymatic activity in the appropriate compartment (3, 5).

Like the other PCs, PCSK9 is synthesized as an inactive proenzyme, and contains a triad of residues (D186, H226, and S386) that are required for catalytic activity (108). The soluble ~74-kDa precursor form of PCSK9 undergoes intramolecular autocatalytic

cleavage in the ER, which produces a 14-kDa prodomain and a ~60-kDa catalytic fragment (10, 86). The cleaved prodomain remains associated with the catalytic domain, forming a complex that is transported to the Golgi apparatus and subsequently secreted (10, 108). Several studies have shown that the secreted mature form of PCSK9 contains an intact prodomain, with no evidence of secondary proteolytic processing (10, 28, 71, 72, 94).

The genetic data from humans and the *in vivo* studies in mice demonstrate that PCSK9 reduces the number of the LDLRs; however, the mechanism by which PCSK9 carries out this function is only partially known. Evidence is consistent with the secreted form of PCSK9 binding directly to the LDLR and resulting in degradation of the receptor (19, 72, 94). Zhang *et al*. (127) localized the binding site of PCSK9 in the LDLR to the first epidermal growth factor-like repeat (EGF-A) of the extracellular domain and showed that PCSK9 binding to this site is required for LDLR degradation. For the secreted form of PCSK9 to destroy LDLRs, the PCSK9/LDLR complex must be internalized into endosomal/lysosomal compartments (72).

Although binding and internalization of PCSK9 and the LDLR are required for PCSK9 to promote degradation of the receptor, it is not known whether PCSK9 acts catalytically in the process, either to cleave the LDLR or an accessory protein that affects LDLR stability. Inactivation of the catalytic activity using routine mutagenesis results in either PCSK9 remaining sequestered in the ER or in improper folding of the protein. Therefore, this question is addressed by expressing the prodomain and an inactive catalytic domain *in trans* in cells and purifying the resultant recombinant protein complex from the medium. Using this reagent, evidence is provided that PCSK9 catalytic activity

is not required for PCSK9 to bind and degrade LDLRs in cultured human hepatoma HepG2 cells.

RESULTS

Among the PC family of mammalian serine proteases, autocatalytic cleavage of the prodomain is required for entry of the protease into the secretory pathway. Accordingly, mutation of the conserved serine (S386) of the catalytic triad in PCSK9 prevents autocatalytic cleavage and results in retention of the protein within the ER (86, 90). Therefore, to determine whether catalytic activity is required for exogenous PCSK9 to destroy LDLRs, an alternative strategy was employed to obtain secreted catalytically inactive PCSK9. An expression plasmid was constructed that contained the signal peptide and prodomain of PCSK9 followed by a V5 epitope tag. A second expression plasmid was constructed that contained the signal sequence, catalytic, and C-terminal portions of PCSK9 followed by a FLAG-tag. This is shown schematically in Figure 3-1. The two plasmids were co-transfected into HEK 293 cells to determine whether the PCSK9 fragments expressed *in trans* could associate and be secreted from the cell. As shown in Figure 3-2*A*, the prodomain and catalytic fragments were similarly expressed in the transfected cells (*lanes 3-5*); however, secretion of either peptide only occurred when both fragments were co-expressed (*lane 10*). Because PCSK9 from co-expression of the prodomain and catalytic fragment of PCSK9 was secreted, it provided a means to mutate key amino acid residues of the catalytic triad to determine whether catalytic activity was required for PCSK9 activity.

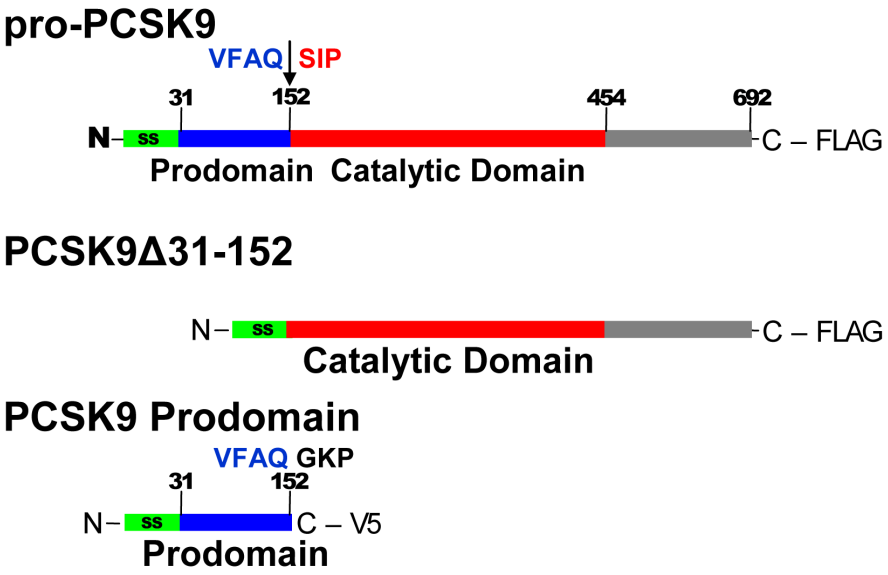

FIGURE 3-1. ***Trans*- PCSK9 constructs.**
Constructs used to for PCSK9 expression are diagramed. PCSK9 contains a signal sequence (green), prodomain (blue), catalytic domain (red), and C-terminal domain (grey). Full-length and prodomain deleted constructs contain a C-terminus FLAG tag and the prodomain construct contained a C-terminus V5 tag. Arrow and sequence indicate the site of PCSK9 intramolecular cleavage. Sequence above the prodomain construct indicates the site of V5 tag fusion.

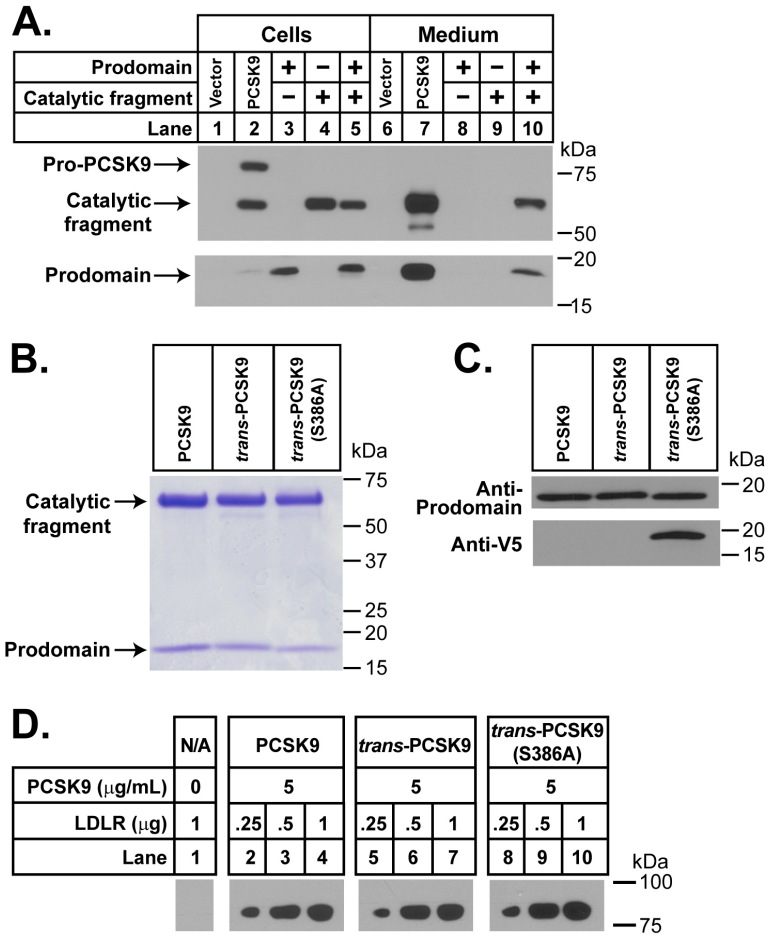

FIGURE 3-2. **PCSK9 is secreted and binds the LDLR when expressed *in trans*.**
A, HEK 293 cells were transiently transfected with wild-type PCSK9, prodomain of PCSK9, catalytic fragment of PCSK9, or both the prodomain and catalytic fragment of PCSK9. Medium and cell extracts were subjected to SDS-PAGE and immunoblot analysis. The catalytic fragment of PCSK9 was detected with IgG-15A6 and the prodomain with IgG-1A1. *B,* PCSK9, *trans*-PCSK9, and *trans*-PCSK9(S386A) were purified from stable transfected HEK 293S cells. 5 μg of each protein was resolved on 4-15% SDS-PAGE and stained with Coomassie Brilliant Blue R-250. *C,* Purified wild-type PCSK9, *trans*-PCSK9, and *trans*-PCSK9(S386A) were analyzed for the presence of the prodomain by 4-15% SDS-PAGE and immunoblotting. The prodomain was detected with the IgG-3C12 anti-prodomain and anti-V5 antibodies. *D*, The indicated amount of purified extracellular domain of the LDLR was resolved under nonreducing conditions by SDS-PAGE and transferred to nitrocellulose. Filters were incubated with 5 μg/mL of the indicated purified PCSK9 or buffer control (N/A) for 1 h and then incubated with 2.5 μg/mL anti-FLAG M2 antibody.

An HEK 293S cell line was subsequently established that stably expressed the "*trans*-PCSK9" or a *trans*-PCSK9 protein containing an alanine substituted for the serine at position 386 (S386A) of the catalytic triad. This amino acid change abolishes the autocatalytic cleavage of PCSK9 (90, 108). From these cell lines, large amounts of the recombinant purified proteins could be obtained to characterize their binding properties and test for activity. Secreted *trans*-PCSK9 proteins were purified using the FLAG epitope as previously described (72). Figure 3-2*B* shows that the catalytic fragment and prodomain co-purify with both proteins expressed *in trans*, indicating the two fragments interact and are secreted together in a manner similar to that of the wild-type PCSK9 purified from HEK 293S cells stably transfected with a single plasmid encoding the full-length PCSK9 protein. The alanine to serine change at position 386 of the purified protein was confirmed by sequencing using mass spectrometry. Further evidence that the S386A mutation produces a catalytically inactive protein was the immunoblot data using an antibody that recognizes the V5 tag present at the C-terminus of the prodomain. Immunoblot of purified PCSK9 or *trans*-PCSK9 using an anti-V5 or anti-PCSK9 prodomain antibody revealed that only the *trans*-PCSK9(S386A) retained the V5 tag (Figure 3-2*C*). This indicates that the wild-type *trans*-PCSK9 could cleave the V5 tag from the prodomain and the *trans*-PCSK9(S386A) could not. The sequence of the cleavage site in *trans*-PCSK9 (VFAQ^{152}↓GKP) was verified by mass spectrometry and was found to occur at the same residue as the prodomain is normally cleaved from full-length PCSK9 (VFAQ^{152}↓SIP).

It was first determined whether the secreted recombinant *trans*-PCSK9 proteins could bind to the LDLR by ligand blotting using purified LDLR protein. Figure 3-2*D*

shows that the purified *trans*-PCSK9 and *trans*-PCSK9(S386A) proteins bound the LDLR with affinities similar to that measured with purified PCSK9 protein derived from a single plasmid encoding the full-length protein. Next, it was tested whether catalytic activity was required for PCSK9 to degrade LDLRs when added to the medium of HepG2 cells cultured in sterol-depleted medium to induce LDLR expression (72). After incubation with purified PCSK9, the surface proteins of the cells were covalently modified with a cell-impermeable biotinylation reagent and then isolated using streptavidin beads. Total cellular LDLRs in whole cell extracts and cell surface LDLRs were measured by SDS-PAGE and immunoblotting (72). The amounts of whole-cell and cell surface PCSK9 were also measured by SDS-PAGE and immunoblotting using an anti-FLAG antibody that detected only exogenously added PCSK9.

Figure 3-3 shows that PCSK9 purified from the full-length plasmid (PCSK9), *trans*-PCSK9, and *trans*-PCSK9(S386A) had nearly identical potencies in reducing the number of LDLRs on the cell surface at all concentrations tested without affecting another cell surface receptor, the transferrin receptor (compare *lanes 6-10* of Figure 3-3*A*, *B*, and *C*). FLAG-tagged PCSK9 was detected in whole-cell extracts in a concentration-dependent manner (*lanes 2-5,* Figure 3-3*A, B, C*) but was not detected among the biotin-labeled cell surface proteins (*lanes 7-10,* Figure 3-3*A, B, C*), suggesting that most of the cell-associated PCSK9 had been internalized. Of note, the minimum concentration of the catalytically inactive PCSK9 required to degrade LDLRs was 0.5 μg/ml, a concentration similar to that found in human plasma (Figure 3-3*C, lane 7*) (72).

These results indicate that catalytic activity of PCSK9 is not required to degrade LDLRs when PCSK9 is added exogenously to HepG2 cells. Previously, point mutations

in human PCSK9 have been identified that result in a gain-of-function and hypercholesterolemia (1). One gain-of-function PCSK9 mutation, PCSK9(D374Y) binds to the LDLR with ~25-fold greater affinity and is ~10-fold more active in reducing LDLRs than the wild-type protein (28, 72). If the hypothesis that binding of PCSK9 to LDLR but not catalytic activity is required for PCSK9 to degrade the LDLR is correct, then the introduction of the D374Y mutation into the catalytically inactive PCSK9(S386A) should still confer increased binding and enhanced degradation capacity. To test this possibility, an HEK 293S cell line was established that stably expressed PCSK9 in *trans* that contained both the D374Y and S386A mutations in the catalytic fragment [*trans*-PCSK9(D374Y-S386A)].

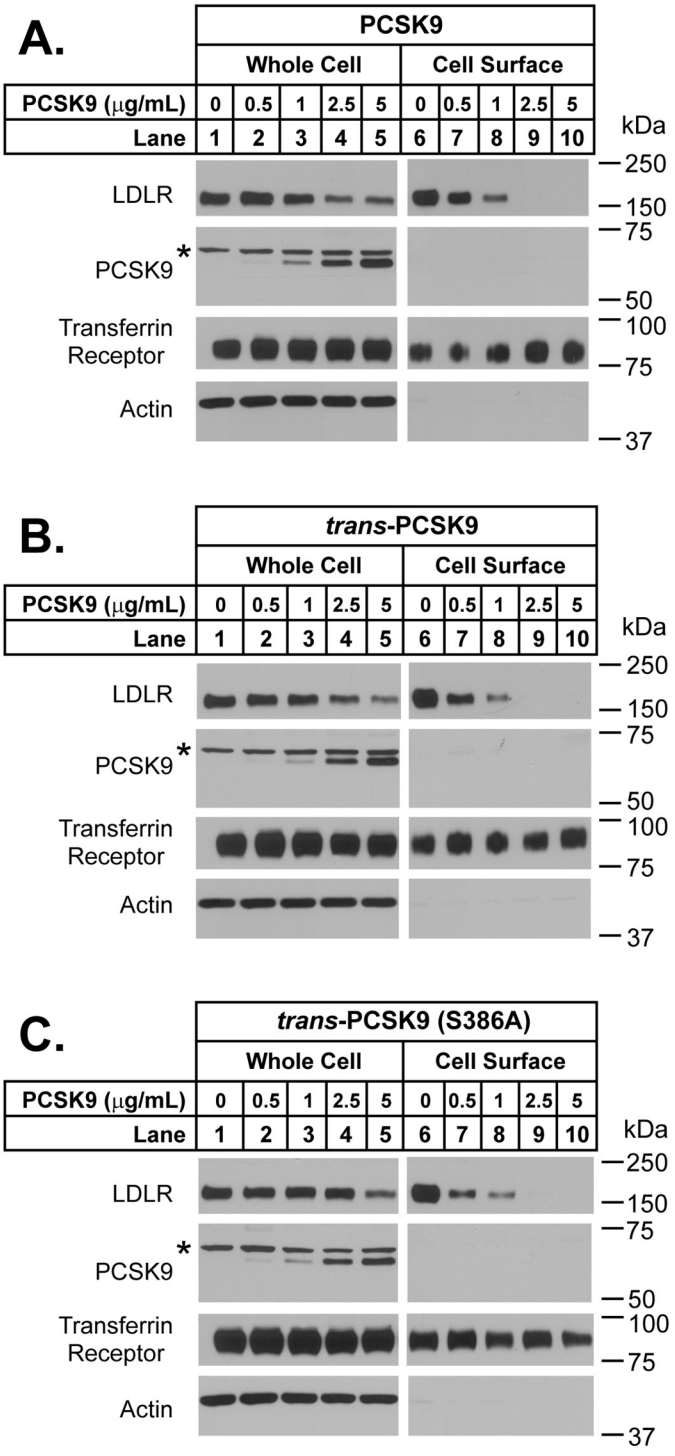
A.
PCSK9
Whole Cell
Cell Surface
PCSK9 (μg/mL) 0 0.5 1 2.5 5 0 0.5 1 2.5 5
Lane 1 2 3 4 5 6 7 8 9 10
kDa
LDLR
PCSK9 *
Transferrin Receptor
Actin
250
150
75
50
100
75
37
B.
trans-PCSK9
Whole Cell
Cell Surface
PCSK9 (μg/mL) 0 0.5 1 2.5 5 0 0.5 1 2.5 5
Lane 1 2 3 4 5 6 7 8 9 10
kDa
LDLR
PCSK9 *
Transferrin Receptor
Actin
250
150
75
50
100
75
37
C.
trans-PCSK9 (S386A)
Whole Cell
Cell Surface
PCSK9 (μg/mL) 0 0.5 1 2.5 5 0 0.5 1 2.5 5
Lane 1 2 3 4 5 6 7 8 9 10
kDa
LDLR
PCSK9 *
Transferrin Receptor
Actin
250
150
75
50
100
75
37

FIGURE 3-3. **Catalytically inactive PCSK9 degrades the LDLR when added to HepG2 cells.** Cells were cultured with the indicated concentrations of: *A,* PCSK9; *B, trans*-PCSK9; or *C, trans*-PCSK9(S386A) for 4 h. Cell surface proteins were biotinylated and whole cell and cell surface extracts resolved by 8% SDS-PAGE. Immunoblot analysis was performed for LDLR using IgG-HL1 and FLAG-tagged PCSK9 using anti-FLAG M2. Transferrin receptor was detected as control for loading and non-specific protein degradation. Actin was detected as a control for loading and biotinylation of non-cell surface proteins. * indicate non-specific cross-reacting proteins.

The binding of the *trans*-PCSK9(D374Y-S386A) was first evaluated by ligand blotting (Figure 3-4*A*). The affinity of *trans*-PCSK9(D374Y-S386A) for the LDLR was similar to that of the D374Y protein, both of which had an apparent higher affinity for the LDLR than the wild-type PCSK9 protein. When added to the medium of HepG2 cells at one-tenth the concentration of wild-type PCSK9, the *trans*-PCSK9(D374Y-S386A) and the PCSK9(D374Y) proteins were able to degrade the LDLRs on the cell surface (*lanes 6-10*, Figure 3-4*C* and *D*). These data further support the conclusion that the binding of PCSK9 to the LDLR facilitates the degradation of the LDLR through a mechanism that does not require proteolytic activity of PCSK9.

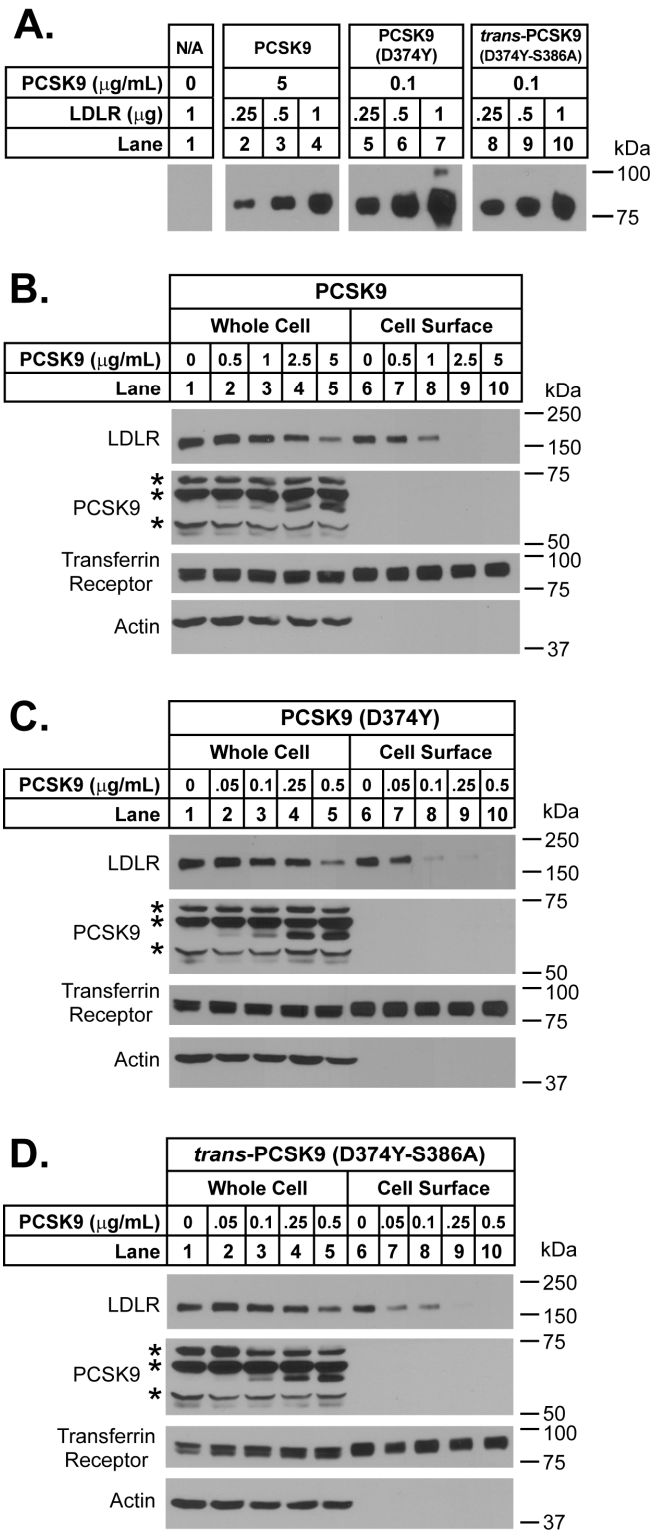
A.
N/A
PCSK9
PCSK9 (D374Y)
trans-PCSK9 (D374Y-S386A)
PCSK9 (μg/mL) 0 5 0.1 0.1
LDLR (μg) 1 .25 .5 1 .25 .5 1 .25 .5 1
Lane 1 2 3 4 5 6 7 8 9 10
kDa
100
75
B.
PCSK9
Whole Cell
Cell Surface
PCSK9 (μg/mL) 0 0.5 1 2.5 5 0 0.5 1 2.5 5
Lane 1 2 3 4 5 6 7 8 9 10
kDa
LDLR
250
150
PCSK9
75
50
Transferrin Receptor
100
75
Actin
37
C.
PCSK9 (D374Y)
Whole Cell
Cell Surface
PCSK9 (μg/mL) 0 .05 0.1 .25 0.5 0 .05 0.1 .25 0.5
Lane 1 2 3 4 5 6 7 8 9 10
kDa
LDLR
250
150
PCSK9
75
50
Transferrin Receptor
100
75
Actin
37
D.
trans-PCSK9 (D374Y-S386A)
Whole Cell
Cell Surface
PCSK9 (μg/mL) 0 .05 0.1 .25 0.5 0 .05 0.1 .25 0.5
Lane 1 2 3 4 5 6 7 8 9 10
kDa
LDLR
250
150
PCSK9
75
50
Transferrin Receptor
100
75
Actin
37

FIGURE 3-4. **The D374Y gain-of-function mutation increases the ability of catalytically inactive *trans*-PCSK9 to bind and degrade LDLRs.** *A,* Ligand blotting of the extracellular domain of LDLR with 5 μg/mL of PCSK9 or 0.1 μg/mL of PCSK9(D374Y) or *trans*-PCSK9(D374Y-S386A) was performed as described in the legend of Figure 3-2*C,* HepG2 cells were treated with the indicated concentration of *B,* wild-type PCSK9, *C,* PCSK9(D374Y), or *D, trans*-PCSK9(D374Y-S386A) for 4 h, and LDLR, PCSK9, transferrin receptor, and actin protein levels were measured by immunoblot analysis as described in the legend of Figure 3-2. * indicate non-specific cross-reacting proteins.

Next, it was determined if an intact catalytic site was required for PCSK9-mediated degradation of hepatic LDLRs *in vivo*. Wild-type PCSK9 or *trans*-PCSK9(S386A) was infused into *Pcsk9*$^{-/-}$ mice at a rate of 32 μg/h and the effects on hepatic LDLRs were assessed by immunoblot analysis (Figure 3-5). Similar reductions in hepatic LDLRs were seen with the catalytically inactive and wild-type protein, confirming that catalytic activity is not required for PCSK9 to mediate the degradation of hepatic LDLRs *in vivo*.

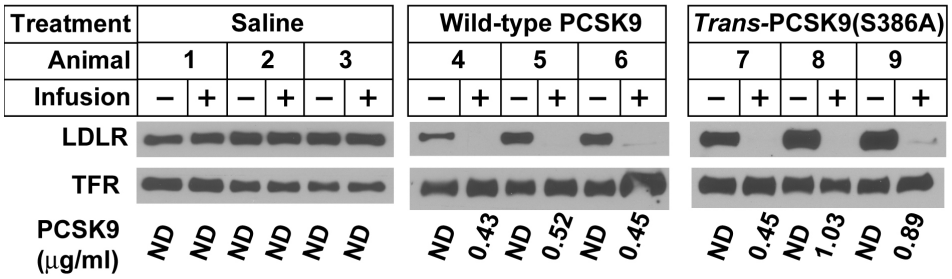

FIGURE 3-5. **Catalytically inactive PCSK9 reduces LDLR *in vivo.***
Hepatic LDLR protein levels in mice infused with catalytically inactive recombinant *trans*-PCSK9(S386A) protein. Male *Pcsk9*$^{-/-}$ mice were infused with saline, 32 μg/h of recombinant human wild-type-PCSK9, or 32 μg/h of *trans*-PCSK9(S386A) for 3 h. A liver sample was obtained before (-) and after infusion (+). Liver membrane proteins were isolated and 5 μg protein was subjected to 8% SDS-PAGE for immunoblot analysis. The TFR protein was used as a control for loading. Immunoblots show protein levels from individual mice before and after infusion. Plasma human PCSK9 concentrations were determined by ELISA from blood samples obtained at the end of the 3 h infusion (72).

DICUSSION

In the current report, it is demonstrated that the introduction of a mutation in PCSK9 that abolishes catalytic activity but does not interfere with the secretion of the protein fails to alter the mutant protein's ability to bind to the LDLR or to mediate the destruction of LDLRs when added to the medium of cultured HepG2 cells. These results support a model in which exogenous PCSK9 binds to the LDLR, which then either targets the LDLR to the lysosome for degradation or prevents the recycling of the receptor in a manner that is independent of inherent catalytic activity of the protein. These data indicate that unlike other PCs, PCSK9 is unique as a subtilisin-like serine protease in that the protein carries out a biological function that is independent of its proteolytic activity.

Studies have demonstrated that PCSK9 and the LDLR interact directly and that the association of PCSK9 with the cell surface and its subsequent internalization is dependent upon the presence of LDLRs (72, 94, 127). In addition, both proteins co-localize to a late endocytic/lysosomal compartment and internalization is required for PCSK9 to reduce LDLR protein levels since this activity is blocked in the absence of autosomal recessive hypercholesterolemia (ARH), an endocytic adaptor protein required in hepatocytes for LDLR internalization in clathrin-coated pits (72, 94, 127). Inasmuch as PCSK9 is a member of the proteinase K subfamily of subtilisin-related serine endoproteases, it seemed likely that PCSK9 cleaved the LDLR, which then facilitated degradation. A second possibility was that PCSK9 cleaved another as yet unidentified protein that ultimately mediated the destruction of LDLRs. The data of Figures 3-3, and 3-5 indicate that catalytic activity is not required for PCSK9 to mediate the destruction of

LDLRs when added exogenously to HepG2 cells or infused into mice. The data of Figure 3-4 further support the conclusion that binding of PCSK9 to the LDLR is sufficient to target LDLRs for degradation, since inactivating the catalytic site in the hyperactive protein PCSK9(D374Y) did not change the ~10-fold higher specific activity of the protein (72). These data also support the conclusion that the gain-of-function of PCSK9(D374Y) is a result of its increased affinity for the LDLR.

Previous studies have suggested that cleavage of PCSK9 is required for the protein to be secreted from cells (10). In the current study, it was found that if catalytically inactive mutants are highly overexpressed, a significant amount of unprocessed PCSK9 is secreted into the medium. The secreted full-length but catalytically inactive protein was purified and tested *in vitro* as described in Figure 3-2; however, the uncleaved PCSK9 protein did not bind to the LDLR nor did it reduce LDLRs in HepG2 cells (Figure 3-6). Thus, cleavage of the prodomain may be required for PCSK9 to adopt a conformation that mediates LDLR binding.

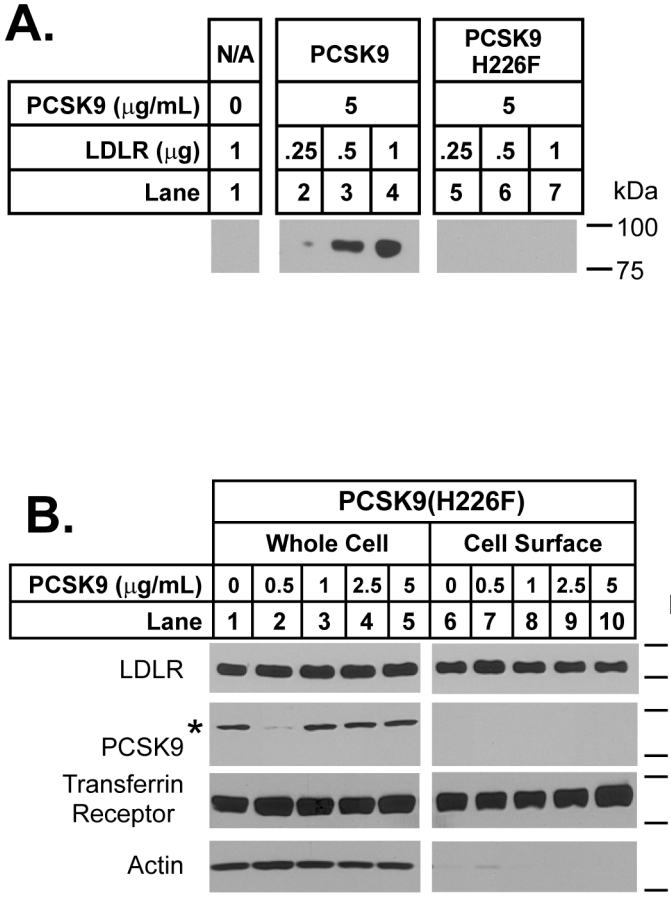

FIGURE 3-6. **Uncleaved, full-length PCSK9 does not bind or degrade LDLRs.** *A,* Ligand blotting of the extracellular domain of LDLR with 5 μg/mL of PCSK9 or PCSK9(H226F) was performed as described in the legend of Figure 3-2*C*. *B*, HepG2 cells were treated with the indicated concentration of PCSK9(H226F) for 4 h, and LDLR, PCSK9, transferrin receptor, and actin protein levels were measured by immunoblot analysis as described in the legend of Figure 3-2. * indicate non-specific cross-reacting proteins.

The data of Figure 3-2 demonstrate that the PCSK9 prodomain is capable of performing a chaperone function *in trans*, as evidenced by the ER exit and secretion of *trans*-PCSK9, and the uncompromised ability of the protein to bind to the LDLR. Previously, it has been shown that mature active furin can be formed in monkey kidney

BSC-40 cells by the co-expression of the furin prodomain and a furin fragment lacking the prodomain on separate plasmids (3). In the case of PCSK9, the ability of the prodomain to function *in trans* allowed for studies of the effect of catalytic function on LDLR degradation independent of effects on PCSK9 trafficking in the secretory pathway. The crystal structure of PCSK9 was recently solved at the 2.0-Å resolution (28). The prodomain failed to contain an apparent target loop that is found in the prodomains of other proprotein convertases and typically is the site of a second cleavage event that results in exposure and activation of the protease. The absence of a target loop in the prodomain of PCSK9 has been interpreted as evidence that catalytic activity may not be involved in the LDLR-lowering function of PCSK9 (28). The current studies provide direct experimental evidence that exogenously added PCSK9 reduces LDLRs in a manner that requires LDLR binding but not catalytic activity.

Studies by Maxwell and Breslow (76) showed that overexpression of PCSK9 in HepG2 cells induced the degradation of LDLRs intracellularly in a post-ER compartment, and Nassoury *et al*. (85) have suggested the two proteins interact in the ER and co-localize in the Golgi apparatus in hepatocytes. The results of the current studies do not preclude the possibility that PCSK9 can function intracellularly in a manner that requires catalytic activity.

Previously, Cohen *et al*. (24) reported that one out of every 50 African-Americans inherits a nonsense mutation in *PCSK9* that lowered LDL cholesterol levels by ~40%. In a 15-year prospective study, nonsense mutations in PCSK9 reduced LDL cholesterol levels by 28%, which was associated with a reduction in the frequency of coronary heart disease of 88% in African-Americans (25). In addition, individuals that

carry these cholesterol-lowering loss-of-function mutations in PCSK9 appear to have a normal life-span (25). Thus, genetic data from humans with loss-of-function mutations in *PCSK9* validate PCSK9 as a potential target for the treatment of hypercholesterolemia and suggest that inhibitors of the protease would be of therapeutic benefit. The lack of a requirement for PCSK9 catalytic activity in reducing LDLRs has important implications for the development of PCSK9 inhibitors. It has been previously shown that LDLR levels do not change when a catalytically dead enzyme that is not secreted is expressed in liver (90) or in cultured liver cells (76, 118). Thus, the current data now suggest that inhibitors of PCSK9's catalytic activity will have to function intracellularly in the ER to block PCSK9 secretion and, hence, its ability to reduce LDLR protein levels.

Materials and Methods

PCSK9 Activity Assays. HepG2 cells (ATCC, HB-8065) were incubated with PCSK9 and proteins prepared as described (72). Ligand blotting of purified human LDLR was performed as described (72), except all steps were performed in buffer containing 50 mM Tris-maleate at pH 6.0, 90 mM NaCl, 2 mM $CaCl_2$, 2.5% (w/v) milk, and the monoclonal anti-FLAG antibody M2 (2.5 μg/ml) was used in place of IgG-15A6.

Construction of Trans and Mutant PCSK9 Expression Vectors. All DNA manipulations were performed using standard molecular biology techniques (106). pCMV-PCSK9(AA1-152)-V5, a vector encoding the signal sequence and prodomain of PCSK9 (amino acids 1-152) and a C-terminal V5 epitope tag (GKPIPNPLLGLDST), was generated by PCR using the pCMV-PCSK9-FLAG vector (90) as a template and the following primers: forward primer 5'-GGAATTCGCCACCATGGGCACCG-3'; and

reverse primer 5'-CTTATCACGTAGAATCGAGACCGAGGAGAGGGTTAGGGATAGGCTTACCCTGGGCAAAGACAGAGGAGTCCTC-3'. The PCR fragment was cloned into pCR2.1-TOPO (Invitrogen) and the insert was then digested with *Hind*III and *Xba*I before ligation into pcDNA3.1/Hygro(+) (Invitrogen). A vector containing a deletion of the prodomain (amino acids 31-152) of PCSK9 (pCMV-PCSK9Δ31-152-FLAG) was generated through site-directed mutagenesis of the pCMV-PCSK9-FLAG vector using the oligonucleotide 5'-CCCGCGGGCGCCCGTGCGAGCATCCCGTGGAACCTG-3'. A S386A change was introduced into the pCMV-PCSK9Δ31-152-FLAG vector by site-directed mutagenesis using the primer 5'-ACAGAGTGGGACAGCCCAGGCTGCTGCCC-3'; the resulting plasmid was designated pCMV-PCSK9Δ31-152(S386A)-FLAG. Site-directed mutagenesis was then used to introduce a D374Y amino acid in pCMV-PCSK9Δ31-152(S386A)-FLAG to produce the plasmid (pCMV-PCSK9Δ31-152(D374Y-S386A)-FLAG) as described (72). Primer 5'-GCAAGTGTGACAGTTTTGGCACCCACCTGG-3' was used too introduce the H226F mutation into pCMV-PCSK9-FLAG to make (pCMV-PCSK9(H226F)-FLAG).

Tissue Culture Medium. Medium A contained Dulbecco's Modified Eagle Medium (DMEM) (Cellgro) supplemented with 100 units/ml penicillin, 100 μg/ml streptomycin sulfate and 1 g/L glucose. Medium B contained Medium A supplemented with 10% (v/v) fetal calf serum (FCS). Medium C contained Medium A supplemented with 1% Insulin-Transferrin-Selenium (ITS) (Cellgro). Medium D contained DMEM supplemented with 2.5% (v/v) newborn calf lipoprotein-deficient serum (NCLPDS), 100

units/ml penicillin, 100 μg/ml streptomycin sulfate, 10 μM sodium compactin, 50 μM sodium mevalonate, and 4.5 g/L glucose.

Transient Transfection of Human Embryonic Kidney (HEK) 293 Cells with PCSK9 Mutants. HEK 293 cells were plated at 5 x 10^5 cells/60-mm dish in Medium B on day 0. On day 3, plasmids were transfected using Lipofectamine 2000 transfection reagent (Invitrogen) per the manufacturer's instructions. For transfection of the full-length PCSK9 plasmid, 0.4 μg of DNA was co-transfected with 1.2 μg of empty vector DNA. For *trans*-PCSK9 experiments, 0.4 μg of pCMV-PCSK9Δ31-152-FLAG was co-transfected with 1.2 μg of pCMV-PCSK9 (AA1-152)-V5. On day 4, Medium B was replaced with Medium C. On day 5, cells and medium were harvested. Cells were washed 3 times in cold phosphate-buffered saline and lysed in buffer A (50 mM Tris-HCl, pH 7.4, 150 mM NaCl, 5 mM EDTA, 5 mM EGTA, 1% (v/v) NP-40, and 0.5% (w/v) sodium deoxycholate) with protease inhibitors (1 mM dithiothreitol, 1 mM PMSF, 0.5 mM Pefabloc, 10 μg/ml leupeptin, 5 μg/ml pepstatin A, 25 μg/ml ALLN, and 10 μg/ml aprotinin). Samples were subjected to SDS-PAGE and immunoblot analysis as described (90).

Stable Transfection and Purification of Epitope-tagged PCSK9 Mutants. For stable lines expressing *trans*-PCSK9, HEK 293S cells were cultured in Medium B in 100-mm dishes and transfected with 0.5 μg of pCMV-PCSK9(AA1-152)-V5 using Lipofectamine 2000 transfection reagent (Invitrogen). Colonies surviving hygromycin selection were isolated and expression of PCSK9 prodomain was verified by immunoblot analysis using an anti-V5 antibody (see below). The colony with highest prodomain

expression was transfected with 0.5 μg of pCMV-PCSK9Δ31-152-FLAG, pCMV-PCSK9Δ31-152(S386A)-FLAG or pCMV-PCSK9Δ31-152(D374Y-S386A)-FLAG as above. Colonies surviving neomycin/hygromycin selection were assessed for PCSK9 secretion by immunoblot analysis of the medium with anti-FLAG M2 antibody. FLAG-tagged human PCSK9, PCSK9(D374), PCSK9(H226F), *trans*-PCSK9, *trans*-PCSK9(S386A), and *trans*-PCSK9(D374Y-S386A) were purified from stably expressing HEK 293S cells as described (72).

Antibodies and Immunoblot Analysis. Monoclonal antibody 3C12 (IgG subclass 1) resulted from immunization with full-length human PCSK9 (130). Monoclonal antibody 1A1 (IgG subclass 2a) resulted from immunization with recombinant human PCSK9 prodomain purified from *E. coli*. Both antibodies recognize epitopes in the prodomain of PCSK9. Mouse monoclonal antibodies were generated against purified recombinant human PCSK9 proteins as described (130). Additional monoclonal antibodies used include: anti-PCSK9 IgG-15A6 (72); anti-human LDLR IgG-HL1 (121); anti-human transferrin receptor (Zymed Laboratories); anti-V5 (Invitrogen); anti-FLAG M2 (Sigma-Aldrich); anti-Actin AC40 (Sigma-Aldrich). The secondary antibody used for immunoblot analysis was horseradish peroxidase-conjugated donkey anti-mouse IgG (Jackson ImmunoResearch Laboratories) with detection using SuperSignal West Pico Chemiluminescent Substrate System (Pierce).

Animals. Experiments were performed in *Pcsk9*$^{-/-}$ (97) mice on a mixed C57BL/6J;129S6/SvEv background. All studies were approved by the Institutional Animal Care and Research Advisory Committee at the University of Texas Southwestern Medical Center.

PCSK9 continuous infusion. Dr. Aldo Grefhorst performed all infusion studies. Male wild-type and *Pcsk9*$^{-/-}$ mice were anaesthetized with sodium pentobarbital, and a small lobe of the liver was removed through an abdominal incision. The tissue was snap frozen in liquid nitrogen, and the wound closed with a suture. A blood sample was obtained immediately prior to initiating a continuous infusion of PCSK9 in a saline solution for 1, 2, 3, or 6 h via the jugular vein under anesthesia. Blood samples were collected during infusion at the indicated time points via the tail vein and the concentration of human PCSK9 was determined by ELISA (72). Animals were killed by cardiac puncture prior to harvesting the liver and the adrenals.

Immunoblot analysis of liver membranes. Liver membranes were prepared (35) and the protein concentrations were determined using the BCA Protein Assay kit (Pierce). For immunoblot analyses, individual or pooled samples were mixed with loading buffer and heated for 5 min at 96 °C prior to being subjected to SDS-PAGE as described (90). Immunoblot analyses were performed with rabbit polyclonal LDLR antiserum (90) and a horseradish peroxidase-conjugated anti-rabbit IgG from donkey (Amersham Pharmacia Bioscience). The invariant control protein, transferrin receptor (TFR), was detected using monoclonal anti-TFR IgG raised in mice (Zymed, San Francisco, CA) and horseradish peroxidase-conjugated rabbit anti-mouse IgG as the secondary. Immuncomplexes were detected using the SuperSignal West Pico Chemiluminescent Substrate System (Pierce).

CHAPTER FOUR
Molecular Basis for LDLR Recognition by PCSK9 [f]

Summary

PCSK9 post-translationally regulates hepatic low-density lipoprotein receptors (LDLRs) by binding to LDLRs on the cell surface, leading to their degradation. The binding site of PCSK9 has been localized to the epidermal growth factor-like repeat A (EGF-A) domain of the LDLR. Here, the crystal structure of a complex between PCSK9 and the EGF-A domain of the LDLR is determined. The binding site for the LDLR EGF-A domain resides on the surface of PCSK9's subtilisin-like catalytic domain containing ASP374, a residue for which a gain-of-function mutation (ASP374TYR) increases the affinity of PCSK9 towards LDLR and increases plasma LDL-cholesterol (LDL-C) levels in humans. The binding surface on PCSK9 is distant from its catalytic site, and the EGF-A domain makes no contact with either the C-terminal domain or the prodomain. Point mutations in PCSK9 that altered key residues contributing to EGF-A binding (ARG194 and PHE379) greatly diminished binding to the LDLR's extracellular domain. The structure of PCSK9 in complex with the LDLR EGF-A domain defines potential therapeutic target sites for blocking agents that could interfere with this interaction *in vivo*, thereby increasing LDLR function and reducing plasma LDL-C levels.

[f] This chapter is adapted from (71). Used with permission.

Introduction

The overall domain structure of PCSK9 is similar to other PC family members. It includes a signal peptide, followed by a prodomain, a subtilisin-like catalytic domain and a variable C-terminal domain (51). The prodomain serves a dual role both as a chaperone for folding and as an inhibitor of catalytic activity (3, 4, 83). Autocatalysis between GLN152 and SER153 (VFAQ:SIP) separates the prodomain from the catalytic domain, but the prodomain remains bound, occluding the catalytic site (10, 72). For other PC family members, a second catalytic cleavage is required to release the prodomain, which unmasks the catalytic site resulting in an active protease (3). No site of secondary cleavage has been identified that activates PCSK9.

The crystal structure of apo-PCSK9 revealed a tightly bound prodomain that is predicted to render the active site inaccessible to exogenous substrates (28, 47, 91). The structure of the PCSK9 prodomain and catalytic domain is similar to that of other subtilisin-like serine proteases. The C-terminal domain of PCSK9 contains three six-stranded β-sheet subdomains arranged with quasi-three fold symmetry. This domain shares structural homology to the adipokine resistin, and has been speculated to mediate protein-protein interactions (28, 47, 91).

Recent studies have provided insights into the site and mode of PCSK9's action. Addition of recombinant PCSK9 to the medium of cultured hepatocytes results in a dramatic reduction in LDLR number. PCSK9 binds directly to the LDLR on the cell surface and PCSK9-stimulated degradation of the LDLR requires autosomal recessive hypercholesterolemia (ARH), an adaptor protein needed for internalization of LDLRs (72). The affinity of PCSK9 binding to the LDLR is enhanced at acidic pH, suggesting

that PCSK9 binds more avidly to LDLRs in the lysosomal/endosomal compartments (28, 36, 127). One gain-of-function mutant, ASP374TYR was ~10-fold more active than wild-type PCSK9 in mediating degradation of LDLRs owing to a ~5-30 fold increased affinity of PCSK9 for the LDLR (28, 36, 72). Although autocatalysis of PCSK9 is required for proper folding and secretion, catalytic activity was not required for PCSK9-mediated LDLR degradation when added to cultured cells as shown in Chapter 3.

The LDLR is a multidomain protein whose extracellular domain (ECD) consists of an N-terminal ligand binding domain (7 cysteine-rich repeats (R1-R7) that mediate binding to LDL and β-VLDL), followed by the epidermal growth factor (EGF)-precursor homology domain (a pair of EGF-like repeats (EGF-A and EGF-B) separated from a third EGF-like repeat (EGF-C) by a β-propeller domain), and an 'O-linked sugar' domain (100, 103). Following endocytosis of the receptor:ligand complex, bound lipoproteins are released in the acidic environment of the endosome and the LDLR recycles to the cell surface. Ligand release has been proposed to result from a pH-dependent conformational change in the LDLR-ECD due to an intramolecular interaction between ligand binding modules R4 and R5 with the β-propeller domain (101).

Zhang *et al.* (127) recently mapped the residues of the LDLR that are required for binding to PCSK9. PCSK9 binds in a calcium-dependent manner to the first EGF-like repeat (EGF-A) of the EGF-precursor homology domain of the LDLR. The integrity of the EGF-precursor homology domain is essential for normal LDLR turnover. Deletion of this region results in a failure of internalized LDLRs to release bound ligand and prevents recycling to the cell surface (30). Several natural mutations in the EGF-precursor homology domain of *LDLR* that hinder receptor recycling are present in patients with FH

(55, 120). The EGF-A domain itself forms several intramolecular interactions proposed to be important for LDLR stability. The EGF-A and EGF-B tandem pair form an extended rod-like conformation stabilized by calcium binding and interdomain hydrophobic packing interactions (70, 104). The interaction of EGF-A with ligand binding module R7 confers a rigid conformation on this region of the LDLR across a wide pH range (7). This rigidity has been proposed to facilitate the acid-dependent closed conformation of the LDLR (6).

To determine the residues of PCSK9 that interact with the LDLR, the crystal structure of PCSK9 in complex with the EGF-A domain of the LDLR was determined. The structure defines the mode of binding of PCSK9 to the EGF-A domain and demonstrates that LDLR binding does not require dissociation of the prodomain from PCSK9. This information may facilitate the development of therapeutic antibodies or peptides that could be used to disrupt the PCSK9:LDLR interaction and thus function as an inhibitor of PCSK9's action.

Results and Discussion

For structural studies, a recombinant PCSK9 protein lacking the N-terminal 21 amino acids of the prodomain region (Δ53-PCSK9) was used. Δ53-PCSK9 was processed normally when expressed in HEK 293S cells (data not shown). To test the relative binding affinity of Δ53-PCSK9 compared to full-length PCSK9, competition binding assays were performed at pH 7.4 using a fluorophore-labeled PCSK9 and purified LDLR-ECD. Unexpectedly, Δ53-PCSK9 displayed a >7-fold greater affinity for the LDLR-ECD compared to the full-length PCSK9 protein (EC_{50} of 27.8 nM for Δ53-PCSK9 *versus* 203

nM for wild-type PCSK9) (Table 4-1 and Figure 4-1*A*). The affinity of binding of both PCSK9 and Δ53-PCSK9 increased ~3-fold when the pH was lowered from 7.0 to 6.0 (Table 4-1 and Figure 4-1*B*).

The binding studies were repeated using a purified LDLR fragment consisting of the EGF-AB tandem pair that was found to be more stable in solution than the EGF-A domain alone. Compared to the ECD, EGF-AB was ~3-fold less efficient at competing for binding of fluorophore-labeled LDLR-ECD to PCSK9 (EC_{50} of 119 nM for EGF-AB *versus* 35.3 nM for LDLR-ECD). As previously reported for the LDLR-ECD, Δ53-PCSK9 had a ~3-4-fold higher affinity for the EGF-AB at pH 6.0 compared to pH 7.0 (Table 4-1 and Figure 4-1*C* and 4-1*D*).

TABLE 4-1. ***In vitro*** **binding**

PCSK9 protein	Competition of DyLight800-PCSK9 binding to LDLR at pH 7.4 (EC_{50})	Fold increase in binding to LDLR pH 7.0 → pH 6.0
Wild-type	202.6 nM	3.3
Δ53-PCSK9	27.8 nM	3.1
LDLR protein	Competition of DyLight800-LDLR-ECD binding to PCSK9 at pH 7.4 (EC_{50})	Fold increase in binding to Δ53-PCSK9 pH 7.0 → pH 6.0
LDLR-ECD	35.3 nM	3.3
EGF-AB	119.2 nM	3.8

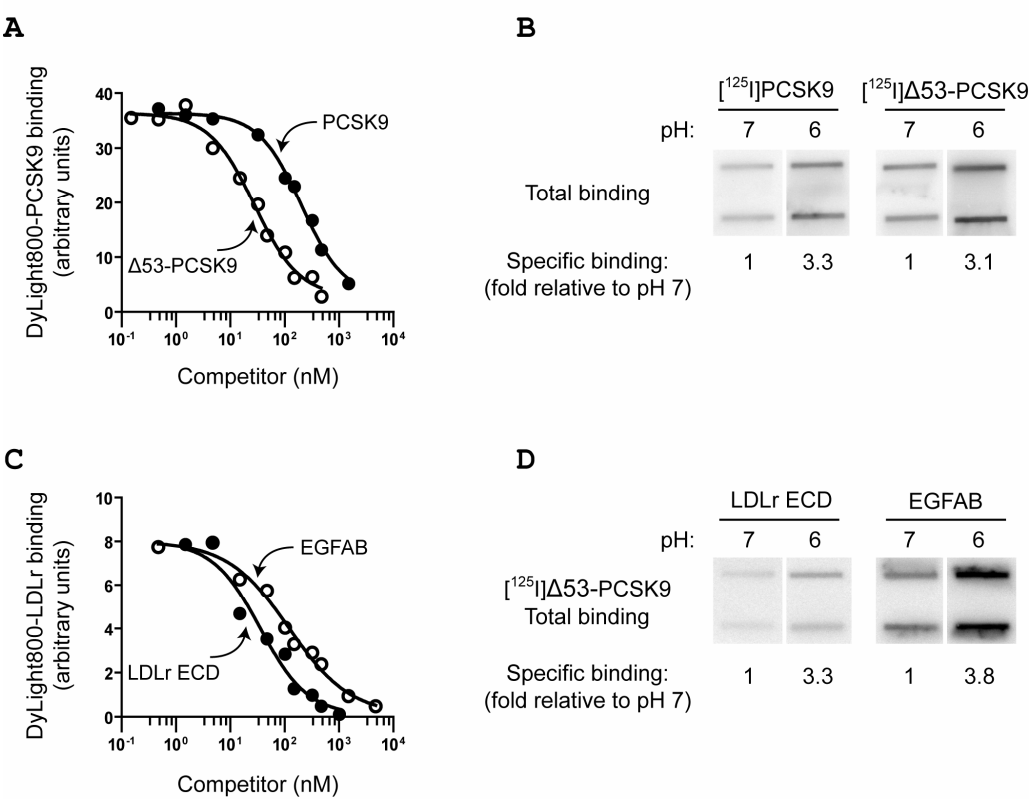

FIGURE 4-1. **Binding of wild-type and truncated PCSK9 to LDLR proteins.**
A, competition binding of wild-type PCSK9 and Δ53-PCSK9 to the LDLR. LDLR-ECD was prebound to slot-blotted anti-LDLR mAb (IgG-C7). Blots were incubated for 90 min with 0.1 μg/ml DyLight800-labeled PCSK9 at pH 7.4 in the presence of increasing concentrations of unlabeled wild-type PCSK9 (closed circles) or Δ53-PCSK9 (open circles) and bound fluorophore-labeled PCSK9 was detected and quantified. B, pH dependence of LDLR binding by wild-type and truncated PCSK9. Slot-blotted LDLR-ECD (2 μg) was incubated with 1 μg/ml [^{125}I]-labeled wild-type PCSK9 or Δ53-PCSK9 for 90 min at the indicated pH. Dried blots were exposed to a PhosphorImager plate and the resulting signals were quantified using a Molecular Dynamics Storm 820 system (GE Healthcare). Non-specific binding was determined in the presence of a 100-fold excess of unlabeled PCSK9 and was <10% of total binding values for all determinations. Specific binding values represent total binding minus non-specific binding and are expressed relative to binding at pH 7. C, competition binding of LDLR-ECD and EGF-AB to PCSK9. Wild type PCSK9 was prebound to slot-blotted anti-FLAG M2 mAb as described in Experimental Procedures. Blots were incubated for 90 min with 0.1 μg/ml DyLight800-labeled LDLR-ECD at pH 7.4 in the presence of increasing concentrations of unlabeled LDLR-ECD (closed circles) or EGF-AB (open circles) and bound fluorophore-labeled LDLR was detected and quantified. D, pH dependence of LDLR-ECD and EGF-AB binding to truncated PCSK9. Slot-blotted LDLR-ECD (2 μg) or EGF-

AB (4 μg) was incubated with 1 μg/ml [^{125}I]-labeled Δ53-PCSK9 for 90 min at the indicated pH. Bound radiolabeled Δ53-PCSK9 was quantified and relative binding values at different pH were determined as described above.

Structure of the complex

Crystals of Δ53-PCSK9 in complex with the EGF-AB pair of the LDLR were grown at pH 4.8 and the structure was refined to 2.4Å (Table 4-2). Electron density for the EGF-B domain was poor and EGF-B was not included in the final model. Electron density is visible for the entire EGF-A domain of the LDLR (residues 293-331) and for a calcium ion within the EGF-A domain. In the structure of the PCSK9:EGF-A complex (Figure 4-2*A*), PCSK9 adopts a fold that is identical to apo-PCSK9, except for a sub domain within the C-terminal variable domain (residues 532-601) that is visible in the apo-PCSK9 structures (28, 47, 91) but is disordered in the PCSK9:EGF-A complex (Figure 4-2*B*). Aside from this domain, the structures of apo-PCSK9 and PCSK9 bound to EGF-A are virtually identical, with a root-mean-square deviation of 1.5Å across Cα atoms. The first ordered residue of the prodomain is THR61, similar to the apo-PCSK9 structures (28, 47, 91). The lack of an ordered N-terminus in the prodomain of the PCSK9:EGF-A complex and the increased affinity of Δ53-PCSK9 for the LDLR-ECD (Table 4-1) suggest that residues 31-60 do not play a direct role in binding to LDLR.

TABLE 4-2. **Data Collection and Refinement Statistics**

Space group	P4(1)2(1)2
a,b (Å)	116.952
c (Å)	134.878
Resolution (Å) (final shell)	40.0 – 2.41 (2.47-2.41)
Reflections	
Total	162854
Unique	36583
Completeness (%)	98.9 (90.0)
Rsym (%)	6.2
Rcryst (%)	20.3 (25.9)
Rfree(%)	24.0 (31.4)
RMSD	
Bond length (Å)	0.014
Bond angle (o)	1.483

EGF-A binds a surface of PCSK9 that is formed primarily by residues 367-381. This region is over 20Å from the catalytic site of PCSK9 and ~500Å^2 of solvent accessible surface are buried on each molecule (Figure 4-3*A*). The prodomain and the C-terminal domain of PCSK9 do not contact the EGF-A domain. PCSK9 primarily contacts the N-terminal region of EGF-A, making no contacts with the C-terminus of EGF-A. An anti-parallel beta sheet is formed between residues 377-379 of PCSK9 and 308-310 of EGF-A. In addition, key interactions with EGF-A are made by ARG194 and ASP238 of PCSK9 (Figure 4-3*B*). The N-terminus of the catalytic domain of PCSK9, residues 153-155, also contributes to the interface (Figure 4-3*C*). The interface between PCSK9 and EGF-A is primarily hydrophobic with a number of specific polar interactions surrounding

the interface. PHE379 is at the center of this hydrophobic surface and makes a number of contacts to EGF-A. Numerous salt bridges and hydrogen bonds formed between PCSK9 and EGF-A likely contribute to the specificity of PCSK9 binding to the EGF-A domain of LDLR over other EGF-like domains. Hydrogen bonds between PCSK9-ASP238 and EGF-A-ASN295, PCSK9-THR377 and EGF-A-ASN309, and a salt bridge between the N-terminal amine of PCSK9-SER153 to EGF-A-ASP299 contribute to this specificity. The corresponding residues in EGF-B (ASP335, ASP339, VAL348) or the EGF-A domain of the closely related very low-density lipoprotein receptor (VLDLR: ASN331, VAL335, LYS345) or apolipoprotein E receptor-2 (apoER2: ASN338, HIS342, THR352) cannot participate in all of these interactions (Figure 4-4). Mutation of ASN295 to ALA in the LDLR decreases binding to PCSK9, demonstrating the importance of this interaction (127). The repositioning of PCSK9-SER153 after autocatalysis (>25 Å removed from GLN152 (28, 47, 91)) is required for forming the observed salt bridge to EGF-A-ASP299, consistent with the inability of secreted, uncleaved PCSK9 to bind to the LDLR-ECD (Chapter 3). Nassoury *et al*. (85) reported that the uncleaved proform of PCSK9 binds to the LDLR in the endoplasmic reticulum when both proteins are overexpressed in cells. In this study uncleaved PCSK9 was also shown to bind to an LDLR chimera protein lacking the EGF-precursor homology domain. Therefore, PCSK9 may form weak contacts with other regions of the LDLR that are revealed by high expression levels. This could also explain a recent report of PCSK9 binding to the VLDLR and apoER2 (92).

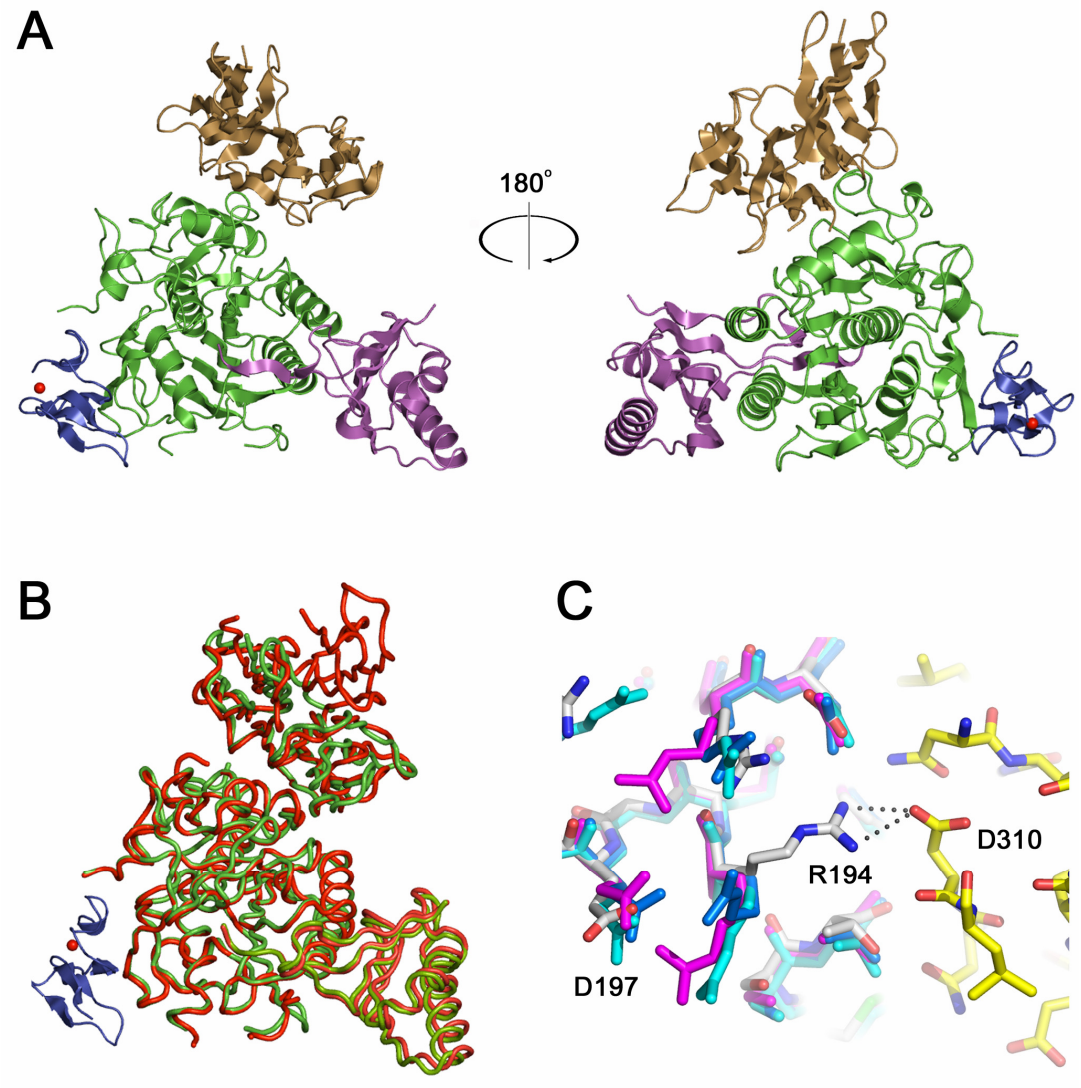

FIGURE 4-2. **The PCSK9:EGF-A complex.**
A, PCSK9, with the prodomain (magenta), the subtilisin-like catalytic domain (green), and the C-terminal domain (brown), and the EGF-A domain of LDLR (blue) are represented as a ribbon diagram. The bound calcium ion within the EGF-A domain is shown as a red sphere. B, superposition of the PCSK9:EGF-A complex and apo-PCSK9. The PCSK9:EGF-A complex is shown with PCSK9 in green, EGF-A in blue, and bound calcium as a red sphere. Apo-PCSK9 is shown in red. C, the apo-PCSK9 (2P4E, blue; 2PMW, cyan; 2QTW, magenta) structures superimposed onto the PCSK9:EGF-A complex (carbon, grey (PCSK9) or yellow (EGF-A); nitrogen, blue; oxygen, red). ARG194 from PCSK9 forms a salt bridge with ASP310 of EGF-A, breaking an intramolecular salt bridge with ASP197.

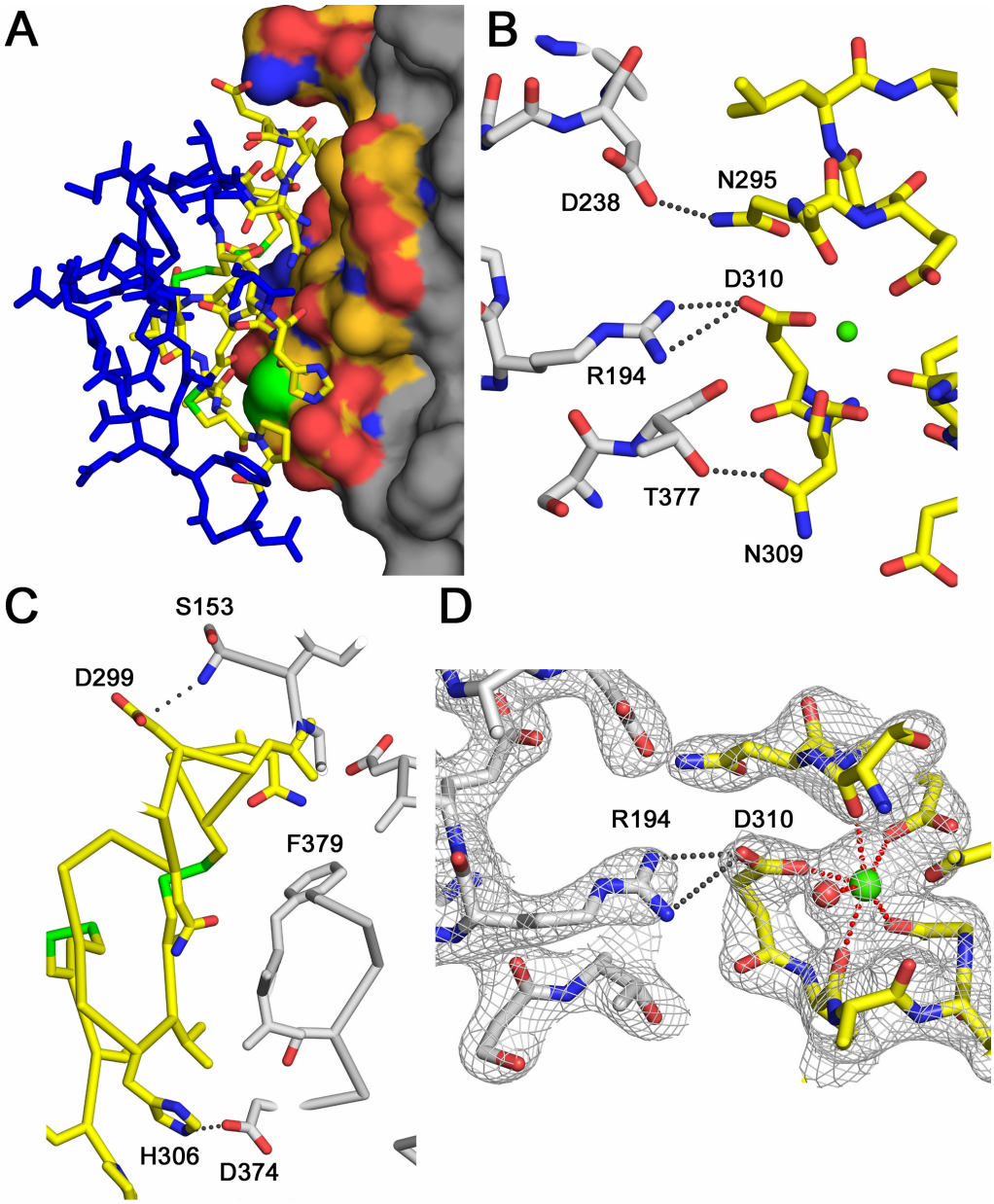

FIGURE 4-3. **Interface between PCSK9 and EGF-A.**
A, the surface of PCSK9 buried upon binding of EGF-A. The surface of PCSK9 buried upon binding to EGF-A is colored according to element type: carbon, orange; nitrogen, blue; oxygen, red; sulfur, green. Areas of PCSK9 not involved in binding are colored grey. EGF-A is represented as a stick model. Residues within EGF-A involved in binding

are colored according to element type: carbon, yellow; nitrogen, blue; oxygen, red. Residues not involved in binding are colored blue. B, interactions between PCSK9 (grey) and EGF-A (yellow) near the calcium (green sphere) binding site of EGF-A. C, autocatalysis of PCSK9 is required for binding to EGF-A. Autocatalysis of PCSK9 (grey) between residues 152-153 results in a free N-terminal amine that interacts with EGF-A (yellow). The site of the gain-of-function mutation, ASP374, on PCSK9 is positioned to interact with HIS306 of EGF-A. D, calcium coordination within the EGF-A domain after binding to PCSK9. The *sigmaA* weighted, 2Fo-Fc electron density map contoured at 1σ shows the calcium ligands arranged as a pentagonal bipyramid. ASP310 coordinates calcium (green sphere) and forms a salt bridge with ARG194 of PCSK9. A water molecule (red sphere) acts as an additional ligand.

```
                 O *       *O O

EGF-A LDLR     GTNECLDNNGGCSHVCNDLKIGYECLCPDGFQL VAQRRCE
EGF-A vLDLR    HINECLVNNGGCSHICKDLVIGYECDCAAGFEL IDRKTCG
EGF-A apoER2   GLNECLHNNGGCSHICTDLKIGFECTCPAGFQL LDQKTCG
EGF-B LDLR     DIDECQD PDTCSQLCVNLEGGYKCQCEEGFQLDPHTKACK
EGF-B vLDLR    DIDECQN PGICSQICINLKGGYKCECSRGYQMDLATGVCK
EGF-B apoER2   DIDECKD PDACSQICVNYKGYFKCECYPGYEMDLLTKNCK
```

FIGURE 4-4. **Sequence alignment of EGF-A and EGF-B domains of LDLR, vLDLR, and apoER2.** Calcium coordinating residues of the EGF-A domain of LDLR are indicated by ∗ (side chain oxygen ligand) or **O** (main chain carbonyl oxygen ligand). Hydrogen bond acceptors or acidic residues involved in binding to PCSK9 are shaded red and Hydrogen bond donors or basic residues are shaded blue. Residues involved in hydrophobic contacts with PCSK9 are shaded grey. THR352 (colored red) of apoER2 is at an unfavorable distance to hydrogen bond with PCSK9.

A comparison of the EGF-A binding surface in apo-PCSK9 to the PCSK9:EGF-A complex shows that ARG194 is the only residue of PCSK9 that makes a significant conformational change upon binding to EGF-A (Figure 4-2*C*). In apo-PCSK9, ARG194 forms an intramolecular salt bridge with ASP197. In the structure of the complex, ARG194 is bent away from ASP197 and forms a salt bridge with EGF-A-ASP310, a calcium coordinating residue in the EGF-A domain (7, 70, 101, 104). Mutations of ASP310 of EGF-A to GLU severely decrease binding of LDLR to PCSK9, demonstrating the specificity of this interaction (127). The equivalent aspartate residue (ASP64) from an EGF-like domain of factor IX uses both of its side chain oxygens to coordinate calcium (96); however, in the structure of the PCSK9:EGF-A complex, ASP310 coordinates calcium through only one of its side chain oxygen atoms, while the other is involved in the salt bridge with ARG194 of PCSK9 (Figure 4-3*D* and 4-5). The calcium coordination seen in PCSK9-bound EGF-A is similar to the coordination geometry seen in the EGF-like domain of C1s where an ASN residue replaces ASP310 and contributes only one ligand (46) (Figure 4-5). The other calcium ligands in EGF-A include: a side chain oxygen from GLU296; the carbonyl oxygens of THR294, LEU311, and GLY314; and a water molecule arranged as a pentagonal bipyramid. The carbonyl oxygen of CYS292 (MET in the crystal) is 2.9Å from the calcium and is positioned to act as a 7th ligand. Removal of calcium coordinating residues within the EGF-A domain has been shown to impair LDL release and uncouple the fixed orientation between ligand binding module R7 and EGF-A (7). The observed calcium coordination in the PCSK9:EGF-A complex could signify a conformational change in the EGF-A domain upon PCSK9 binding.

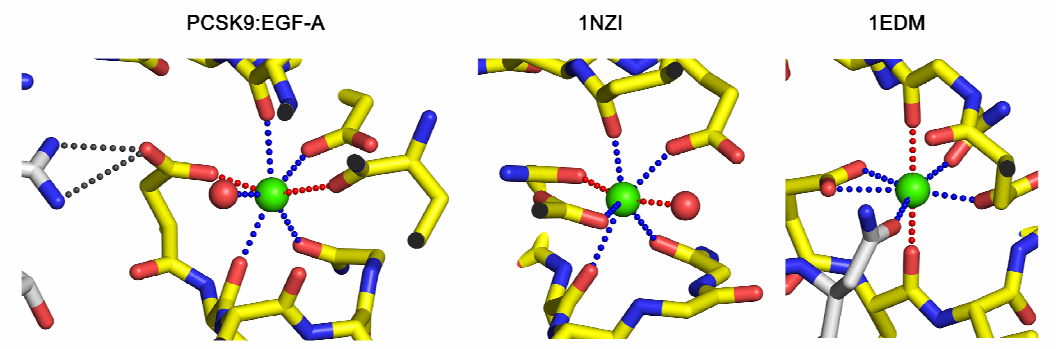

FIGURE 4-5. **Comparison of the Calcium coordination geometry of PCSK9:EGF-A to other EGF-like domains.**
The Calcium coordination within the PCSK9:EGF-A complex, the C1s EGF-like domain (1NZI), and the factor IX EGF-like domain (1EDM) are shown. Calcium is shown as a green sphere and water molecules are shown as red spheres. The equatorial ligands are indicated by blue dots and the axial ligands are indicated by red dots.

Mutagenesis of PCSK9

The crystal structure of the PCSK9:EGF-A complex identified ARG194 and PHE379 of PCSK9 as critical residues for EGF-A binding, with ARG194 forming a salt bridge with EGF-A-ASP310 and PHE379 making several contacts, through both its main chain and side chain, to EGF-A (Figure 4-3) To confirm that these residues are critical for PCSK9 binding to full-length LDLR, purified proteins were prepared harboring amino acid changes in these key residues (ARG194GLN or PHE379ALA) and the mutant proteins were tested for their ability to bind to the LDLR-ECD. Neither mutation affected PCSK9 auto-catalysis or secretion rate (Figure 4-6*A*). As with wild-type PCSK9, the catalytic fragment of the mutant proteins co-purified with bound prodomain as revealed by SDS-PAGE and Coomassie staining of the purified mutant proteins (Figure 4-6*B*).

Ligand blotting was performed to assess the ability of immobilized mutant PCSK9 proteins to associate with fluorophore-labeled LDLR-ECD. To ensure equivalent

amounts of PCSK9 were present in each lane, blots were co-incubated with a fluorophore-labeled anti-PCSK9 mAb that does not interfere with LDLR binding (data not shown). The gain-of-function mutant PCSK9(ASP374TYR) bound LDLR-ECD with greater affinity than wild-type PCSK9 (Figure 4-6*C*), in agreement with previous reports (28, 36, 72). Mutation of either ARG194 or PHE379 decreased PCSK9 binding to LDLR-ECD by >90%. Thus, ARG194 and PHE379 in the catalytic domain of PCSK9 represent critical surface residues for the binding of PCSK9 to the LDLR.

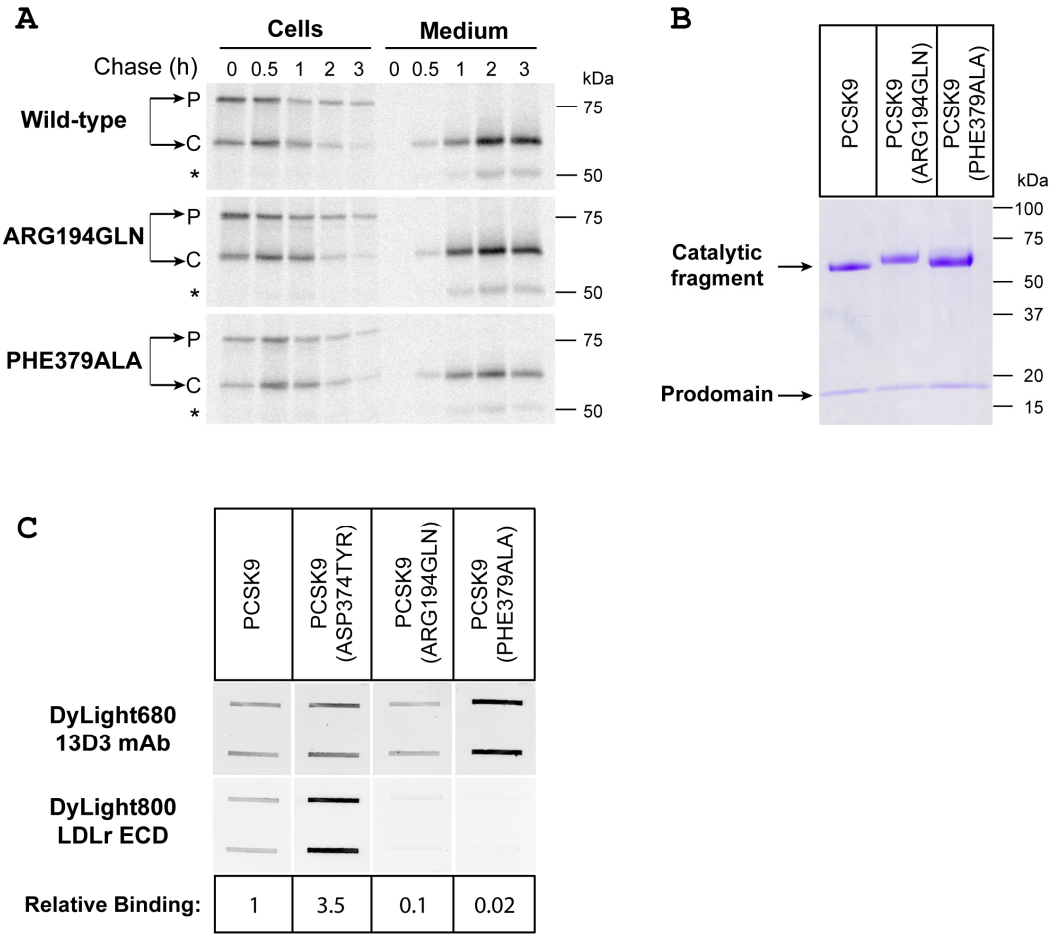

FIGURE 4-6. **ARG194GLN and PHE379ALA mutations in EGF-A binding region of PCSK9 diminish binding to the LDLR-ECD.**
A, mutations in PCSK9 do not affect auto-catalysis and secretion rates. HEK 293 cells were transiently transfected with PCSK9 expression constructs 24 hours prior to labeling for 30 minutes with [^{35}S]methionine/cysteine. After washing, cells were incubated in chase medium for the indicated times. Cells were lysed and PCSK9 was immunoprecipitated from cells lysates and medium. Samples were subjected to 8% SDS-PAGE and the gel was dried, exposed to a PhosphorImager plate and scanned. P and C denote proprotein and cleaved forms of PCSK9, respectively. The asterisk denotes a band consistent with a furin/PC5/6A-cleaved form of PCSK9 (11). B, Coomassie staining of purified PCSK9 proteins. Purified PCSK9 proteins were subjected to SDS-PAGE on 4-15% gradient gels followed by staining with Coomassie R-250 dye. C, binding of fluorophore-labeled LDLR-ECD to mutant PCSK9 proteins. Purified FLAG-tagged

PCSK9 proteins were prebound to blotted anti-FLAG M2 mAb followed by simultaneous incubation with DyLight800-labeled LDLR-ECD and DyLight680-labeled anti-PCSK9 (IgG-13D3). Bound fluorophore-labeled proteins were visualized by infrared scanning and quantified. Shown are duplicate blots and resulting quantification from a representative experiment performed three times with similar results. Binding values represent the ratio of bound LDLR to 13D3 mAb expressed relative to the ratio obtained for wild-type PCSK9 binding.

Natural mutations in PCSK9

The gain-of-function mutation ASP374TYR increases the affinity of PCSK9 for LDLR ~5-30 fold (28, 47, 72, 91). PCSK9-ASP374 is positioned 4Å from EGF-A-HIS306. In the crystal structure at pH 4.8, EGF-A-HIS306 is presumably protonated and forms a salt bridge with PCSK9-ASP374. A mutation of ASP374 to TYR would place the hydroxyl group of tyrosine ~3Å from EGF-A-HIS306, allowing for a favorable hydrogen bond (Figure 4-7*A*). Of note, the FH-associated mutation HIS306TYR would create the reciprocal change, suggesting that this mutation in LDLR would increase its affinity toward PCSK9 (Figure 4-7*B*), thereby causing enhanced degradation of the LDLR.

Other gain-of-function mutations, SER127ARG and PHE216LEU, display modest changes in affinity for the LDLR (28, 36) suggesting that the hypercholesterolemic phenotype associated with these mutations is not directly a result of an increase in affinity for LDLR. PCSK9 containing the SER127ARG mutation is internalized at approximately the same rate as wild type PCSK9 (36), but processing and secretion are less efficient for this mutant (10, 90). SER127 is located in the prodomain and is over 40Å from the EGF-A binding site. While it is possible that other domains of LDLR interact with PCSK9, these domains are not absolutely required for binding (127), making it unlikely that SER127 or neighboring residues contribute significantly to the

binding affinity of PCSK9 for the LDLR through other direct contacts. The distance of SER127 from the EGF-A binding surface suggests that the phenotype of this mutation is likely a result of another mode of PCSK9 regulation *in vivo*.

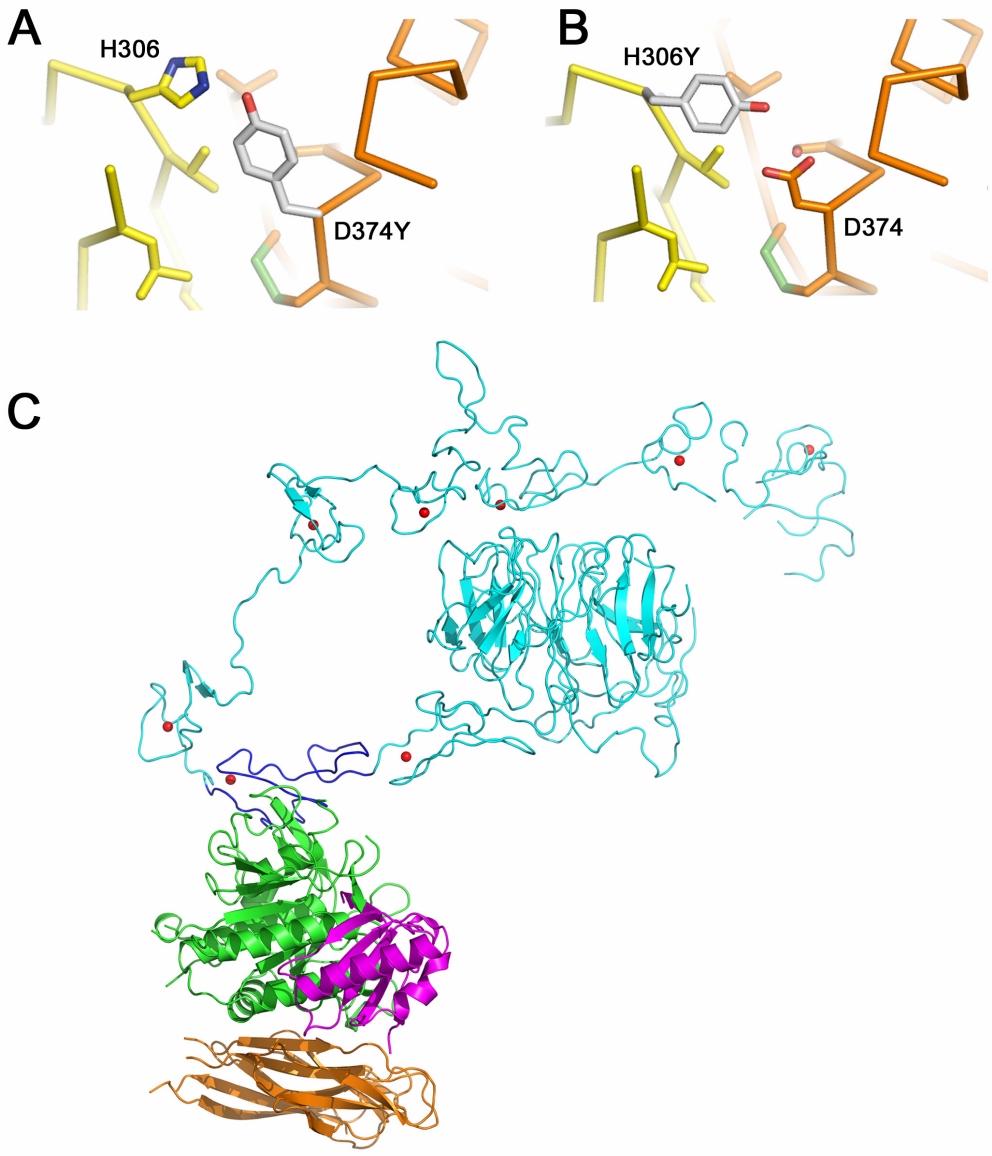

FIGURE 4-7. **Mutations in PCSK9 and LDLR.**
A, the gain-of-function mutation ASP347TYR in PCSK9 increases binding to LDLR. ASP347 in PCSK9 mutated to Tyrosine (grey) is in position to hydrogen bond to HIS306 of LDLR. B, the FH mutation HIS307TYR in LDLR. HIS306 in LDLR mutated to Tyrosine (grey) is in position to hydrogen bond to ASP347 of PCSK9. C, model for full-length LDLR-ECD bound to PCSK9. The EGF-A domain (blue) of the LDLR-ECD (cyan) at acidic pH and the PCKSK9:EGF-A complex were superimposed. PCSK9 (prodomain, magenta; subtilisin-like catalytic domain, green; C-terminal domain, brown) binds on the outside surface of LDLR and would not interfere with the interaction of ligand binding module R4 and R5 with the β-propeller domain.

PHE216 of PCSK9 is located within a disordered loop in the structure of the PCSK9:EGF-A complex and apo-PCSK9 (28, 47, 91). PCSK9 carrying the PHE216LEU gain-of-function mutation does not have increased affinity for LDLR (28) and PHE216 does not interact with the EGF-A domain in the structure of the PCSK9:EGF-A complex. The PHE216LEU mutation has been proposed to reduce a Furin/PC5/6A-dependent cleavage of PCSK9 after residue ARG218 (11). This cleavage event would remove two residues (SER153 and ARG194) that form key salt bridges in the PCSK9:EGF-A complex, presumably weakening or destroying the interaction. Indeed, alteration of ARG194 in PCSK9 by site-directed mutagenesis decreased binding to the LDLR-ECD by 90% (Figure 4-6*C*). Thus, the structure of the PCSK9:EGF-A complex provides a molecular basis for the FH phenotype associated with the PHE216LEU mutation.

Loss-of-function mutations in PCSK9 resulting in missense or nonsense mutations generally result in lowered levels of secreted PCSK9 (130). Among the loss-of-function mutations that are processed and secreted normally, ALA443THR is ~20Å from the EGF-A binding site and does not play a direct role in binding to EGF-A. It has been suggested that the ALA443THR mutation results in a higher susceptibility to Furin/PC5/6A-dependent cleavage (11) and may result in lower levels of functional PCSK9. PCSK9 carrying the ARG46LEU mutation has been shown to have a modest decrease in affinity toward the LDLR (36). ARG46 is not present in the current structure. Since THR61 and is ~55Å from EGF-A, it is unlikely that ARG46 could interact with EGF-A without a significant conformational change occurring in the prodomain. It should be noted that Δ53-PCSK9 binds with increased affinity to the LDLR-ECD at

physiological pH (Table 4-1), suggesting that the region of the prodomain containing ARG46 could affect binding of PCSK9 to the LDLR in an indirect manner.

pH dependence of binding

The LDLR is proposed to undergo a conformational change at acidic pH from an opened to a closed conformation, thereby facilitating ligand release (6, 101). A model of the low pH form of LDLR bound to PCSK9 was generated by superimposing the EGF-A domain from the LDLR-ECD structure (101) onto the corresponding residues in the PCSK9:EGF-A structure (Figure 4-7*C*). In the model, PCSK9 binds on the outside of the closed, low pH form of the LDLR and would not sterically interfere with the intramolecular interaction of ligand binding modules R4 and R5 to the β-propeller domain or with lipoprotein binding. However, an effect imposed by PCSK9 on either lipoprotein binding or adoption of the closed conformation by the LDLR cannot be excluded.

The crystal structure of the LDLR-ECD at pH 5.3 shows an alternative orientation of EGF-A relative to EGF-B from that observed in the isolated EGF-AB domain NMR structure obtained at pH 6.5 (70, 104). Given the lack of change in apo-PCSK9 domain organization and structure at pH values ranging from 4.6 to 10.5 (28, 47, 91) and in PCSK9 in complex with EGF-A, it is possible that the enhanced affinity of PCSK9 toward LDLR at acidic pH is due to a conformational change in the LDLR. Consistent with this model, *in vitro* binding studies comparing association and dissociation rates between PCSK9 and LDLR reveal that the major difference at neutral versus acidic pH is a change in the association rate. At low pH, the association rate

increases ~100 fold, while the dissociation rate is virtually unchanged (36). The current binding studies indicate that at acidic pH, PCSK9 has increased affinity towards the EGF-AB fragment used in the structural studies. The *in vitro* binding studies with the EGF-AB fragment and the crystal structure of the PCSK9:EGF-A complex suggest that the pH-dependent increase in affinity resides, at least partially, within the EGF-AB fragment.. It has been suggested that a region rich in histidine residues on the surface of the C-terminal domain of PCSK9 might be responsible for the pH-dependent increase in affinity toward LDLR (28, 47, 91). This region of the C-terminal domain is disordered in our structure; therefore, it can not be ruled out that there is a contribution of the C-terminal domain of PCSK9 to the pH-dependent changes in binding affinity, either through interacting with domains other than EGF-A or by influencing the conformation of PCSK9. In the PCSK9:EGF-A structure, only a single histidine contributes to the binding interface, HIS306 of EGF-A. These structural and biochemical data are consistent with a model where LDLR, through a low pH induced conformational change and/or protonation of HIS306, is responsible for the pH dependent increase in affinity toward PCSK9.

PCSK9-dependent LDLR degradation

The cellular mechanism by which PCSK9 increases LDLR degradation remains unresolved. The structure of the PCSK9:EGF-A complex is consistent with a model where enhanced affinity of PCSK9 for the low pH conformation of the LDLR prevents receptor recycling. PCSK9 binding to the LDLR may alter the conformation of the low pH form of the LDLR. For instance, binding of PCSK9 near the N-terminal region of EGF-A might affect known interdomain interactions involving the EGF-A domain, either

through steric hindrance by the PCSK9 molecule itself or by affecting the EGF-A conformation, calcium coordination, and/or stability. Known intramolecular EGF-A interactions include the interdomain packing of EGF-A with EGF-B, which is important for LDLR stability (104), and the interaction of EGF-A with ligand binding module R7, which confers a rigid conformation on this region of the LDLR across a wide pH range (7). This rigidity is proposed to facilitate the acid-dependent closed conformation that allows ligand release and LDLR recycling from the endosomal compartment (6). Alternatively, PCSK9 may bind to an as yet unknown factor that directly promotes degradation of LDLR.

Conclusions

PCSK9 has emerged as one of the most important determinants of plasma LDL-C levels as illustrated by a recent report that described a compound heterozygote with two inactivating mutations in *PCSK9* (130). This healthy individual had no circulating PCSK9 and a strikingly low plasma LDL-C concentration of 14 mg/dl. The effects of heterozygous loss-of-function mutations in *PCSK9* (TYR142X and CYS679X in African-Americans, and ARG46LEU in Caucasians) on CHD have been reported in a large biracial 15-year prospective study (25). The TYR142X and CYS679X nonsense mutations in *PCSK9* reduced LDL-C levels by 28% and decreased the frequency of CHD by 88%. Caucasians with an ARG46LEU allele had a mean reduction in LDL-C levels of 15% and manifest a 47% reduction in CHD (25). Thus, PCSK9 represents a new and validated therapeutic target for the treatment of hypercholesterolemia; however the demonstration that catalytic activity is required for PCSK9 maturation and secretion but

not for degradation of LDLRs suggests that small molecule inhibitors of PCSK9 will need to function in the endoplasmic reticulum (Chapter 3). The elucidation of the structure of the PCSK9:EGF-A complex now provides the structural foundation for the development of alternative approaches to inhibit PCSK9-mediated LDLR degradation. If PCSK9 functions primarily as a secreted protein in plasma, agents that interfere with the PCSK9:LDLR interaction at the cell surface also have the potential to lower plasma LDL-C levels in individuals with hypercholesterolemia.

Materials and Methods

Expression constructs for truncated and mutant forms of PCSK9. A full-length human PCSK9 cDNA followed by a FLAG-epitope tag (DYKDDDDK) under control of the cytomegalovirus promoter-enhancer (pCMV-PCSK9-FLAG) was used for generation of truncated (Δ53-PCSK9) and mutant forms of PCSK9 (90). Δ53-PCSK9, ARG194GLN and PHE379ALA mutant forms of PCSK9 were generated using the QuikChangeTM site-directed mutagenesis kit (Stratagene) according to manufacturer's instructions.

Purification of recombinant proteins. Δ53-PCSK9 was stably expressed in HEK-293S cells (98). PCSK9(ARG194GLN) and PCSK9(PHE379ALA) were expressed in HEK-293 cells following transient transfection using FuGene 6 transfection reagent (Roche) according to manufacturer's instructions. FLAG-tagged proteins were purified from conditioned medium as previously described (72). The EGF-AB fragment (residues 293-372) was expressed as a GST fusion in Rosetta-gamiB cells (Novagen) and purified by glutathione chromatography. The GST tag was removed by TEV protease cleavage and the EGF-AB fragment was further purified by ion exchange and size exclusion

chromatography. Reverse phase chromatography and mass spectrometry were used to monitor proper folding and disulfide bond formation. The LDLR-ECD was expressed and purified as previously described (101).

Crystallization and structure determination. Dr. Hyock Kwon performed the crystallization and structure determination studies. The complex of Δ53-PCSK9 and EGF-AB was formed by adding a 4-fold molar excess of EGF-AB to Δ53-PCSK9 and further purified by size exclusion chromatography. Initial crystals were obtained using the Fluidigm TOPAZ system. Crystals of PCSK9:EGF-A were formed by mixing equal volumes of the complex (6 mg/ml in 10 mM Tris pH 7.5, 50 mM NaCl, 0.25 mM $CaCl_2$, 0.01% NaN3) with 0.3 M $(NH_4)H_2PO_4$ and equilibrating the mixture under Al's oil (Hampton Research) against H_2O. Crystals were transferred stepwise into a solution of 0.05 M $(NH_4)H_2PO_4$, 5 mM $CaCl_2$, and 35% glycerol and flash frozen in a -160^oC nitrogen stream. Crystals belong to space group P4(1)2(1)2 (a=b=117.0Å, c=134.9Å). Diffraction data were collected at the Advanced Photon Source, beam line 19-ID. And were processed with HKL2000 (87) and the CCP4 suite (26). The structure was determined by molecular replacement using the program PHASER (116). The search model included residues 61-449 of PCSK9 (PDB ID:2P4E). The model was built with the program COOT (34). Initial refinement was performed with CNS (18) and the final cycles of refinement were performed with REFMAC (82). Figures were generated with PYMOL (W. L. Delano, www.pymol.org).

Pulse-chase analysis. HEK 293A cells (Q-Biogene) were plated on day 0 at 2.0 x 10^5 cells in 60-mm dishes and cultured in DMEM (Cellgro) supplemented with 10% (v/v) fetal calf serum (FCS), 100 units/ml penicillin, 100 μg g/ml streptomycin sulfate and 1

g/L glucose (Medium A). Dishes were transfected on day 2 with PCSK9 cDNA expression plasmids (1 μg) using FuGene 6 transfection reagent (Roche) as per manufacturer's instructions. On day 3, cells were incubated for 60 min in L-methionine- and L-cysteine-free Medium A (Medium B), prior to pulse-labeling for 30 min with 150 μCi/ml Redivue PRO-MIX [^{35}S] Cell Labeling Mix (GE Healthcare) in Medium B. Cells were then washed twice with PBS and incubated for various times in 1.5 ml chase medium consisting of Medium A containing 10 mM and 3 mM amounts of unlabeled L-methionine and L-cysteine, respectively. Immunoprecipitation of cell and medium extracts was performed as described using a polyclonal anti-PCSK9 antibody (72).

In vitro binding measurements. The pH dependence of ^{125}I-labeled PCSK9 binding to LDLR-ECD or EGF-AB fragment was analyzed by ligand blotting as previously described (127). Other binding assays were performed using purified PCSK9 and LDLR-ECD proteins labeled through amine-linkage with DyLight800 fluorophore dye using the DyLight antibody labeling kit as per manufacturer's instructions (Pierce). Bound PCSK9 was detected using monoclonal antibody (mAb) IgG-13D3 (72) labeled with DyLight680 dye (Pierce). LDLR-ECD or EGF-AB was diluted in TBS-C (50 mM Tris pH 7.4, 90 mM NaCl, 2 mM $CaCl_2$) and blotted directly onto 0.22 μm pore size nitrocellulose membranes (GE Healthcare) using a BioDot SP slot-blot apparatus (BioRad) according to manufacturer's instructions. Purified PCSK9 proteins were radioiodinated as previously described (107) with the exception that the labeling reaction was carried out using IODO-GEN pre-coated iodination tubes (Pierce). Bound PCSK9 was detected using monoclonal antibody (mAb) IgG-13D3 (72), recognizing an epitope in the catalytic domain of PCSK9, labeled with DyLight680 dye (Pierce). For

immobilization of LDLR-ECD or PCSK9, mAbs IgG-C7 (3 μg) (8) or anti-FLAG M2 (5 μg) (Sigma-Aldrich), respectively, were slot-blotted onto nitrocellulose as described above. Blots were blocked for 30 min in Odyssey blocking buffer (LI-COR Biosciences). All incubations (90 min) and subsequent washes (3 x 15 min) were carried out at room temperature with gentle oscillation in TBS-C buffer containing 2.5% non-fat milk. Blots were initially incubated with LDLR-ECD to bind to IgG-C7 mAb or PCSK9 (5 μg/ml) to bind to anti-FLAG M2 mAb followed by incubation with fluorophore-labeled proteins in the absence or presence of unlabeled competitor proteins. Blots were scanned using the Li-COR Odyssey infrared imaging system and band intensity was quantified using Odyssey v2.0 software (LI-COR Biosciences). For competition binding assays, the amount of competitor protein required for 50% inhibition of fluorophore-labeled protein binding (EC_{50}) was determined by fitting data to a sigmoidal dose response curve using nonlinear regression (GraphPad Software, Inc.).

Data deposition: Coordinates have been deposited in the protein data bank under accession code **3BPS**.

CHAPTER FIVE
Increased Binding of PCSK9 to a Mutant LDL Receptor: A Sixth Class of LDLR Mutations that Cause Familial Hypercholesterolemia

Summary

The secreted protease PCSK9 mediates degradation of the low-density lipoprotein receptor (LDLR) in liver via a non-catalytic mechanism requiring direct binding to the epidermal growth factor-like repeat A (EGF-A) domain of the LDLR. Here, it is shown that an *LDLR* mutation (H306Y) within the EGF-A domain that causes familial hypercholesterolemia (FH) results in increased LDLR binding and degradation by PCSK9. Crystallographic structural analysis showed that the H306Y mutation in the EGF-A domain mimics a low pH conformational change undergone in wild-type EGF-A-His306, resulting in an improved hydrogen bond with PCSK9-Asp-374. Recombinant LDLR sub-fragments harboring the H306Y mutation inhibited binding of PCSK9 to cell surface LDLRs and increased LDLR expression and function in HepG2 human hepatoma cells stably overexpressing wild-type PCSK9 or gain-of-function PCSK9 mutants associated with hypercholesterolemia (S127R or D374Y). These studies define a new class of *LDLR* mutation that cause FH, and support the concept that pharmacological inhibition of the PCSK9:LDLR interaction at the cell surface would increase liver LDLR number and lower plasma LDL levels.

Introduction

Circulating plasma levels of low-density lipoprotein cholesterol (LDL-C) are a primary risk factor for the development of coronary heart disease (CHD). Clearance of LDL from the plasma occurs mainly by the liver through the action of the LDL receptor (LDLR), a cell surface glycoprotein that binds to circulating LDL particles with high affinity and mediates their endocytic uptake (43). Autosomal dominant hypercholesterolemia (ADH) is associated with gene mutations that negatively affect plasma LDL clearance, mainly occurring in genes encoding the LDLR (ie, familial hypercholesterolemia (FH)) (56) or apolipoprotein B100 (apoB100; ie, familial defective apoB100) (62). Recently, mutations in a third gene, *PCSK9*, were discovered that caused ADH (1). Functional studies have shown that PCSK9 regulates circulating LDL-C levels through its ability to mediate LDLR degradation in liver (75, 90). Mutations in PCSK9 resulting in hypercholesterolemia have been classified as gain-of-function due to their mode of inheritance (1, 74, 119)}. Loss-of-function mutations in *PCSK9* have also been identified that result in lowered plasma LDL-C levels and significant protection from CHD without apparent adverse effects on other aspects of human physiology (24, 25, 130). Thus, PCSK9 represents a validated therapeutic target for the treatment of hypercholesterolemia.

PCSK9 is a member of the mammalian proprotein convertase (PC) family of subtilisin-like serine endoproteases. PCSK9 consists of a signal sequence, followed by a prodomain which serves as both a folding chaperone and an inhibitor of cognate enzymatic activity, a conserved catalytic domain, and a cysteine- and histidine-rich C-terminal domain of unknown function (47, 108). Autocatalytic processing of PCSK9 in

the endoplasmic reticulum (ER) results in release of the ~14 kDa prodomain, which remains associated with the ~60 kDa catalytic/C-terminal domains, occluding the catalytic site (28, 86, 91). PCSK9 is rapidly and efficiently secreted from liver-derived cells in culture, and is abundant in human plasma. Unlike other PCs, in which the prodomain is further proteolytically processed to activate the serine protease, the prodomain of secreted PCSK9 remains intact and tightly bound (10, 28, 72, 91).

PCSK9 mRNA is primarily expressed in liver, with low levels of expression in intestine, kidney, and brain (108). *PCSK9* and *LDLR* expression in liver is co-regulated by sterol regulatory element binding protein (SREBP)-2 (33, 60, 64), a transcription factor which displays increased activity when cellular cholesterol levels are depleted (59). Cell culture and animal studies support that LDL-C lowering statin drugs increase liver LDLR protein expression by increasing SREBP-2 activity. Therefore, it is widely anticipated that pharmacological inhibitors of PCSK9 would work synergistically with statins in further raising liver LDLR levels and decreasing plasma LDL-C. In support of this theory, plasma PCSK9 levels have been shown to be increased in humans undergoing statin therapy (20, 79) and *Pcsk9*$^{-/-}$ mice were hyper-responsive to statins (97).

Early over-expression studies demonstrated that PCSK9 promotes LDLR protein degradation within the lysosomal compartment of cells (10, 75). However, it remains unclear whether PCSK9-mediated LDLR degradation occurs through the rerouting of nascent LDLRs from the Golgi apparatus to lysosomes (intracellular mechanism), or following PCSK9 secretion and reuptake in the endocytic pathway (extracellular mechanism). Direct experimental support for an intracellular mechanism has come from a study in which expression of autosomal recessive hypercholesterolemia (ARH), an

endocytic adaptor required for LDLR internalization in hepatocytes, was shown to be dispensable for enhanced degradation of mouse liver LDLR in vivo following adenoviral-mediated PCSK9 over-expression (90). In addition, Maxwell *et al.* (76) showed that adenoviral-mediated over-expression of PCSK9 enhanced degradation of newly-synthesized mature LDLR, and to a lesser extent precursor LDLR, in a post-ER compartment in HepG2 human hepatoma cells.

In support of an extracellular mechanism, numerous studies have now established that exogenous PCSK9, either present in conditioned medium or in a purified form, mediates cell surface LDLR degradation in the endosomal/lysosomal compartment of cells (19, 36, 72, 127). In addition, circulating plasma PCSK9 is active in lowering mouse liver LDLR levels *in vivo* in studies using a parabiosis model (72) or PCSK9 infusion techniques (45).

Secreted PCSK9 binds directly to the first epidermal growth factor-like repeat (EGF-A) of the EGF precursor homology domain of the LDLR, and this binding is required for exogenous PCSK9 to promote LDLR degradation (127). The physiological significance of the binding of secreted PCSK9 to the LDLR is underscored by studies showing that this interaction i) occurs at physiological circulating concentrations of PCSK9 (45, 72), ii) is enhanced dramatically at acidic pH (28, 36, 127), consistent with the ability of PCSK9 to cause LDLR degradation within acidic cellular compartments, and iii) accounts for the cellular phenotype of a *PCSK9* gain-of-function mutation (D374Y) associated with a severe form of hypercholesterolemia (84), as this mutant protein displays an ~10-fold increased ability to promote cell surface LDLR degradation owing to a 5- to 30-fold increased affinity for the LDLR (28, 36, 72). Although

autocatalytic activity is obligatory for PCSK9 maturation and secretion, catalytic function was not required for LDLR degradation by exogenous PCSK9 in cultured HepG2 cells, nor in mouse liver in vivo (Chapter 3). These data are consistent with PCSK9 acting as a molecular chaperone to divert the LDLR from its normal endocytic recycling route and into a degradation pathway.

The LDLR is a modular protein consisting of an N-terminal ligand binding domain (seven cysteine-rich repeats (R1-R7) that mediate binding to LDL and β-VLDL), followed by the EGF-precursor homology domain (a pair of EGF-like repeats (EGF-A and EGF-B) separated from a third EGF-like repeat (EGF-C) by a β-propeller domain), an "O-linked sugar" domain rich in serine and threonine residues that undergo O-linked glycosylation, a transmembrane region, and a cytoplasmic tail of 50 amino acids containing an NPxY motif that directs the receptor to clathrin-coated pits as well as sequence determinants required for sorting to the basolateral membrane in polarized cells (22, 68, 100, 103)}. FH-associated loss-of-function mutations in the gene encoding the LDLR represent one of the most common inborn errors of metabolism. FH heterozygotes number 1 in every 500 persons worldwide and >1000 mutant *LDLR* alleles implicated in causing FH have been identified. Many insights of LDLR function, as well as the general process of receptor-mediated endocytosis, have come from studies of defective receptors in cells from patients with FH (43). Greater than 150 loss-of-function FH-associated *LDLR* alleles have been characterized at the cellular and/or molecular level (55). Traditionally these mutations have been categorized based on the nature of the LDLR defect: null alleles (class 1); transport-defective alleles, which partially or completely fail to reach the cell surface (class 2); ligand binding-defective alleles (class 3);

internalization-defective alleles, which fail to cluster in coated pits (class 4); and recycling-defective alleles (class 5) (44).

In Chapter 4, the crystal structure of a complex between PCSK9 and the EGF-A domain of the LDLR is described. The binding site for the LDLR EGF-A domain resides on a surface of PCSK9's subtilisin-like catalytic domain >20 Å removed from the PCSK9 catalytic site containing Asp-374 which forms a hydrogen bond with EGF-A-His306. It is predicted that the gain-of-function D374Y mutation in PCSK9 would result in a more favorable bond distance for this interaction. Interestingly, the same histidine residue that binds to PCSK9-Asp374 is replaced by tyrosine in FH patients reported in Great Britain (31) and the Netherlands (37). The mechanism by which this mutation causes FH is not known.

Here, it is investigated whether increased affinity for PCSK9 underlies the FH-phenotype associated with the His306Tyr *LDLR* allele. Structural, biochemical, and cellular studies indeed showed that the His306Tyr mutation within the EGF-A domain of the LDLR enhanced PCSK9 binding affinity resulting in increased PCSK9-mediated cellular LDLR degradation. Low micromolar concentrations of blocking peptides comprised of LDLR sub-fragments containing the H306Y mutation prevented secreted PCSK9 reuptake and resulted in nearly complete recovery of LDLR number and function in HepG2 human hepatoma cells stably overexpressing wild-type PCSK9 or gain-of-function PCSK9 mutants implicated in hypercholesterolemia (D374Y or S127R). These studies define a novel class of FH-associated mutation based on the affected aspect of LDLR function, and identify the first *LDLR* mutation to cause FH due to a gain-of-function, namely increased PCSK9 binding affinity. Furthermore, potent inhibitors of the

cell surface LDLR:PCSK9 interaction allowed for the demonstration that PCSK9 acts predominantly as a secreted factor in causing LDLR degradation in liver-derived cells.

Results

Addition of purified PCSK9 to cultured cell medium (36, 72) or the circulation of mice (45) results in LDLR degradation in liver, suggesting that pharmacological inhibitors of the PCSK9:LDLR interaction could be effective within the extracellular milieu. To test this hypothesis, the binding of secreted PCSK9 to cell surface LDLRs was inhibited. The purified secreted form of PCSK9 binds specifically to the first EGF-like repeat (EGF-A) within the EGF precursor homology domain of the LDLR (127). In Chapter 4 it was shown that a stable 80-amino acid LDLR-derived peptide consisting of the tandem EGF-like repeats A and B (EGF-AB) binds to PCSK9, albeit with ~3-fold lower affinity than full-length LDLR extracellular domain (ECD) protein. EGF-AB can be readily purified in large quantities following its expression in *E. coli*, making it a potentially suitable reagent for blocking the interaction of PCSK9 with cell surface LDLRs. For this purpose, mutations in the EGF-AB sequence that would increase PCSK9 affinity were introduced. Based on structural data obtained from co-crystallization of PCSK9 with the LDLR EGF-A domain at pH 4.8, it was predicted that an FH-associated H306Y mutation in the EGF-A domain of the LDLR would result in increased binding to PCSK9. EGF-AB harboring the His306Tyr mutation was purified, and the PCSK9 binding affinity of this mutant peptide was compared to that of wild-type EGF-AB. To test the effect of the His306Tyr mutation on binding affinity for PCSK9, competition binding assays were performed at pH 7.4 to assess the ability of EGF-AB peptides to

compete with fluorophore-labeled LDLR-ECD (DyLight-800) for binding to immobilized PCSK9. In assays using wild-type PCSK9, EGF-AB(H306Y) displayed a 2.5-fold greater binding affinity than wild-type EGF-AB (EC50 of 195.6 nM for EGF-AB(H306Y) versus 497.6 nM for wild-type EGF-AB) (Figure 5-1*A*).

To further characterize the FH associated mutation His306Tyr in the *LDLR*, a full-length LDLR cDNA construct was created with a His306Tyr mutation. The full-length mutant LDLR was transfected into the human hepatoma cell line HuH-7. The mutant LDLR was tested for its ability to internalize PCSK9 and for its susceptibility to PCSK9 degradation. Transfected HuH-7 cells were treated with various concentrations of purified FLAG-tagged PCSK9 for 1 hour. Cells were then lysed and subjected to SDS-PAGE and immunoblot analysis. Internalized PCSK9 was detected with anti-FLAG antibody. The LDLR was detected using a monoclonal anti-human LDLR to show expression of the transfected LDLR construct. TFR was detected with a monoclonal anti-human TFR antibody and used as a control for loading. Figure 5-1*B* shows that the LDLR(H306Y) binds and internalizes PCSK9 when added to the medium of transfected cells with at least 3-times greater efficiency than that of wild-type LDLR.

To determine the susceptibility of LDLR(H306Y) to PCSK9 degradation, transfected HuH-7 cells were treated with 0-10 μg/mL PCSK9 for 4 hours before isolation of the cell surface protein fraction. The cell surface was biotinylated before lyses of the cells and the capture of the biotinylated protein fraction with neutravidin beads. Cell surface protein fractions were subjected to SDS-PAGE and immunoblot analysis. LDLR and TFR were detected using a DyLight-800 labeled secondary and the LI-COR Odyssey infrared imaging system. LDLR levels were quantified and normalized

to TFR expression. Figure 5-1*C* shows LDLR(H306Y) is more readily degrade in the presence of PCSK9, with ~85% reduction when subjected to 10 μg/mL PCSK9. This is in contrast to only a 15% reduction in wild-type LDLR levels.

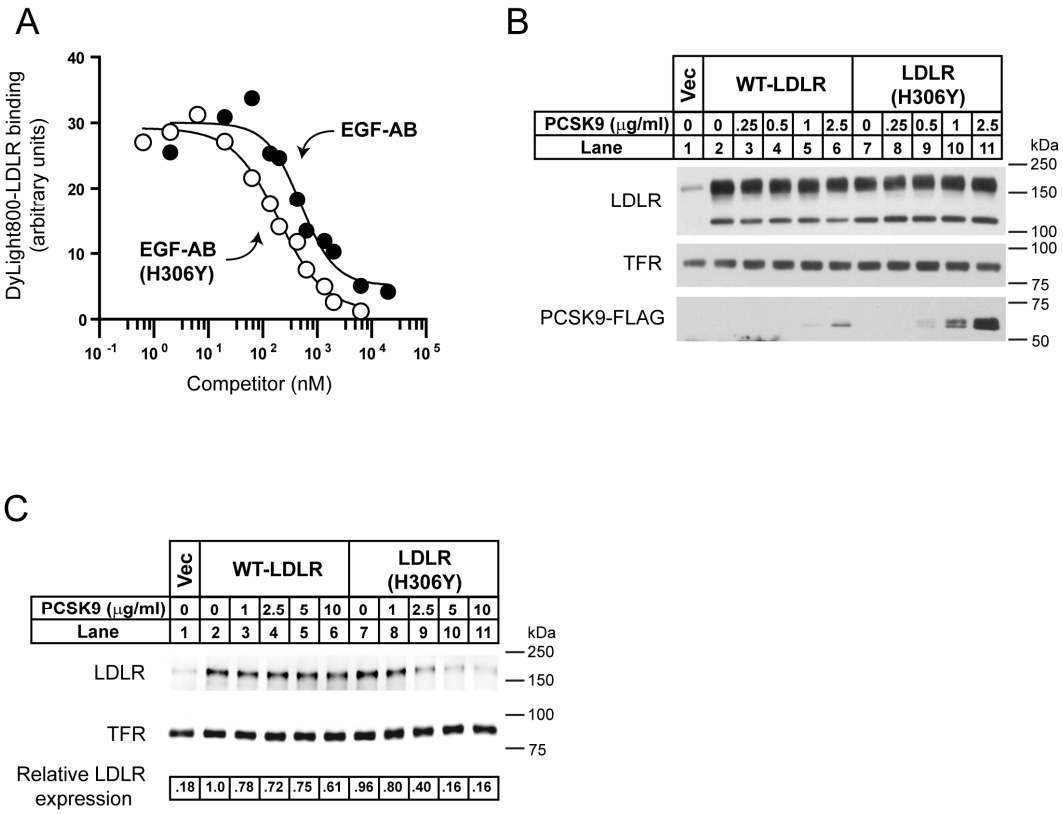

FIGURE 5-1. **EGF-AB(H306Y) has increased affinity for PCSK9.**
A, competition binding of EGF-AB and EGF-AB(H306Y) to PCSK9. Wild-type PCSK9 was prebound to slot-blotted anti-FLAG M2 mAb. Blots were incubated for 90 min with 0.1 μg/ml DyLight800-labeled LDLR-ECD at pH 7.4 in the presence of increasing concentrations of unlabeled EGF-AB (closed circles) or EGF-AB(H306Y) (open circles) and bound fluorophore-labeled LDLR was detected and quantified. *B,* HuH-7 cells were transfected with wild-type or H306Y full-length LDLR. Cells were then treated for 1 hour with the indicated amount of purified FLAG-tagged PCSK9. Following incubation with PCSK9, cells were lysed and subjected to SDS-PAGE and immunoblot analysis. Internalized PCSK9 was detected with anti-FLAG antibody. Transfected LDLR was

detected with anti-human LDLR IgG HL-1. TRF was detected as a loading control using anti-human TFR mAb. *C,* HuH-7 cells were transfected as in *B* and treated with the indicated amount of PCSK9 for 4 hours. Following PCSK9 incubation, cell surface proteins were isolated by biotinylation and pulldown with neutravidin beads. Isolated cell surface proteins were subjected to SDS-PAGE and immunoblot analysis. LDLR and TFR were detected as in *B*. Secondary detection used a DyLight800 bound antibody. Blots were visualized and quantified using the LI-COR Odyssey infrared imaging system. LDLR levels are normalized to TFR expression.

Increased binding and susceptibility to PCSK9-mediated degradation could explain why the H306Y mutation in the LDLR causes FH; however this mutation could also affect other aspects of LDLR maturation or degradation. To rule out a defect in maturation of the LDLR(H306Y), HuH-7 cells were transiently transfected with LDLR or LDLR(H306Y) expression constructs and treated with sterol-supplemented medium to lower endogenous LDLR before labeling with [^{35}S]methionine/cysteine. Cells were incubated in chase medium for 2 hours. Cells were lysed and LDLR was immunoprecipitated from cell lysates. Samples were subjected to SDS-PAGE and phosphoimaging. The LDLR(H306Y) was made and processed in at a rate similar to the wild-type receptor (Figure 5-2*A*). HuH-7 cells were transfected with LDLR or LDLR(H306Y) and assayed for there ability to bind LDL. Transfected cells were incubated with DiI-LDL and the mean fluorescence of each sample determined by counting 10,000 cells by flow cytometry. The LDLR cells bound significantly more DiI-LDL than vector transfected cells. LDLR(H306Y) transfected cells bound a similar amount of DiI-LDL as the wild-type LDLR transfected cells (Figure 5-2*B*). This rules out the possibility that the His306Tyr FH mutation has defective LDL binding.

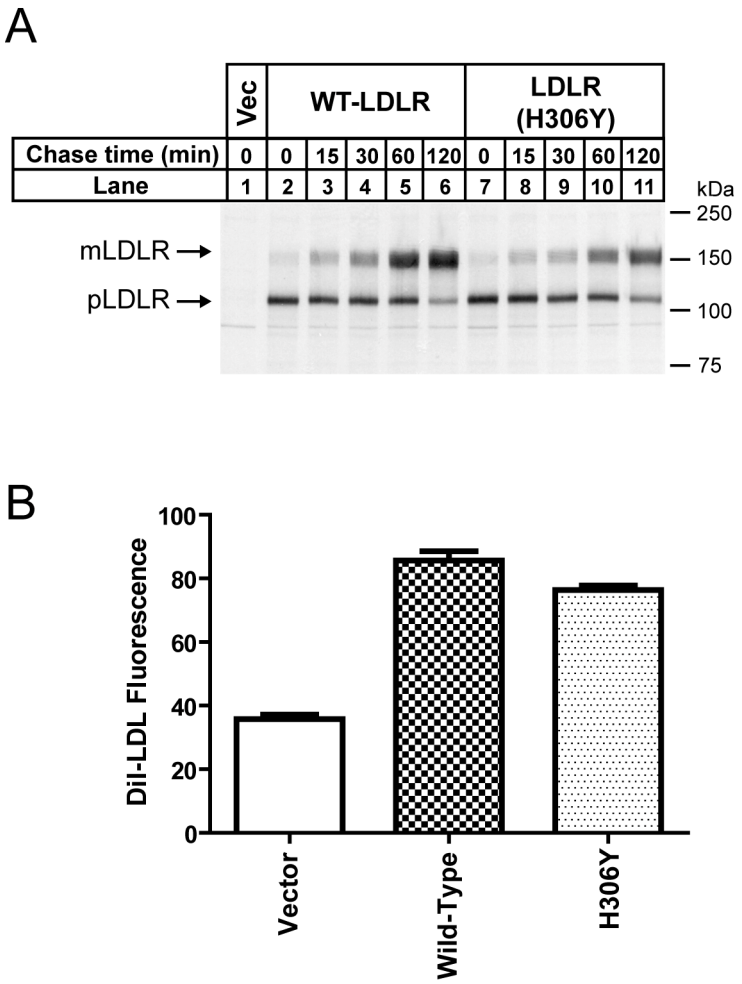

FIGURE 5-2. **LDLR(H306Y) is not defective in processing or LDL uptake.**
A, HuH-7 cells were transiently transfected with LDLR or LDLR(H306Y) expression constructs and treated with sterol-supplemented medium, 24 hours prior to labeling for 30 minutes with [^{35}S]methionine/cysteine. After washing, cells were incubated in chase medium for the indicated times. Cells were lysed and LDLR was immunoprecipitated from cells lysates. Samples were subjected to 8% SDS-PAGE and the gel was dried, exposed to a PhosphorImager plate and scanned. Labels indicate the mature (mLDLR) and unprocessed (pLDLR) forms of the LDLR. *B,* HuH-7 cells were transfected with vector, LDLR, or LDLR(H306Y) and treated with sterol-supplemented medium, 24 hours prior to incubation for 2 hours with 100 μg/mL DiI-LDL. After incubation, Cells were trypsinized and the mean fluorescence intensity of 10,000 cells for each sample measured by flow cytometry. Three replicate samples were used per condition.

To determine the mechanism responsible for the increased binding of PCSK9 to LDLR(H306Y), structural analysis was performed. Crystals of Δ53-PCSK9 in complex with either wild-type EGF-AB or EGF-AB(H306Y) were grown at pH 4.8 and transferred to pH 7.4 prior to data collection and the structures were refined to 2.7 Å (Table 5-1). The structures of both complexes are nearly identical with the previously determined structure of Δ53-PCSK9:EGF-AB determined at pH 4.8 in Chapter 4, with a root mean square deviation across all Cα atoms of 0.3 Å (EGF-AB wt at neutral pH) and 0.4 Å (EGF-AB H306Y) when compared to the low pH structure. Similar to the previous structure determined at acidic pH, electron density is not visible for the EGF-B domain. At acidic pH, His306 of EGF-AB is 4 Å from Asp374 of PCSK9, forming an intermolecular salt bridge. However, at neutral pH His306 of EGF-AB is rotated away from Asp374 of PCSK9 and is 3.1Å from Ser305 forming an intramolecular hydrogen bond (Figure 5-3B). At neutral pH, His306Tyr of EGF-AB forms a hydrogen bond with Asp374 of PCSK9. His306Tyr is in a conformation that is similar to that seen for His306 at acidic pH, placing the hydroxyl group of His306Tyr 3.0 Å from Asp374 (Figure 5-3C).

TABLE 5-1. **Data Collection and Refinement Statistics**

EGF-AB	Wt pH 7.4	H306Y pH 7.4
Space group	P4(1)2(1)2	P4(1)2(1)2
a,b (Å)	116.047	115.661
c (Å)	133.629	133.401
Resolution (Å) (final shell)	40.0 – 2.70 (2.77 – 2.70)	40.0 – 2.70 (2.77-2.70)
Reflections		
Total	110489	117756
Unique	24921	25367
Completeness (%)	96.6 (81.9)	99.3 (92.8)
Rsym (%)	8.4	8.1
Rcryst (%)	22.6 (34.7)	23.4 (33.2)
Rfree(%)	26.1 (46.5)	27.8 (41.2)
RMSD		
Bond length (Å)	0.006	0.006
Bond angle (°)	0.973	0.971

A

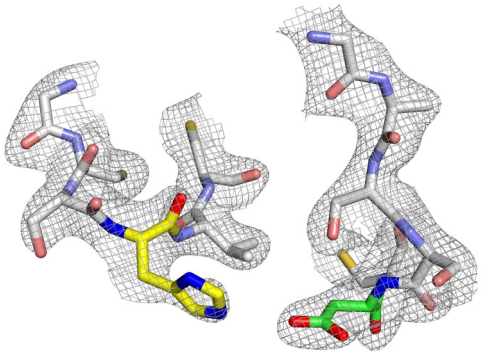

WT
pH 4.8

B

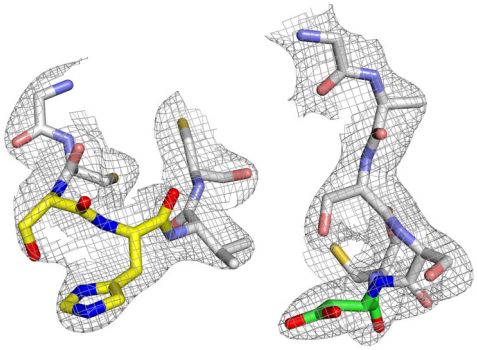

WT
pH 7.4

C

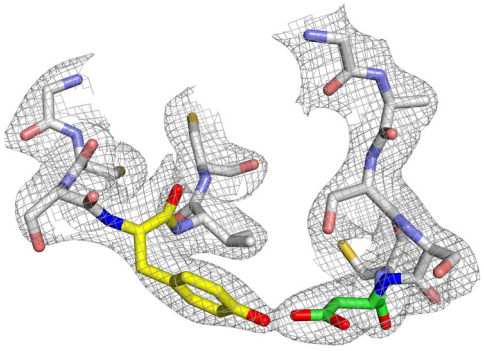

H306Y
pH 7.4

FIGURE 5-3. **The structure of the PCSK9:EGF-A complex.**
The *sigmaA* weighted $2F_o$-F_c electron density map contoured at 1σ shows the conformational change that occurs upon protonation of His306. EGF-A and PCSK9 are represented as a stick model. Residues involved in the pH dependant conformational change are colored according to element type: nitrogen, blue; oxygen, red; EGF-A carbon, yellow; PCSK9 carbon, green. All other residues are colored grey. A, at acidic pH, His306 of EGF-A forms a salt bridge with Asp374 of PCSK9. B, at neutral pH, His306 of EGF-A forms an intramolecular hydrogen bond with Ser305. C, the FH mutation H306Y of EGF-A is able to form a hydrogen bond with Asp374 of PCSK9 at neutral pH.

To test whether EGF-AB(H306Y) could prevent cell surface LDLR binding and uptake of exogenous PCSK9, indirect immunofluorescence and immunoblot blot analysis was carried out in HuH7 human hepatoma cells cultured in sterol-depleted medium to induce LDLR expression. For use as a control for non-specific effects of EGF-AB peptides in cultured cell experiments, a EGF-AB protein was purified in which a residue (L318) previously shown to be important for binding of PCSK9 to full-length LDLRs (127) was mutated to alanine. PCSK9 was detected using a polyclonal antibody raised against the full-length human protein, and fluorescence intensity settings were kept constant for all conditions. In the absence of exogenous PCSK9, weak immunostaining of endogenous PCSK9 was detected predominantly in a reticular pattern throughout the cytoplasmic space, consistent with the endoplasmic reticulum (ER) (Figure 5-4*A*, upper left panel). Addition of 5 μg/ml of exogenous PCSK9 to the culture medium for 1 hour resulted in robust cellular uptake of PCSK9 and immunostaining of punctate vesicular structures throughout the cytoplasm and the perinuclear region, indicative of early/late endosomal localization of internalized PCSK9 (Figure 5-4*A*, upper right panel). In contrast, only weak fluorescence similar to that of endogenous PCSK9 immunostaining

was evident upon simultaneous addition of a 5 μM concentration of EGF-AB(H306Y), indicating that this LDLR sub-fragment prevented exogenous PCSK9 uptake (Figure 5-4*A*, lower left panel). The addition of a 5 μM concentration of the negative-control EGF-AB(L318A) peptide had a no effect on exogenous PCSK9 uptake (Figure 5-4*A*, lower right panel). To quantify the blocking efficiency seen in the immunofluorescence, whole cell extracts from cells treated at the same time and with the same conditions were subjected to SDS-PAGE and immunoblotting with anti-FLAG antibody to detect exogenous PCSK9. Figure 5-4*B* shows that PCSK9 is efficiently taken up when added to HuH7 cells exogenously (Lane 2) and that this uptake in inhibited by 90% in the presence of 5 μM EGF-AB(H306Y) (Lane2).

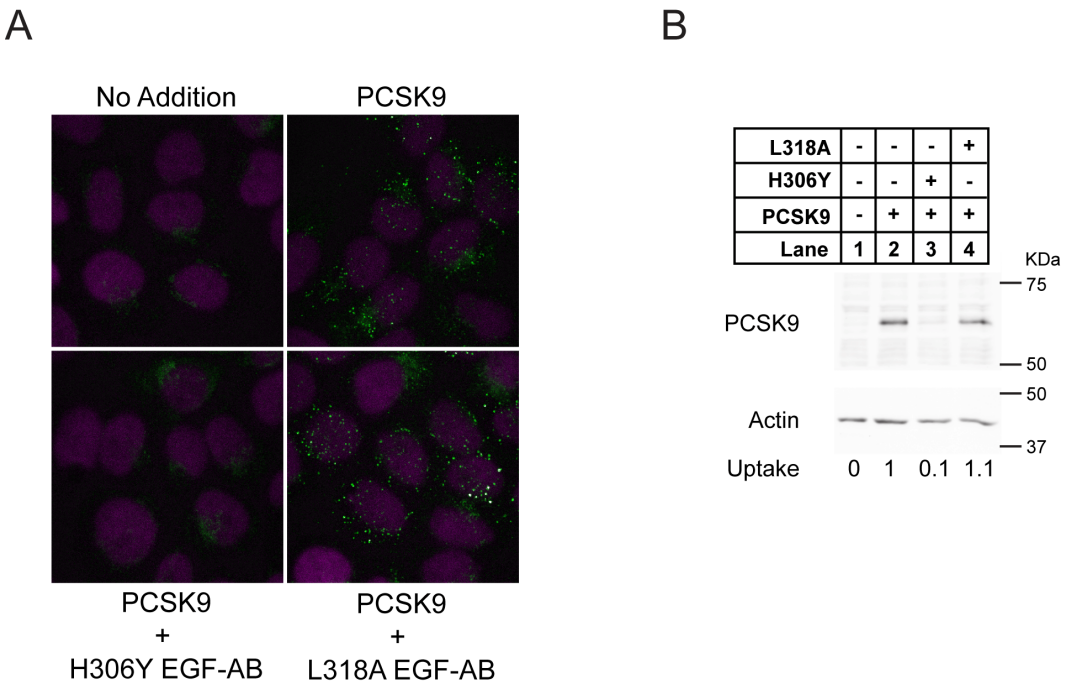

FIGURE 5-4. **EGF-AB blocks uptake of PCSK9 in HuH-7 cells.**
HuH-7 cells were treated 30 minutes with or without purified, full-length, FLAG-tagged PCSK9 and EGF-AB(H306Y) blocking peptide or EGF-AB(L318A) negative control. *A,* cells were immunostained for PCSK9 (green) and nuclear stained with DAPI (magenta). *B,* cells were lysed and subjected to SDS-PAGE and immunoblotting for FLAG-tagged PCSK9. Actin was detected as a control for loading. The PCSK9 bands were quantified and normalized to actin levels to determine PCSK9 uptake in each sample.

For experiments examining the cellular site of action of PCSK9, HepG2 human hepatoma cell-lines stably expressing empty vector (HepG2-Vec) or C-terminal FLAG-tagged versions of wild-type PCSK9 or either of two PCSK9 gain-of-function mutants (S127R and D374Y) associated with hypercholesterolemia were constructed. The S127R and D374Y PCSK9 mutants were chosen for study due to the severity of the associated FH phenotype (1, 84). To assess PCSK9 autocatalytic processing and secretion rates in stably transfected HepG2 cells, [^{35}S]methionine/cysteine was added to culture media for a followed by a chase period in isotope-free medium. Radiolabeled over-expressed PCSK9

proteins were isolated by immunoprecipitation from cells and medium at various times using an anti-FLAG monoclonal antibody. The S127R mutation is in the C-terminal region of the prodomain and it has previously been shown that the mutation reduces PCSK9 autocatalysis and secretion (10). As expected, over-expressed PCSK9(S127R) was processed from proprotein to cleaved form at a slower rate than wild-type PCSK9 or PCSK9(D374Y), but the appearance of the mature cleaved form of the protein in the medium was not significantly delayed (Figure 5-5*A*). ELISA measurements determined that media PCSK9 concentration was increased by ~10-fold for HepG2-PCSK9 and HepG2-PCSK9(S127R) cells and ~5-fold in HepG2-PCSK9(D374Y) cells compared to HepG2-Vec cells following a 24 h period in sterol-depleting medium (Figure 5-5*B*). HepG2-PCSK9, HepG2-PCSK9(S127R) and HepG2-PCSK9(D374Y) cells had 18-, 12- and 7-fold elevated PCSK9 mRNA levels compared to HepG2-Vec control cells, respectively (Figure 5-5*C*). There were only small differences in LDLR mRNA levels between the different cell lines (Figure 5-5*D*).

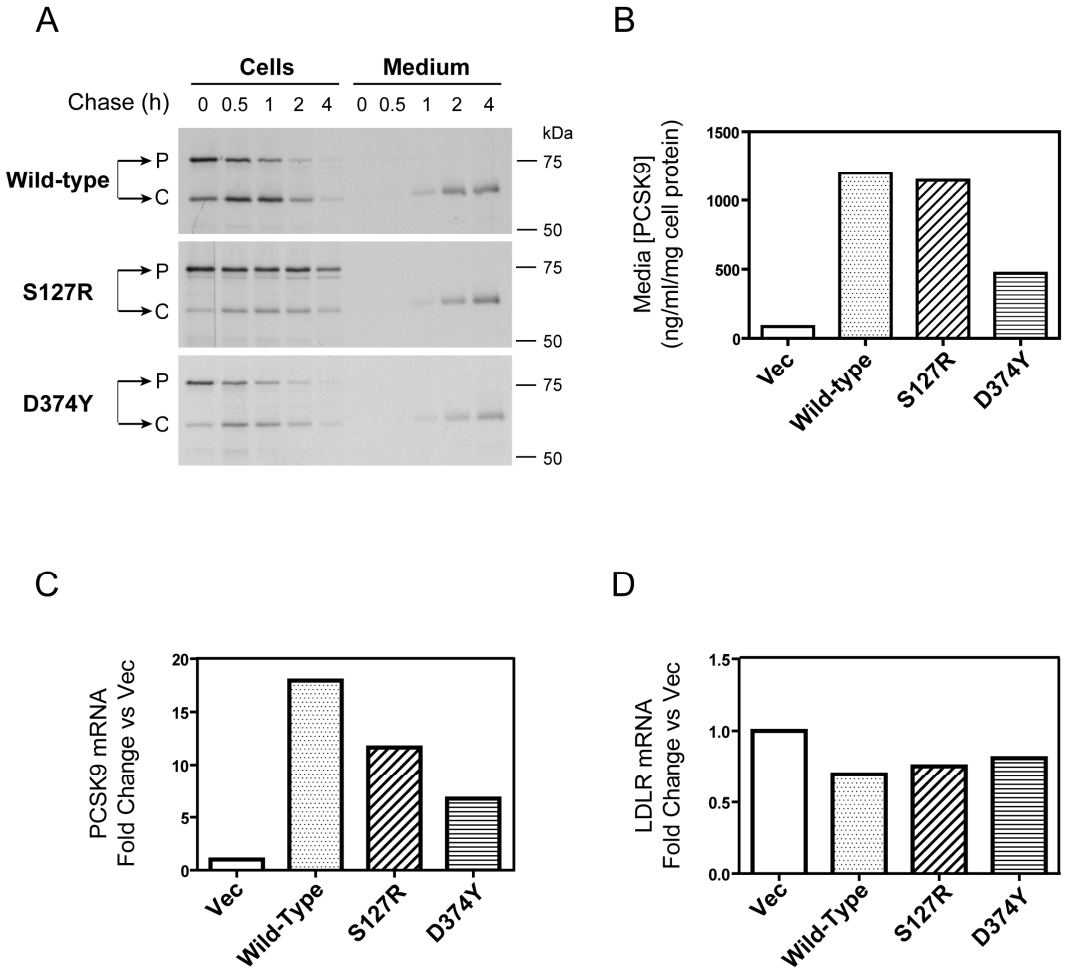

FIGURE 5-5. **Characterization of stably expressing PCSK9 cell lines.**
A, HuH-7 cells stably transfected with PCSK9, PCSK9(S127R), or PCSK9(D374Y) were labeled for 30 minutes with [^{35}S]methionine/cysteine. After washing, cells were incubated in chase medium for the indicated times. Cells were lysed and PCSK9 was immunoprecipitated from cell lysates and medium. Samples were subjected to 8% SDS-PAGE and the gel was dried, exposed to a PhosphorImager plate and scanned. P and C denote proprotein and cleaved forms of PCSK9, respectively. *B,* Medium from HuH-7 cells stably transfected with vector, PCSK9, PCSK9(S127R), or PCSK9(D374Y) was subjected to ELISA to determine PCSK9 concentrations. *C,* RNA was harvested from HuH-7 cells stably transfected with vector, PCSK9, PCSK9(S127R), or PCSK9(D374Y) and subjected to RT-QPCR to determine PCSK9 expression levels and *D,* LDLR expression levels.

Next, it was tested whether addition of EGF-AB(H306Y) to the culture medium inhibited PCSK9-mediated LDLR degradation in PCSK9 over-expressing HepG2 cells. The effect of incubation with the EGF-AB(H306Y) blocking peptide on LDLR protein expression in PCSK9 over-expressing HepG2 cells was determined by immunoblot analysis using a monoclonal antibody. Following treatments, cell surface proteins were covalently modified with a cell-impermeable biotinylation reagent and isolated using streptavidin beads. Protein quantification was performed on immunoblots using infrared dye (IRDye-800)-labeled secondary antibodies and the LICOR Odyssey infrared imaging system. Under basal conditions, LDLR levels were reduced by 70%, 80%, and 90% among cell surface proteins in cells over-expressing wild-type, S127R, and D374Y PCSK9, respectively compared to vector-transfected controls (Figures 5-6 and 5-7). There was no effect of PCSK9 over-expression on levels of another cell surface protein, the transferrin receptor. Incubation with 5 μM EGF-AB(H306Y) for 18 h resulted in the recovery of cell surface LDLR protein levels in HepG2-PCSK9, HepG2-PCSK9(S127R), and HepG2-PCSK9(D374Y) cells to that of HepG2-Vec control cells cultured under basal conditions. Incubation with a 5 μM concentration of the negative-control EGF-AB(L318A) peptide had no effect on cell surface LDLR protein levels (Figure 5-6 and 5-7).

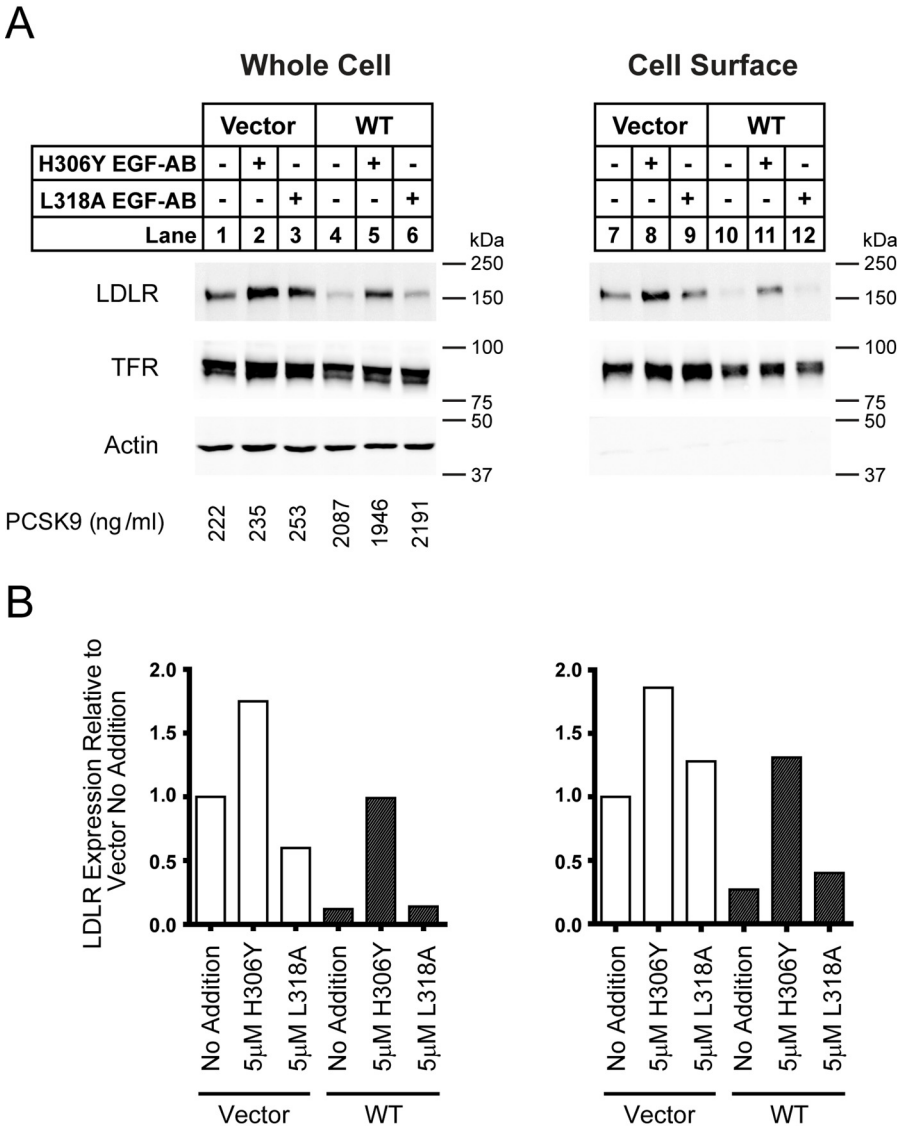

FIGURE 5-6. **EFG-AB restores LDLR numbers in PCSK9 overexpressing cells.** HepG2 cells stably overexpressing empty vector or wild-type PCSK9 (WT) were treated for 18 hours with the indicated concentration of EGF-AB(H306Y) or EGF-AB(L318A). *A,* cell surface proteins were biotinylated and whole-cell and cell surface extracts subjected to SDS-PAGE and immunoblot analysis for LDLR. TFR was detected as a control for loading and non-specific protein degradation. Actin was detected as a control for loading and biotinylation of non-cell surface proteins. PCSK9 concentrations in the medium of each sample were detected by ELISA. *B,* the LDLR bands in *A* were quantified using the LI-COR Odyssey infrared scanning system. Values were normalized to TFR and graphed relative to the vector cell line, no addition condition.

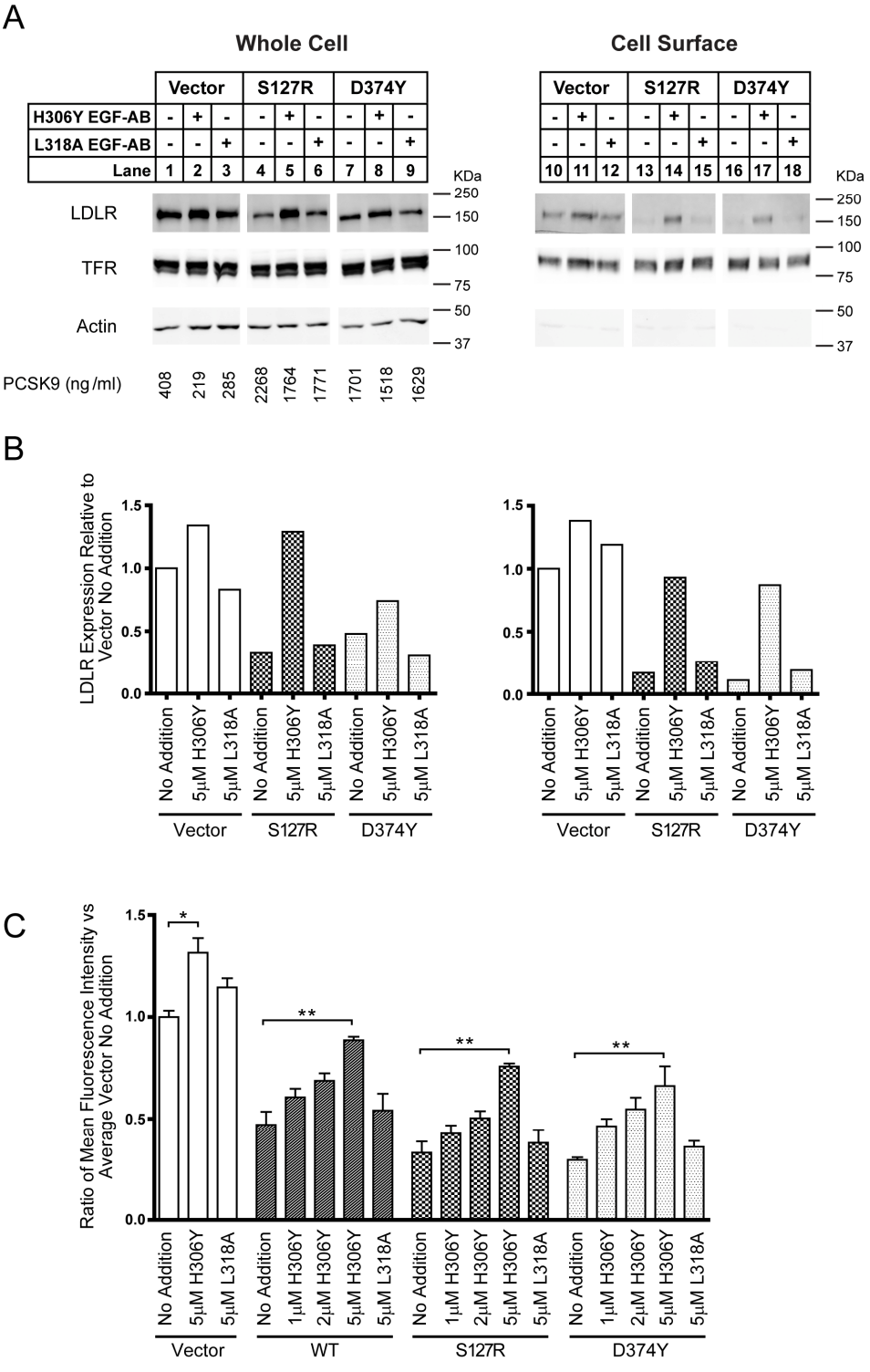
A
Whole Cell
Cell Surface
Vector
S127R
D374Y
H306Y EGF-AB
L318A EGF-AB
Lane
KDa
LDLR
TFR
Actin
PCSK9 (ng/ml)
408
219
285
2268
1764
1771
1701
1518
1629
B
LDLR Expression Relative to Vector No Addition
No Addition
5μM H306Y
5μM L318A
C
Ratio of Mean Fluorescence Intensity vs Average Vector No Addition
1μM H306Y
2μM H306Y
WT

FIGURE 5-7. **EGF-AB restores LDLR numbers and function in gain-of-function PCSK9 overexpressing cell lines.** HepG2 cells stably overexpressing empty vector, PCSK9(S127R), or PCSK9(D374Y) were treated for 18 hours with the indicated concentration of EGF-AB(H306Y) or EGF-AB(L318A). *A,* cell surface proteins were biotinylated and whole-cell and cell surface extracts subjected to SDS-PAGE and immunoblot analysis for LDLR. TFR was detected as a control for loading and non-specific protein degradation. Actin was detected as a control for loading and biotinylation of non-cell surface proteins. PCSK9 concentrations in the medium of each sample were detected by ELISA. *B,* the LDLR bands in *A* were quantified using the LI-COR Odyssey infrared scanning system. Values were normalized to TFR and graphed relative to the vector cell line, no addition condition. *C,* empty vector, PCSK9(WT), PCSK9(S127R), or PCSK9(D374Y) overexpressing cells were treated for 18 hours with the indicated concentration of EGF-AB(H306Y) or EGF-AB(L318A) and then incubated for 2 hours with 100 μg/mL DiI-LDL. Cells were trypsinized and the mean fluorescence intensity of each sample measured by flow cytometry. Six replicate samples were used per condition. Asterisk indicates a statistical difference between columns with significance $p<0.05$ by one-way ANOVA and post-test pair wise comparison using Tukey's method. Double asterisk $p<0.001$.

As a measure of LDLR function, cellular uptake of fluorescent DiI-labeled LDL was assessed by FACS analysis. Under basal conditions, DiI-LDL uptake was decreased >50% in HepG2-PCSK9 cells compared to HepG2-Vec controls (Figure 5-7*C*). LDLR function was more severely affected in cells overexpressing PCSK9 gain-of-function mutants, with a ~70% and 75% reductions in DiI-LDL uptake in HepG2-PCSK9(S127R) and HepG2-PCSK9(D374Y) cells, respectively. Addition of 1 – 5 μM EGF-AB(H306Y) for 18 hours prior to DiI-LDL incubation resulted in a dose-dependent increase in DiI-LDL uptake in all PCSK9 over-expressing cells. In HepG2-PCSK9 cells, a dose of 5 μM resulted in DiI-LDL uptake levels equal to that of untreated control cells. Treatment with 5 μM EGF-AB(H306Y) peptide caused a >2-fold increase in DiI-LDL uptake in HepG2-PCSK9(S127R) and HepG2-PCSK9(D374Y) cells; however, overall levels were still suppressed ~20% and 30% compared to untreated control cells, respectively.

Interestingly, 5 μM EGF-AB(H306Y) treatment resulted in a small, but consistently detectable ~30% increase in DiI-LDL uptake in HepG2-Vec cells. Incubation with a 5 μM concentration of the negative-control EGF-AB(L318A) peptide had no effect on DiI-LDL uptake in any cell-line (Figure 5-7*C*).

To rule out the possibility that the EGF-AB blocking peptides entered cells and interfered with PCSK9 action in the endosomal/lysosomal compartment rather than at the cell surface, the uptake and lysosomal degradation of ^{125}I-labeled EGF-AB and PCSK9 proteins was measured. Both ^{125}I-labeled proteins had similar specific activities (1000-1500 cpm/ng protein) and showed no degradation by SDS-PAGE analysis (Figure 5-8*A*). During a 2 h incubation at 37^{o}C, 6 ng ^{125}I-PCSK9 per mg cell protein was recovered in the culture medium as TCA-soluble material (Figure 5-8*B*), indicating protein degradation in lysosomes and conversion of ^{125}I-labeled PCSK9 to mono-^{125}I-tyrosine (42). In contrast, negligible amounts of added ^{125}I-labeled EGF-AB were recoverable as TCA-soluble material in the culture medium, indicating very low cellular uptake of this peptide.

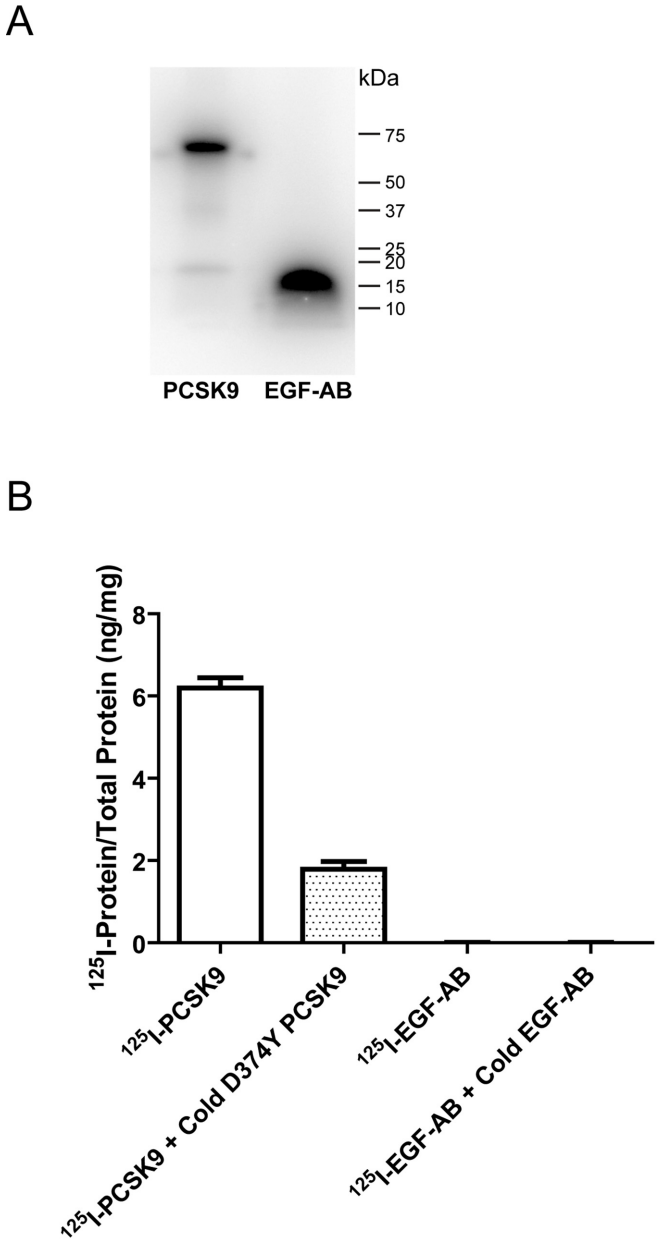

FIGURE 5-8. **^{125}I-Protein uptake in HepG2 cells.**
A, equal counts of ^{125}I-labeled PCSK9 and EGF-AB were subjected to 4-15% SDS-PAGE. The gel was dried, exposed to a PhosphorImager plate and scanned. *B,* equal count of ^{125}I-labeled PCSK9 or EGF-AB was added to HepG2 cells plus or minus an excess of cold competitor and incubated for 1 hour followed by 2 hours in medium lacking added proteins. The medium was TCA precipitated. The TCA soluble medium fraction was counted for radioactivity.

Discussion

The co-crystal structure of PCSK9:LDLR presented in Chapter 4 provided insight into the mechanism of the D374Y mutation in *PCSK9*. It also suggested that there was a previously unrecognized class of *LDLR* mutations that cause FH by increased susceptibility to PCSK9-mediated degradation. The His306Tyr mutation in *LDLR*, previously identified in human patients (31, 37), was one possible mutation of this new class. Figure 5-1 clearly shows an increased binding and susceptibility of LDLR(H306Y) to PCSK9. It was possible that the H306Y mutation could also fall into one of the classical *LDLR* mutation classes. The data in Figure 5-2 effectively excludes this possibility. The protein is expressed (excluding class 1), matures at the same rate as WT LDLR (excluding class 2) and binds and internalizes LDL at to the same extent as WT LDLR (excluding class 3, 4, and 5). This leaves increases binding to PCSK9 as the major mechanism contributing to the FH phenotype seen with the His306Tyr mutation. This is the first gain-of-function mutation in the *LDLR* identified to cause FH and represents a new class of FH mutants, designated Class VI. Patients with this class of mutation will be especially important to identify, as they would benefit from anti-PCSK9 therapies when they are developed.

The structure presented in Chapter 4 provided a potential structural mechanism responsible for increased binding of LDLR(H306Y) to PCSK9. The mature secreted form of PCSK9 binds directly to the first EGF-like repeat (EGF-A) within the EGF-precursor homology domain of the LDLR (127), a region critical for LDLR recycling in the endocytic pathway (30). The co-crystal structure of PCSK9 in complex with the LDLR EGF-A domain determined at pH 4.8 revealed that the Asp374 residue of PCSK9 forms a

salt bridge with His306 of the LDLR (Chapter 4). Based on this structural model, it is predicted that the gain-of-function D374Y mutation in PCSK9 would permit a favorable hydrogen bond, and also that the LDLR (H306Y) mutation would cause a reciprocal change, resulting in increased PCSK9 binding affinity.

To verify these predictions, the structure of PCSK9:EGF-AB and PCSK9:EGF-AB(H306Y) were determined at pH 7.4. As predicted, the structure at neutral pH of PCSK9 in complex with EGF-AB harboring the His306Tyr mutation shows that His306Tyr is in a conformation that mimics the interaction observed between His306 and Asp374 at acidic pH (Figure 5-3), thus explaining the increased affinity of PCSK9 for this mutation. Comparing the structures of PCSK9:EGF-A at neutral and acidic pH reveals that a conformational change occurs upon protonation of His306 in EGF-A, allowing for the formation of a salt bridge with Asp374 of PCSK9 and providing an explanation for the increase in affinity of PCSK9 for the LDLR at acidic pH. At neutral pH, His306 is not protonated and unable to form a favorable hydrogen bond with Asp374 of PCSK9, instead forming an intramolecular hydrogen bond with Ser305. Movement to the acidic environment of the endosome/lysosome would presumably lead to the protonation of His306, allowing for the formation of the observed salt bridge with Asp374, resulting in increased affinity of PCSK9 and the LDLR. The FH mutation His306Tyr adopts this acidic pH conformation, even at neutral pH. It remains to be determined if the interaction between His306 and Asp374 is the sole determinant of the pH dependant increase in affinity or whether other regions of the LDLR contribute to this increase.

While it is well-established that PCSK9 plays a central role in regulating LDLR activity and circulating plasma LDL-C levels, there have been conflicting reports as to whether PCSK9 acts within the secretory pathway (intracellular mechanism), following its secretion and reuptake in the endosomal pathway (extracellular mechanism), or a combination thereof. Determination of the cellular site of action of PCSK9 will facilitate efforts to design inhibitors of PCSK9 function in the treatment of hypercholesterolemia. In this chapter, the provided evidence suggests that PCSK9 acts predominantly as a secreted factor in enhancing the degradation of LDLRs in PCSK9-overexpressing HepG2 human hepatoma cells.

A key prediction of the theory that PCSK9 acts as a secreted factor to degrade LDLRs is that inhibition of the binding of secreted PCSK9 to cell surface LDLRs would prevent enhanced LDLR degradation caused by cellular overexpression of PCSK9; i.e., overexpressed PCSK9 within the secretory pathway would not affect LDLR levels prior to its secretion. To experimentally test this prediction, the recombinant EGF-AB(H306Y) peptide was utilized to inhibit the interaction of cell surface LDLRs with PCSK9 present in culture medium. This blocking peptide was effective at preventing the LDLR-dependent cellular uptake of exogenous purified PCSK9 at low micromolar concentrations (Figure 5-4). Importantly, prolonged (18 h) incubation with EGF-AB(H306Y) resulted in near complete recovery of LDLR protein levels and function in HepG2 cells stably over-expressing either wild-type PCSK9 (Figure 5-6) or gain-of-function PCSK9 mutant proteins associated with hypercholesterolemia (D374Y or S127R) (Figure 5-7). These results provide convincing evidence that PCSK9 does not act

to degrade LDLRs via an intracellular mechanism, but rather following its secretion and reuptake.

A possible caveat is that the EGF-AB(H306Y) blocking peptide could be taken up into cells in sufficient quantity to disrupt PCSK9 action intracellularly in the endosomal/lysosomal compartment. Several lines of evidence dispute this possibility. First, ^{125}I-labeled EGF-AB(H306Y) peptide was not internalized and degraded in appreciable amounts in HepG2 cells compared to ^{125}I-labeled PCSK9 (Figure 5-8). Second, incubation of PCSK9-overexpressing HepG2 cells with an EGF-AB peptide harboring a mutation (Lys318Ala) had minimal effect on exogenous PCSK9 uptake (Figure 5-4) or LDLR levels (Figures 5-6 and 5-7), indicating that the effect of the EGF-AB(H306Y) peptide on increasing LDLR number and function was due to its ability to specifically bind and sequester secreted PCSK9. Taken together, these studies support that the binding of secreted PCSK9 to the LDLR at the cell surface is the initiating event leading to eventual LDLR degradation.

Direct experimental support of an intracellular site of action for PCSK9 has mainly come from two studies in which cellular PCSK9 was overexpressed using adenoviral vectors (76, 90). The absolute level of PCSK9 overexpression was not determined in either study, but was likely very high since the CMV protmoter was used to express PCSK9. It is demonstrated in the current study that stably transfected HepG2 cells overexpressing wild-type PCSK9 had a ~18-fold increased level of PCSK9 mRNA (Figure 5-5*C*) and ~10-fold increase in secreted PCSK9 protein (Figure 5-5*B*). It is possible that extremely high PCSK9 expression achieved using adenoviral vectors could

lead to an intracellular site of LDLR degradation that is not operative at lower PCSK9 expression levels.

Unexpectedly, the EGF-AB(H306Y) blocking peptide also inhibited the action of PCSK9(S127R), a gain-of-function mutation that has impaired cleavage and secretion in vitro. LDLR function was more severely affected in HepG2 cells overexpressing PCSK9(S127R) than wild-type PCSK9 (Figure 5-7), which is consistent with previous studies showing increased potency of purified PCSK9(S127R) at causing LDLR degradation when added exogenously to cultured cells (36, 89). Interestingly, Pandit *et al.* recently showed that the D374Y and S127R mutations impose additive effects when introduced into the same PCSK9 protein, implying different mechanisms for the two mutations in enhancing LDLR degradation (89). Despite a decreased secretion rate, PCSK9(S127R) might reach steady-state levels in human plasma that, which coupled with increased LDLR degrading ability could lead to hypercholesterolemia. These findings are in contrast to those of Homer *et al.* (57), who recently showed decreased ^{125}I-LDL binding in HuH-7 human hepatoma cells transiently over-expressing PCSK9(S127R) despite an apparent lack of mutant PCSK9 secretion, leading to the conclusion that the S127R mutant acts via an intracellular mechanism. In their study, PCSK9 secretion was detected in direct immunoblots of serum-containing conditioned media samples. In the current study, PCSK9 secretion was quantified by ELISA and also detected by [^{35}S]methionine/cysteine pulse-labeling followed by immunoprecipitation of media samples. Therefore, discrepancies between the two studies could reflect different methods used to detect secreted PCSK9.

Recently it was shown that the ER-localized proform of PCSK9 binds to the LDLR in the early secretory pathway when both proteins were over-expressed in primary mouse hepatocytes (85). The observed interaction between the PCSK9 proform and LDLR also occurred with an LDLR chimera protein lacking the EGF-A domain (85), and is therefore fundamentally different than the interaction between secreted mature PCSK9 and LDLRs at the cell surface (127). As such, the EGF-AB peptides used in the current blocking studies should not interfere with this interaction, even if able to access pertinent intracellular sites.

An interaction between the uncleaved proform of PCSK9 and BACE1 (beta-site amyloid precursor protein (APP)-cleaving enzyme 1) has also been demonstrated as evidence in support of a role for PCSK9 in the disposal of non-acetylated BACE1 within the secretory pathway (65). Further characterization of PCSK9's activity within the secretory pathway would be aided by determination of the molecular basis of its interaction with putative binding partners. In this regard, the proposed interactions of the PCSK9 proform with the LDLR (85) or BACE1 (65) are confounding since there is no evidence that the uncleaved proform of PCSK9 represents a single stable protein rather than a complex mixture of folding intermediates. As such, the physiological significance of the reported interactions of LDLR or BACE1 with the proform of PCSK9 within the early secretory pathway remains unclear.

The results reported herein demonstrate that PCSK9 acts predominantly as a secreted factor in causing LDLR degradation in PCSK9-overexpressing HepG2 cells. Verification of this finding in animal models will require the development of reagents, such as blocking antibodies, for inhibiting the interaction of circulating PCSK9 with

hepatic LDLRs. These studies will further define therapeutic targets for inhibiting PCSK9-mediated LDLR degradation in the treatment of hypercholesterolemia.

Materials and Methods

Purification of recombinant proteins. Full-length, FLAG-tagged human wild-type PCSK9 and PCSK9(D374Y) were purified from stably expressing HEK-293 cells as described (72). Plasmids containing EGF-AB mutant forms EGF-AB(H306Y) and EGF-AB(L318A) were generated from an EGF-AB:GST fusion cDNA (Chapter 4) using the Quickchange site-directed mutagenesis kit (Stratagene) according to the manufacturer's instructions. A full length LDLR plasmid containing the His306Tyr mutation (pLDLR-17-H306Y) was generated from pLDLR-17 (102) using site-directed mutagenesis. Δ53-PCSK9, EGF-AB (WT and H306Y), and LDLR-ECD proteins were expressed and purified as described in Chapter 4.

Crystallization and structure determination. Crystals of Δ53-PCSK9:EGF-AB and Δ53-PCSK9:EGF-AB(H306Y) were formed essentially as described previously in Chapter 4. Crystals were transferred stepwise into a solution of 0.05 M $(NH_4)H_2PO_4$, 5 mM $CaCl_2$, and 35% glycerol (final pH 7.4) and flash frozen in a -160^{o}C nitrogen stream or directly into liquid propane. Diffraction data were collected at the Advanced Photon Source, beam line 19-ID and were processed with HKL2000 (87) and the CCP4 suite (26). Refinement was performed with REFMAC (82). Figures were generated with PYMOL (W. L. Delano, www.pymol.org).

Tissue culture medium. Medium A contained DMEM (Mediatech, Inc.), 1 g/L glucose, supplemented with 100 U/mL penicillin and 100ug/mL streptomycin sulfate. Medium B contained Medium A with 10% FCS (vol/vol). Medium C was identical to Medium A, but with 4.5 g/L glucose. Medium D contained Medium C supplemented with 5% (vol/vol) new-born calf lipoprotein-deficient serum (NCLPDS), 10 μM sodium compactin, and 50 μM sodium mevalonate. Medium E contained Medium C supplemented with 5% (vol/vol) NCLPDS, 10 μg/mL cholesterol, and 1 μg/mL 25-OH-cholesterol.

Immunofluorescence. Indirect immunofluorescence for PCSK9 was carried out on cells from the human hepatoma cell line, HuH-7. Cells were grown to 50% confluence on glass coverslips in Medium B. They were then incubated for 18 h in Medium D before 30 minute incubation with or without 5 μg/mL PCSK9 and 5 μM EGF-AB(H306Y) or EGF-AB(L318A). After incubation, cells were washed with phosphate-buffered saline (PBS), fixed in 4% (wt/vol) paraformaldehyde for 15 minutes, quenched in 1% (wt/vol) L-glycine for 10 minutes, and permeabilized in 0.05% (wt/vol) Triton X-100 (Pierce) for 10 minutes at room temperature. Cells were then blocked 30 minutes in PBS supplemented with 5% (wt/vol) BSA, 10% (vol/vol) goat serum (Sigma), and 0.025% (wt/vol) Triton X-100. Cells were stained sequentially with a rabbit polyclonal antibody raised against full length human PCSK9 (228B) (5 μg/ml) and Alexa Fluor 488-congugated goat anti-rabbit IgG (Invitrogen) (2 μg/mL). Both the 16 h primary incubation (4° C) and the 1 h secondary incubation (21° C) were followed by three 20-minute washes in PBS with 0.025% Triton X-100. Coverslips were mounted using

ProLong Gold with DAPI (Invitrogen) and imaged using a Leica TCS SP5 confocal microscope.

PCSK9 blocking in HuH-7 cells. HuH-7 cells were cultured and treated as in the immunofluorescence methods. Following 30 minute incubation of PCSK9 and EGF-AB, cells were washed three times in cold PBS and lysed in 50 mM Tris-HCl, pH 7.4, 150 mM NaCl, 5 mM EDTA, 5 mM EGTA, 1% NP-40, and 0.5% sodium deoxycholate with protease inhibitors (1 mM dithiothreitol, 1 mM PMSF, 0.5 mM Pefabloc, 10 μg/ml leupeptin, 5 μg/ml pepstatin A, 25 μg/ml ALLN, and 10 μg/ml aprotinin). Whole cell extracts were combined with SDS loading buffer and boiled before equal protein amounts were subjected to 8% SDS-PAGE and immunoblot analysis. PCSK9 and actin proteins were detected with mouse anti-FLAG M2 (Sigma) and mouse anti-Actin AC40 (Sigma) primary antibodies. IRDye800-conjugated secondary donkey anti-mouse antibodies (LI-COR Bioscience) were used. Membranes were scanned with the LI-COR Odyssey infrared imaging system and quantified with Odyssey v2.0 software. PCSK9 quantification was normalized against actin.

PCSK9 blocking in Stable HepG2 cells. Human hepatoma cells, HepG2 (ATCC HB-8065), were transfected with empty vector or full length, FLAG tagged human wild-type (pCMV-hPCSK9-FLAG), D374Y (pCMV-hPCSK9(D374Y)-FLAG), or S127R (pCMV-hPCSK9(S127R)-FLAG) PCSK9 cDNA using Fugene 6 (Roche) transfection reagent according to the manufacturer's instructions. The cDNAs pCMV-hPCSK9-FLAG and pCMV-hPCSK9(D374Y)-FLAG were described previously (72). The pCMV-hPCSK9(S127R)-FLAG cDNA was created through site-directed mutagenesis of the pCMV-hPCSK9-FLAG vector. Transfected cells were subjected to selection with G418.

Surviving colonies were isolated and assessed for PCSK9 expression with mouse anti-PCSK9 IgG-15A6 (72). The stably expressing cell lines were grown to confluence in Medium B. Cells were then incubated for 18 h in Medium D with no addition, 5 μM EGF-AB(H306Y), or 5 μM EGF-AB(L318A) protein. After incubation, medium from each condition was subjected to ELISA to determine PCSK9 concentration as described (38). Cells were then biotinylated and whole cell and cell surface proteins isolated as previously described (72). Equal protein fractions were subjected to 8% SDS-PAGE and immunoblot analysis. Mouse anti-human LDLR IgG-HL1 (121), mouse anti-human transferrin receptor (Zymed Laboratories), and anti-actin primary antibodies were used. Secondary detection was with IRDye800-conjugated secondary donkey anti-mouse antibodies. Membranes were scanned and quantified using the LI-COR Odyssey system. LDLR quantification was normalized against TFR.

Pulse-Chase. HuH-7 cells were plated on day 0 at 2.0 x 10^5 cells in 60-mm dishes and cultured in Medium B. Dishes were transfected on day 2 with PCSK9 or LDLR cDNA expression plasmids (1 μg) using FuGene 6 transfection reagent (Roche) as per manufacturer's instructions. On day 3, cells were incubated for 60 min in L-methionine- and L-cysteine-free Medium B, prior to pulse-labeling for 30 min with 150 μCi/ml Redivue PRO-MIX [^{35}S] Cell Labeling Mix (GE Healthcare) in the same medium. Cells were then washed twice with PBS and incubated for various times in 1.5 ml chase medium consisting of Medium B containing 10 mM and 3 mM amounts of unlabeled L-methionine and L-cysteine, respectively. Immunoprecipitation of cell and medium extracts was performed as described using a polyclonal anti-PCSK9 antibody

(72). For cells transfected with LDLR constructs only the cells were immunprecipitated using the mAbs IgG-C7 (8).

PCSK9 uptake and LDLR degradation. HuH-7 cells were cultured and transfected with vector, LDLR, or LDLR(H306Y) as described in the pulse-chase section. The day following transfection, cells were incubated with Medium E. After 18 h, 1-10 μg/mL of purified PCSK9 was added to cells for 4 h. Following incubation, cells used for PCSK9 uptake were lysed and subjected to SDS-PAGE and immunoblot analysis for FLAG-tagged PCSK9, LDLR, and TFR as described above. Cells for LDLR degradation were biotinylated and cell surface proteins subjected to SDS-PAGE and immunoblot analysis. LDLR and TFR were detected and quantified using the LI-COR Infrared imaging system as described above.

In vitro binding measurements. Anti-FLAG M2 (10 μg) (Sigma-Aldrich) was diluted in TBS-C (50 mM Tris pH 7.4, 90 mM NaCl, 2 mM $CaCl_2$) and blotted directly onto nitrocellulose membrane (GE Healthcare) using a BioDot SP slot-blot apparatus (BioRad) according to manufacturer's instructions. Blots were blocked for 30 min in Odyssey blocking buffer (LI-COR Biosciences). All incubations (90 min) and subsequent washes (3 x 15 min) were carried out at room temperature with gentle oscillation in TBS-C buffer containing 2.5% non-fat milk. Blots were initially incubated with PCSK9 (5 μg/ml) to bind to anti-FLAG M2 mAb followed by incubation with DyLight800 (Pierce) dye-labeled LDLR-ECD in the absence or presence of unlabeled competitor proteins. Blots were scanned using the Li-COR Odyssey infrared imaging system and band intensity was quantified using Odyssey v2.0 software (LI-COR Biosciences). The amount of competitor protein required for 50% inhibition of fluorophore-labeled protein binding

(EC_{50}) was determined by fitting data to a sigmoidal dose response curve using nonlinear regression (GraphPad Software, Inc.).

^{125}I-Uptake. Purified PCSK9 and EGF-AB proteins were radioiodinated as previously described (107) with the exception that the labeling reaction was carried out using IODO-GEN pre-coated iodination tubes (Pierce). HepG2 cells were incubated for 18 h in Medium D with human lipoprotein-poor serum (HLPPS) used in place of NCLPDS. Cells were then incubated for 1 h in DMEM with 5% HLPPS and 300,000 CPM of radiolabeled protein with or without cold competitor. For PCSK9 10-fold excess of PCSK9(D374Y) was used; for EGF-AB 50-fold excess of EGF-AB was used. Cells were washed 2x with DMEM with 5% HLPPS and 0.5% BSA and then incubated for 2 h in DMEM with 5% HLPPS. Medium was harvested and the radioactivity of the TCA soluble fraction measured (42). Cells were lysed in 0.5 N NaOH and the radioactivity directly measured.

mRNA determination. RNA has harvested from HepG2 cells stably overexpressing vector, PCSK9, PCSK9(S127R), and PCSK9(D374) using RNA STAT-60 (Tel-Test). DNase I treatment, cDNA synthesis and QPCR were performed as previously described (90).

DiI-LDL uptake. LDL was isolated from the plasma of healthy human subjects by ultracentrifugation as described (15). LDL was labeled with 1,1'-dioctadecyl-3,3,3',3'-tetramethylindocarbocyanine perchlorate (DiI) (Invitrogen). LDL was diluted to 1 mg/mL in PBS with 10 mg/mL NCLPDS and 150 ug DiI was added per mg of LDL. The LDL was labeled 18 h at 37° C. Following labeling, DiI-LDL was re-isolated by ultracentrifugation. The DiI-LDL was then dialyzed for 36 h at 4° C against four changes

of 500 volumes of PBS. DiI-LDL concentration was determined by Modified Lowry Protein Assay kit (Pierce). HepG2 cells stably expressing vector, PCSK9, PCSK9(D374Y), or PCSK9(S127R) were grown to confluence in Medium B. Cells were then incubated in Medium D with no addition, 1, 2, or 5 μM EGF-AB(H306Y), or 5 μM EGF-AB(L318A) protein. After 18 h, 100 μg/mL DiI-LDL was added for 2 h. Cells were washed twice in PBS, trypsinized, and transferred to Medium C supplemented with 2.5% NCLDPS. The mean fluorescence intensity of 10,000 live cells, as determined by scatter characteristics, for each sample was determined in the 585 nm range with a BD FACSCalibur flow cytometer. Replicate samples were assayed for each condition. Experiments were combined by normalization to the average of the vector expressing, no addition condition replicates within each experiment. HuH-7 cells were transfected with vector, LDLR, or LDLR(H306Y) as described in the pulse-chase section. The day after transfection, the cells are incubated in Medium E for 18 h. DiI-LDL was added and uptake measured as above. Three replicates were used per sample.

CHAPTER SIX
High-Throughput Screening Methods

CELL-BASED SCREENING ASSAY FOR INHIBITORS OF PCSK9 CLEAVAGE

Introduction

The serine protease PCSK9 is a major determinant of serum cholesterol levels in humans. Individuals who are heterozygous for inactivation mutations in PCSK9 have on average a 28% reduction in plasma LDL cholesterol and an 88% reduction in risk for coronary heart disease (25, 69). Inhibition of PCSK9 function presents a novel method for therapeutic intervention for the treatment of hypercholesterolemia. The studies in Chapter 3 have shown that although PCSK9's serine protease activity is not directly involved in its regulation of plasma cholesterol levels, proteolytic activity is required for proper maturation and secretion of the protein (90). As a result, cell permeable small-molecule inhibitors of PCSK9 catalytic activity are a valid approach to blocking PCSK9 action.

Currently, there are no known small molecule inhibitors of PCSK9 and no *in vitro* activity assays for PCSK9 activity exist. PCSK9 undergoes intramolecular self-cleavage but it has no other known proteolytic substrates. As a result, cell-based assays that measure PCSK9 secretion have been used as a surrogate for PCSK9 activity. The most common method being the use of a reporter such as luciferase fused to PCSK9. If PCSK9 is active, it undergoes normal secretion and reporter activity can be detected in the medium. If activity is blocked, PCSK9 fails to be secreted and reporter activity goes down. The major downfall of these assays is a high false positive rate that results from non-specific molecules that generally inhibit protein secretion from the cell. Any

compound that affects viability, transcription, translation, or cell trafficking will result in a decrease in reporter signal.

Results and Discussion

Here, a secretion assay has been developed that overcomes these problems and limitations. In Chapter 3, it was shown that PCSK9 could be expressed as two separate peptide chains, a prodomain and a catalytic fragment, which associate resulting in an active secreted protein. These two fragments reflect the cleavage location of full-length PCSK9, thereby eliminating the need for catalytic activity to produce a mature protein. It was also found that a V5 tag placed at the C-terminus of the prodomain was cleaved off of the prodomain once the mature protein formed. Importantly, the V5 tag was not cleaved if an inactivating mutation was made in the catalytic fragment (Figure 6-1). This suggested that the tag recapitulates the natural PCSK9 cleavage site. Building upon these data, it was determined that a GFP reporter could also be cleaved from the prodomain. This is shown schematically in Figure 6-2.

The ability of the PCSK9 to cleave the GFP reporter allowed us to develop a cell-based assay that can be used to screen small molecules for inhibition of PCSK9 catalytic activity. The assay utilizes HEK-293 cells that are stably transfected with two plasmids. The first plasmid expresses the catalytic fragment of human PCSK9 (amino acids 153-692) and the second plasmid expresses the prodomain of human PCSK9 (amino acids 31-152) with a V5-GFP linked to the C-terminus. These cells can be used in a cell-based screen for PCSK9 inhibitors.

As shown in Figure 6-2, top panel, in the basal state GFP will be cleaved from PCSK9. If a compound blocks PCSK9 catalytic activity (Figure 6-2, bottom panel), GFP cleavage will be prevented and a PCSK9-GFP fusion protein will be secreted intact into the medium. Accumulation of PCSK9-GFP in the medium is a direct readout of inhibition of PCSK9 activity. The presence of PCSK9-GFP in the medium is detected using a sandwich ELISA assay. Anti-GFP antibody is used to capture the proteins and an anti-PCSK9 antibody is used for detection. This PCSK9 antibody is a monoclonal antibody that detects an epitope in the catalytic domain of PCSK9. Using this combination of antibodies, the captured epitope is on the prodomain-GFP fusion peptide and the detection epitope is on the catalytic fragment of PCSK9 ensuring that free GFP, PCSK9 without the GFP fusion, and dissociated PCSK9 prodomain and catalytic domain are not detected. Quantification of the ELISA is performed by using a peroxidase linked secondary antibody and a chemiluminescent substrate and by reading luminescence.

The assay cell line will secrete only PCSK9 that has GFP cleaved from the prodomain. This results in only a background signal being detected by the ELISA. If a compound inactivates PCSK9, PCSK9-GFP fusion protein will accumulate in the medium and the ELISA values will become non-zero; if a compound has no effect on PCSK9, ELISA values will remain at background. Inasmuch as this assay looks for an appearance of a signal, compounds that affect the secretion of PCSK9 or the viability of cells will not show up as false positives as they do in other secretion assays.

To determine what ELISA values to expect from an inhibitory compound, a positive control must be used. Because there are no known compounds that inhibit PCSK9 catalytic activity, a second stable cell line was created as a control. This control

cell line expresses PCSK9 as two peptides as described for the assay cell line, but contains an inactivating mutation (S386A) in the catalytic fragment of PCSK9. These cells only secrete a PCSK9-GFP fusion protein. The control cells produce a clear signal in the ELISA (Figure 6-3), which represents the maximum signal that will be seen if a compound is 100% effective at blocking PCSK9 catalytic activity. Using the signal values from the control cell line as a reference, a threshold luminescence value, e.g. 10% of control value, can be set as a cutoff for determining if a compound is a "hit" in the assay.

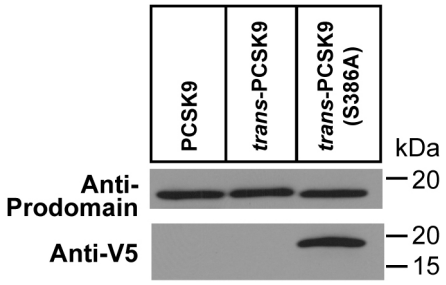

FIGURE 6-1. **PCSK9 can cleave a V5 tag from its prodomain.**
PCSK9 was expressed in full-length form (PCSK9) or as two separate peptides (*trans*-PCSK9). Medium was immunoblotted for PCSK9 prodomain or V5 tag. Full-length catalytically active PCSK9 does not contain a V5 tag and serves as a negative control. Catalytically active PCSK9 expressed as two peptides effectively cleaves a V5 tag from the prodomain, thus the anti-V5 antibody does not produce a signal in the medium. In the absence of catalytic activity (lane 3) the V5-tag remains associated with the prodomain and is detected in the medium. (80)

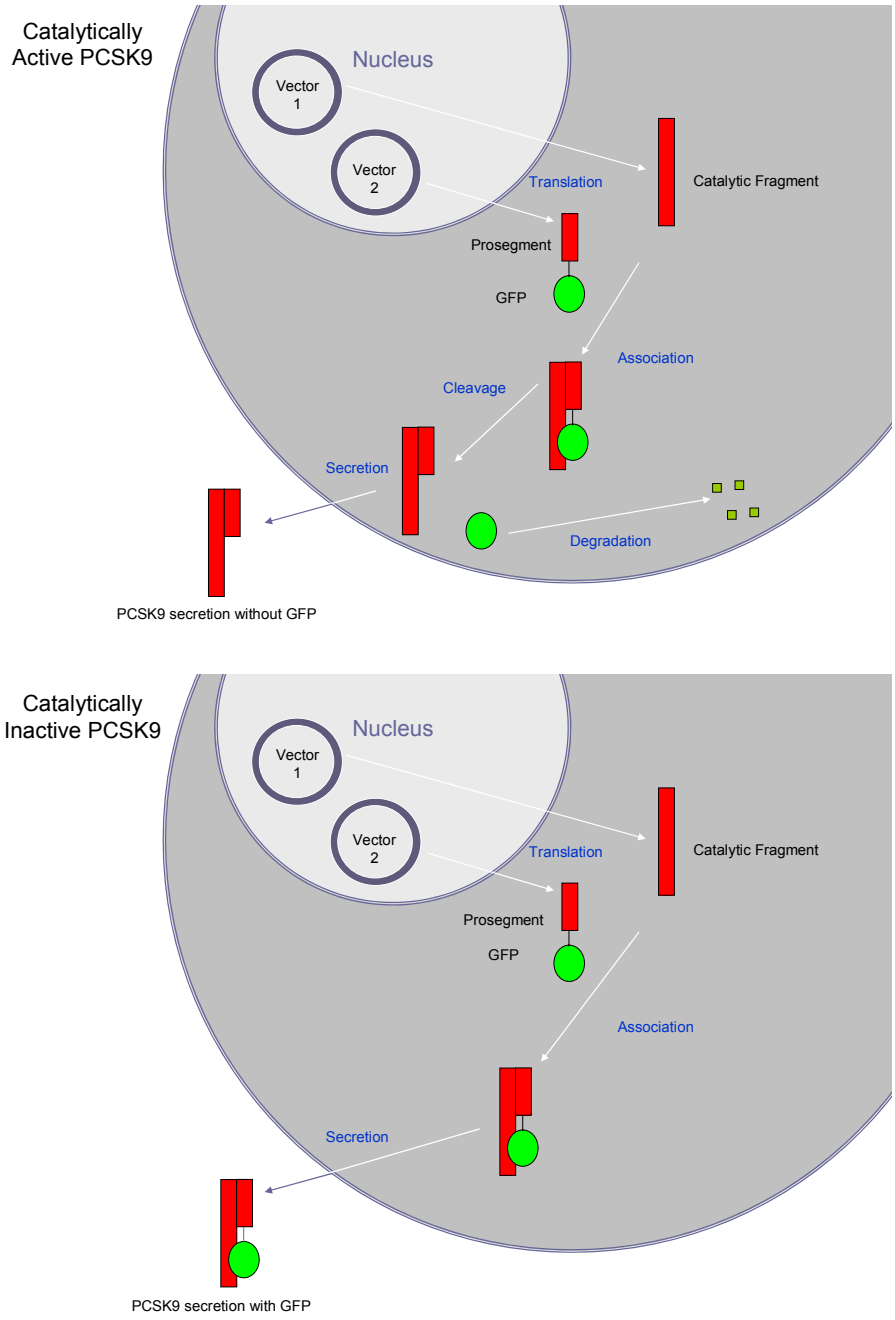

FIGURE 6-2. **Schematic diagram of PCSK9 expressed as two peptides with GFP fused to the prodomain.** If PCSK9 is catalytically active (top panel) GFP is cleaved in the cell and PCSK9 is secreted without GFP. If PCSK9 is inactive (bottom panel), GFP is secreted still linked to PCSK9.

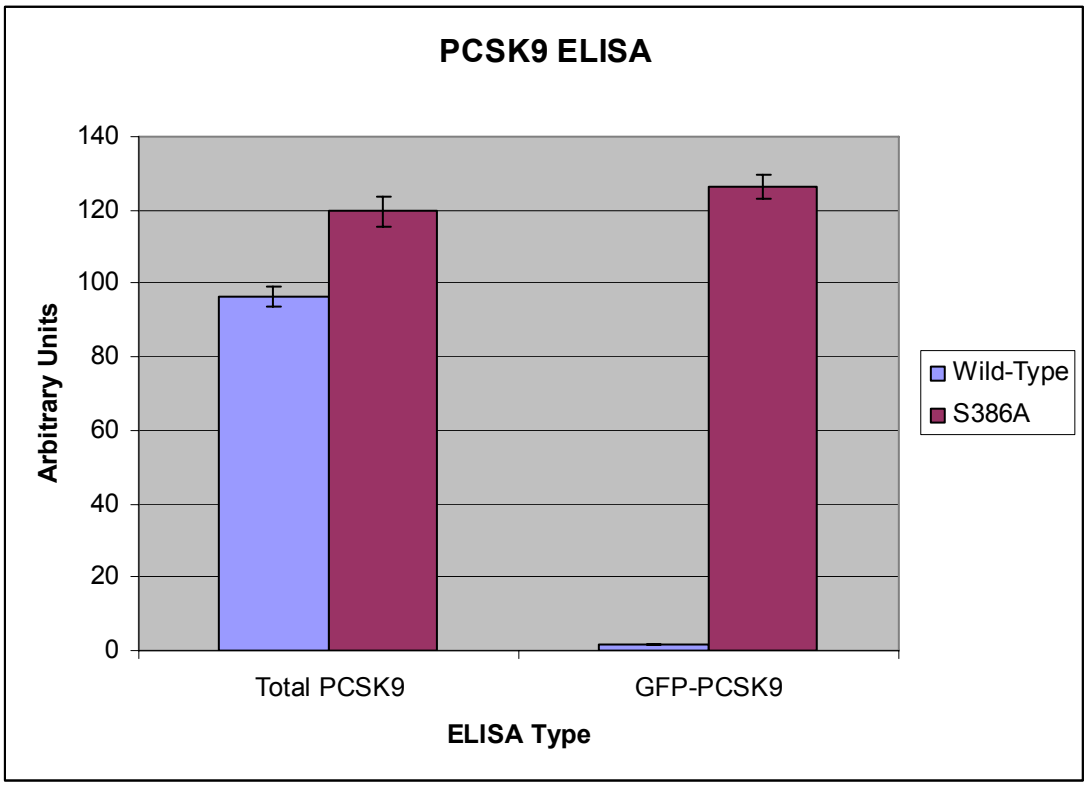

FIGURE 6-3. **A V5-GFP tag is efficiently cleaved from PCSK9.** Cells stably expressing PCSK9 as two peptides, a catalytic fragment (either WT or S386A) and prodomain-V5-GFP, were grown to confluence and the medium harvested. The medium was subjected to ELISA for total PCSK9 and PCSK9 with GFP bound.

Figure 6-3 shows data from the ELISA of stably transfected HEK-293 cell lines expressing catalytically active *trans*-PCSK9-GFP (wild-type) and catalytically inactive *trans*-PCSK9 S386A). The secretion of PCSK9 from the cells is similar based on total PCSK9 protein quantified by an ELISA; however, the wild-type cell line effectively cleaves all the GFP from the secreted PCSK9 and no GFP-PCSK9 is detected in the medium. An inhibitor of PCSK9 catalytic activity should increase the amount of GFP-PCSK9 in the medium of the wild-type cell line.

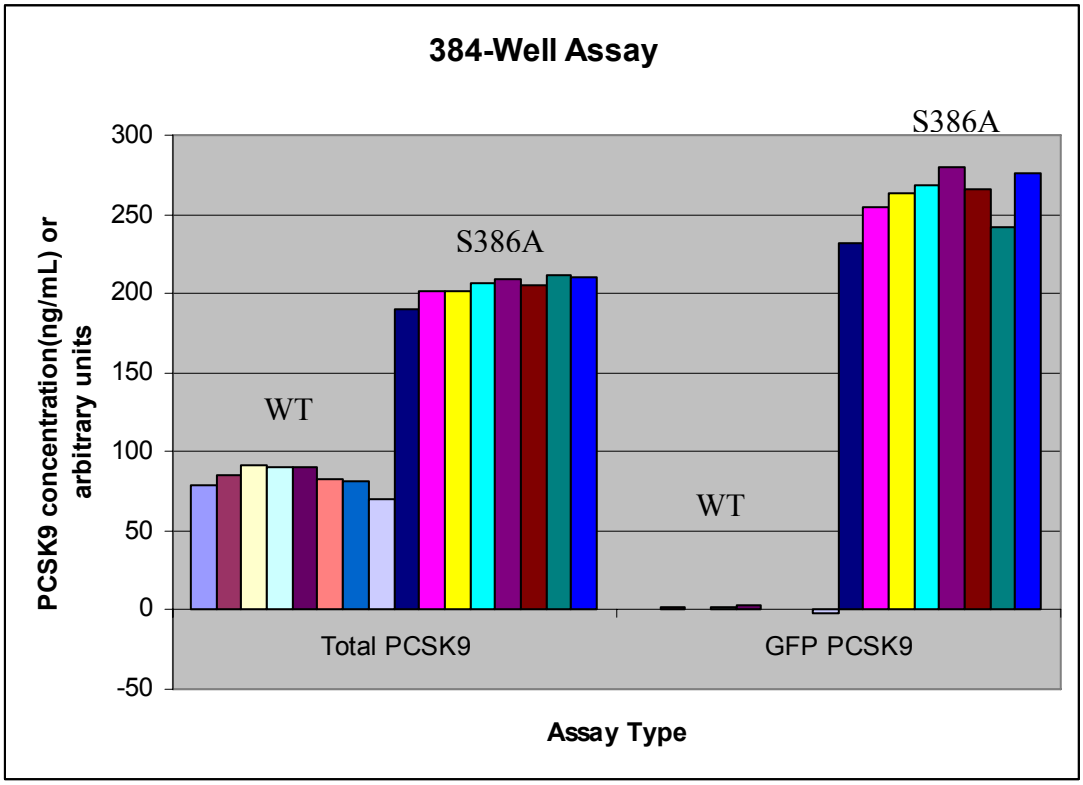

FIGURE 6-4. **Preliminary PCSK9 inhibitor assay data**. Cells expressing PCSK9 as two peptides, a catalytic fragment (either WT or S386A) and prodomain-V5-GFP were cultured in 384 well plate. Eight wells for each cell line (WT or S386A) were assayed by ELISA for total PCSK9 and PCSK9 with bound GFP.

Figure 6-4 shows sample assay data from 8 replicate wells for each cell line. The first 8 bars represent the wild-type cell line (WT) and the last 8 represent the catalytically inactive cell line (S386A). As seen in Figure 6-1, both cell lines secrete PCSK9; however the wild-type cell line cleaves all GFP from the PCSK9 fusion molecule and is not detected in the GFP ELISA. Additionally, these data show the low variance between

wells and the reproducibility of the assay. Total PCSK9 is measured in ng/mL. GFP PCSK9 is measured in arbitrary units.

Materials and Methods

Plasmids. A plasmid containing the prodomain of PCSK9 (amino acids 1-152) followed by a C-terminal V5 tag and green fluorescent protein (GFP) protein from Aequorea victoria (27) was created. The PCSK9 prodomain and V5 sequence were amplified by PCR as described as described in Chapter 3. The PCR fragment was ligated into the pcDNA3.1/CT-GFP-TOPO vector (Invitrogen) using the manufacturer's instructions. The resulting plasmid was mutagenized to move the GFP in frame directly after the V5 tag using the QuikChange site-directed mutagenesis kit (Stratagene) and the primer 5'-CTCCTCGGTCTCGATTCTACGATGGCTAGCAAAGGAGAAGAAC-3'. The prodomain-V5-GFP sequence was transferred to the pcDNA3.1/Hyrgo(+) vector (Invitrogen) through restriction digestion with KPNI and XBAI. Plasmids containing a deletion of the prodomain of PCSK9 with or without a mutation at serine 386 to alanine were previously generated in Chapter 3.

Cell Lines. Human embryonic kidney (HEK) 293 cells (CRL-1573) were stably co-transfected with PCSK9 prodomain-V5-GFP and PCSK9 catalytic and terminal portions with either wild-type sequence or the catalytically inactivating mutation S386A. Cells were cultures in DMEM (cellgro; Mediatech, Inc.) supplemented with 100 U/mL penicillin, 100 μg/mL streptomycin, 1 g/L glucose, and 10% FCS. Cells were plated at $5x10^6$ cells per 100mm dish on day 0. On day 3, the medium was replaced and the cells co-transfected with 1.5 ug prodomain plasmid and 0.5 μg catalytic and C-terminus

plasmid per dish using Lipofectamine 2000 transfection reagent (Invitrogen). On day 4, cells were switched to a selection media containing 500 μg/mL Hygromycin and 700 μg/mL G418. Surviving colonies were selected and screened for secretion of PCSK9 using western blot analysis. The colonies with highest secretion of wild-type and S386A PCSK9 were sub-cloned from single-cells and re-screened for highest PCSK9 expression.

Screening Assay. The cell lines with stable expression of either wild-type or S386A PCSK9 are plated into 384 well plates (Corning, #3701) at densities of 10^5 in 80 μL of the medium described above. The next day the compound to be screened or vehicle can be added directly into the wells. After 18 h incubation, 40 μL of medium are removed to each of 2 assay plates. One plate is a MaxiSorp 384 well plate (NUNC, #460372) pre-coated with the polyclonal anti-PCSK9 antibody 228B and the other plate is a ChoiceCoat Custom-coated anti-GFP plate (Pierce). Detection of captured PCSK9 in both plates is carried out with a monoclonal PCSK9 antibody as described (72).

SCREENING FOR MISSING PROTEINS IN THE PCSK9-LDLR PATHWAY

Introduction

PCSK9 is a secreted serine protease which regulates the LDLR through binding the LDLR at the cell surface and targeting it for degradation as discussed in Chapter 3. As discussed earlier in this chapter, PCSK9 is a major determinant of LDL-C levels and represents an important therapeutic target for the treatment of hypercholesterolemia. The first section of this chapter, based on the work presented in Chapter 3, presents one potential area of inhibiting PCSK9: by blocking its maturation and secretion from cells. A second potential inhibitory mechanism of PCSK9 was presented in Chapter 5: blocking the PCSK9:LDLR interaction extracellularly. This chapter will focus on a high-throughput screening method for determining new targets in the PCSK9 pathway that could be exploited for therapeutic benefit.

PCSK9's action on the LDLR appears to be cell type specific. PCSK9 decreases LDLR receptors in HepG2 cells as shown in Chapter 3, but has no effect on Chinese hamster ovary cells (90). In mice, PCSK9 reduced LDLR in the liver, but leaves LDLRs of the adrenal gland unchanged (45). In humans with PCSK9 mutations, LDLR levels are lower in their lymphoblasts (10) than in the fibroblasts (122). This seems to indicate that another protein factor or factors are involved in the PCSK9:LDLR pathway. These factors could be one of two types: an inhibitor of PCSK9 action or an activator of PCSK9 action. A high-throughput screening assay must be able to address both of these possibilities.

Results and Discussion

The first step in creating a high-throughput assay was to create an assay that could detect PCSK9 mediated degradation of the LDLR. The assay used here is DiI-LDL uptake assessed by flow cytometry. DiI is a lipophilic fluorescent dye that effectively labels LDL cholesterol and does not interfere with the ability of LDL to bind the LDLR (99). When LDLRs are present at the cell surface, they bind DiI-LDL and it is taken into cells. The fluorescence of a cell can then be measured by flow cytometry and will directly relate to the amount of LDLRs on the cell surface. As shown in Chapter 5, this method readily detects changes in LDLR numbers. Because flow cytometry requires very few cells and is easily performed, it lends itself to high-throughput uses.

If there is a factor in the PCSK9:LDLR pathway that specifically activates the pathway in PCSK9-sensitive cells, a cDNA library can be made from these cells. The cDNA library can then be transfected into a cell line that is not sensitive to PCSK9, treated with PCSK9, and assayed for LDLR function. Any cDNA that activates the PCSK9:LDLR pathway should cause a reduction in DiI-LDL uptake. On the other hand, if there is a negative regulator of the PCSK9:LDLR pathway in non-sensitive cells, an siRNA library can be used. In this case, PCSK9-sensitive cells would be transfected with an siRNA library, treated with PCSK9, and assayed for DiI-LDL uptake. Any siRNA that knocked down the negative regulator would increase the DiI-LDL uptake.

To identify an activator of the LDLR:PCSK9 pathway, a cDNA library was created from the liver of a mixed background female mouse and an initial screen of 10,000 cDNAs was undertaken. To determine which cell lines would be useful in the screen, several cell lines were treated with or without PCSK9 and assessed for DiI-LDL

uptake by flow cytometry. Figure 6-5 shows the results for HepG2 cells and SV589 cells. HepG2 cells are a human hepatoma cell line, known to respond to PCSK9. They have intense DiI-LDL fluorescence, which is almost completely abolished after PCSK9 treatment (Figure 6-5*A*). Background fluorescence was established by treating with unlabeled LDL. SV589 cells are a human fibroblast cell line. They have high DiI-LDL fluorescence compared to background, which is not affected by treatment with PCSK9 (Figure 6-5*B*). These data indicate that the HepG2 cell line would be appropriate for an siRNA screen, while the SV589 cells would be appropriate in a cDNA screen.

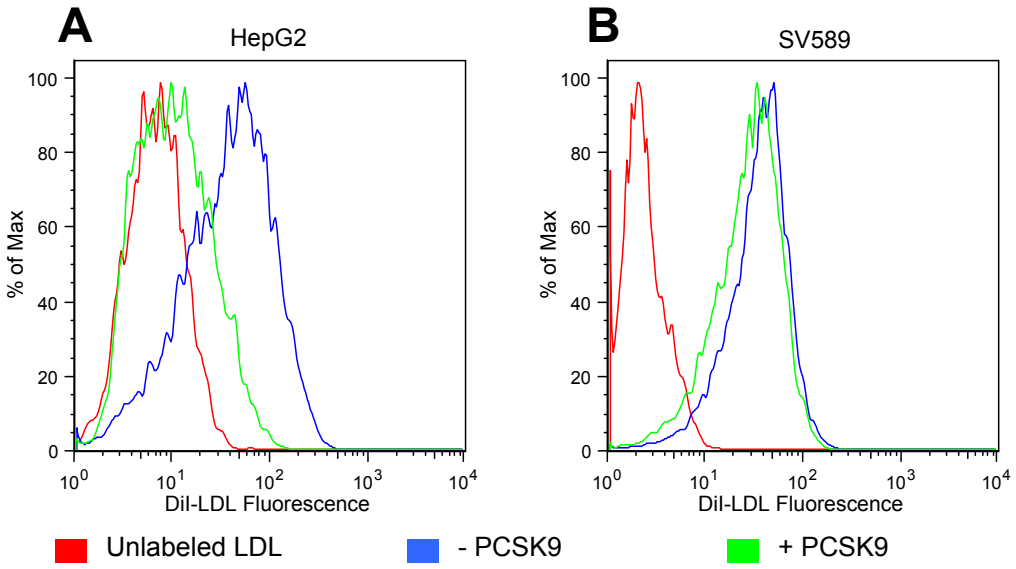

FIGURE 6-5. **PCSK9 reduces DiI-LDL uptake in HepG2, but not SV589 cells.**
A, HepG2 and *B,* SV589 cells were cultured in sterol depleted medium for 18 hours to induce LDLR expression and were then treated for 4 hours with or without 5 μg/mL PCSK9. Two hours into PCSK9 treatment, 80 μg/mL DiI-LDL was added. Ten-thousand cells were measured by flow cytometry and live cells were selected based on scatter charateristics. The histogram of fluorescent intensities is shown. Red: unlabeled LDL, Blue: without PCSK9, Green: PCSK9

SV589 cells were transfected with the cDNA library and treated with or without PCSK9. Within each experiment, several internal controls were used. To control for transfection efficiency, a GFP expressing plasmid was transfected and GFP fluorescence measured. A second control used is insig-1. Insig-1 is a membrane protein that dose dependently blocks activation of sterol regulatory element-binding proteins (SREBPs) (126). Because SREBPs increase the expression of the LDLR (58), blocking SREBP activation with insig-1 will lead to a decrease in DiI-LDL uptake. By transfecting insig-1 in each experiment, it can be verified that the transfection efficiency that is obtained in the experiment is sufficient to see a reduction in DiI-LDL uptake within the population of cells (Figure 6-6*A*).

One hundred pools of approximately 100 cDNAs per pool were screened in SV589 cells. Of those, two pools tested positive by causing a reduction in DiI-LDL uptake after PCSK9 treatment. The two positive pools as well as a representative negative pool are shown in Figure 6-6. The positive pools were subdivided into 16 pools of approximately 12 cDNAs each. Each of the subpools were screened with the same method as the original pools. Four subpools tested positive in the screen and the individual cDNAs within each subpool were sequences and identified by BLAST (129) search against the mouse genome. The identities of each cDNA are listed in Appendix A. Each of the identified cDNAs was screened and only one was positive. The cDNA (53-15-3) was identified as NM_175687. This is an uncharacterized mRNA which has a hypothetical 184AA protein product. According to the GNF SymAtlas (117), the tissue distribution of this mRNA is mainly in the brain and spinal cord. There is little expression of the mRNA in the liver, making this cDNA an unlikely candidate.

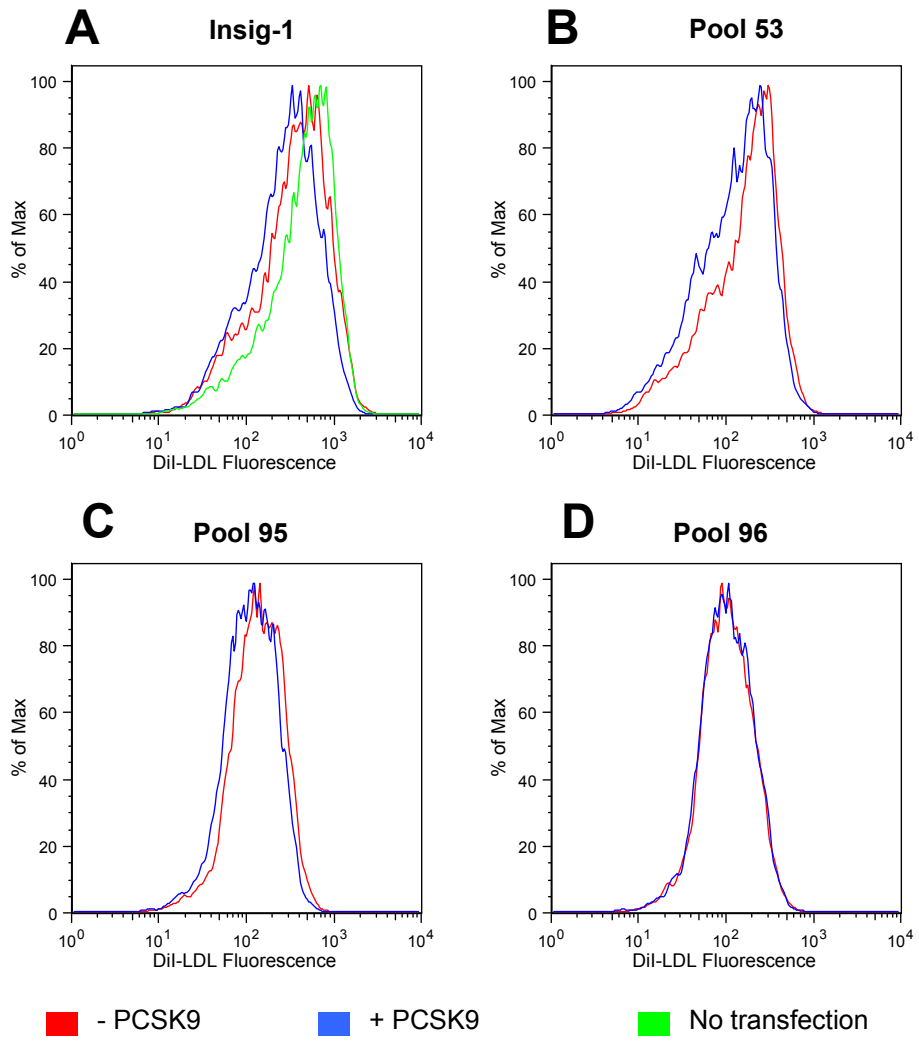

FIGURE 6-6. **Results of cDNA screen in SV589 cells.**
SV589 cells were cultured in sterol depleted medium for 18 hours to induce LDLR expression after transfection with cDNA and were then treated for 4 hours with or without 5 μg/mL PCSK9. Two hours into PCSK9 treatment, 80 μg/mL DiI-LDL was added. Ten-thousand cells were measured by flow cytometry and live cells were selected based on scatter charateristics. The histogram of fluorescent intensities is shown. *A,* Insig-1 transfected cells. *B,* cDNA pool 53. *C,* cDNA pool 95. *D,* cDNA pool 96.

While one potential PCSK9 modulator was identified in this screen, it has not been verified by other experimental means. Additionally, the screen was very limited and should be expanded to a cDNA library of at least 200,000 cDNAs. Despite the limitations of the initial screen, it has proved the power of this assay to identify potential PCSK9 modulating proteins. This assay can now be expanded and to a larger library and to an siRNA screen to comprehensively survey the genome for missing proteins that exist within the PCSK9:LDLR pathway.

Materials and Methods

cDNA library. A female, mixed background, wild-type mouse was killed by cardiac puncture and the liver immediately harvested and homogenized. RNA was generated using the RNeasy kit (Qiagen) according to the manufacturer's instructions. Poly A RNA was generated using an Oligotex kit (Qiagen) according to the manufacturer's instructions. The cDNA library was generated using a SuperScript cDNA synthesis and cloning kit (Invitrogen). Final cDNA was diluted into pools of approximately 100 cDNAs.

Library subcloning. Pools were subcloned by transformation of 10ng of the cDNA pool into One Shot TOP10 chemically competent cells (Invitrogen) according to the manufacturer's instructions. Transformed cells were plated onto agar plated containing ampicillin as a selection antibiotic. After 12 h of culture at 37° C, 192 individual colonies were selected and grown in individual wells of 96 well plated in grown medium containing ampicillin. After 12 h of culture at 37° C, a fraction of medium from each well within a row of a 96 well plate was combined to create a subpool

of 12 cDNAs. The cDNA was isolated with HighPure plasmid isolation kit (Roche) according to the manufacturer's instructions. This created 16 pools for each original pool. If a subpool screened positive, the 12 individual cDNAs could be cloned and sequenced from the original 96 well plate.

Transfection of SV589 cells. Medium A contained Dulbecco's Modified Eagle Medium (DMEM) (Cellgro) supplemented with 100 units/ml penicillin, 100 μg/ml streptomycin sulfate and 1 g/L glucose. Medium B contained Medium A supplemented with 10% (v/v) fetal calf serum (FCS). Medium C contained DMEM supplemented with 5% (v/v) newborn calf lipoprotein-deficient serum (NCLPDS), 100 units/ml penicillin, 100 μg/ml streptomycin sulfate, 10 μM sodium compactin, 50 μM sodium mevalonate, and 4.5 g/L glucose. Medium D contained DMEM supplemented with 5% (v/v) newborn calf lipoprotein-deficient serum (NCLPDS), 100 units/ml penicillin, 100 μg/ml streptomycin sulfate, 10 μg/mL cholesterol, and 1 μg/mL 25-OH-cholesterol, and 4.5 g/L glucose. SV589 cells were plated at 1 x 10^4 cells/24-well dish in Medium B on day 0. On day 3, plasmids were transfected using Lipofectamine LTX transfection reagent (Invitrogen) and PLUS reagent (Invitrogen) per the manufacturer's instructions. 0.5 μg of DNA was transfected in duplicate wells. pCDNA3.1-CT-GFP (Invitrogen) was used as a transfection control plasmid. pCMV-Insig-1-Myc (126) was used for assay control.

DiI-LDL assay and flow cytometry. Human LDL was isolated and labeled with DiI as described in the MATERIALS AND METHODS section of Chapter 5. Twenty-four h after transfection, cells were switched into Medium C. One untransfected well was switched into Medium D to establish background DiI-LDL uptake. After 18 h, 5 μg/mL

PCSK9 was added and incubated for 2 h before 80 μg/mL DiI-LDL was added for an additional 2 h. Cells were washed twice in PBS, trypsinized, and transferred to Medium A supplemented with 2.5% NCLPDS. The mean fluorescence intensity of 10,000 live cells, as determined by scatter characteristics, for each sample was determined in the 585 nm range with a BD FACSCalibur flow cytometer. Transfection efficiency was established by measuring the fluorescence of GFP in the 530 nm range.

CHAPTER SEVEN
Conclusions and Recommendations

The Non-Catalytic conundrum of PCSK9

When PCSK9 was first identified as a protease that regulated LDLR protein levels, it was almost a forgone conclusion that it would act by direct proteolytic cleavage of the LDLR. This was reinforced by the finding that an overexpressed, catalytically inactive mutant of PCSK9 failed to reduce LDLR in the livers of mice (90). The problem was complicated with the recognition that PCSK9 could work as a secreted factor (72). The catalytically inactive PCSK9 used in the mouse studies does not mature and get secreted from the cell. Thus, it did not rule out the possibility that catalytically inactive PCSK9, if it were able to be secreted, could still down regulate the LDLR.

To test whether secreted, catalytically inactive PCSK9 could still degrade the LDLR, some engineering was required. By expressing PCSK9 as two separate peptides, PCSK9 was able to be secreted independent of its catalytic activity. As shown in Chapter 3, using this "*trans*" method of PCSK9 expression, it was determined that PCSK9 does not need to directly cleave the LDLR in order to lead to its degradation. This was very surprising and raises the question: why is a protease needed to perform the function of a chaperone? It seems unnecessary to have a protein with an inherent activity (proteolysis) and not use that activity in its primary biological function. Additionally, it creates a bit of a paradox. While the proteolytic activity of PCSK9 is not required for its direct action on the LDLR, proteolytic activity is required for PCSK9 to mature and reach its site of action.

What is clear from these findings is that pharmacologic inhibition of PCSK9 catalytic activity is a viable target for reducing LDL-C levels. However, it is complicated by the fact that the inhibition must be of the proprotein in the ER of the cell, before the protein has matured. This means any drug of this class must be cell- and ER- permeable. This also complicates drug discovery. If PCSK9 had directly cleaved LDLR, an *in vitro* assay of PCSK9 activity could have been developed. As it stands, a cell-based method is required that assays the maturation and secretion of PCSK9. Chapter 6 presented one such approach to screening for intracellular PCSK9 inhibitors.

It still remains to be determined if there are any proteolytic substrates for PCSK9. It seems unlikely, as the only discovered function of PCSK9 is in cholesterol homeostasis. If it had another substrate, some phenotype would likely have surfaced when PCSK9 was knocked out and overexpressed in mice; although, PCSK9 could have a redundant function with other proteases. The co-crystal structure of PCSK9:LDLR presented in Chapter 5 and the three apo structures of PCSK9 (28, 47, 91) makes it even more unlikely that PCSK9 could cleave any substrate. In all the structures, the prodomain remains bound in the catalytic site, preventing any catalytic activity. The C-domain of the protein, which has been hypothesized as a protein-protein interaction domain, as well as the LDLR binding interface are too distant from the active site to make catalysis likely.

Because PCSK9 does not directly cleave the LDLR, the next step is to understand how PCSK9 targets the LDLR for degradation and what the actual mechanism of degradation is. It is known that the LDLR undergoes a low pH conformational change after endocytosis that allow is to recycle to the plasma membrane (6, 7). It has been suggested that PCSK9 may block this conformational change and cause

trafficking to the lysosome (128). To really determine if this is the case, technically challenging structural studies will be required. A co-crystal structure of the entire LDLR extracellular domain and PCSK9 at low pH will be required for definitive proof of a block in conformational change.

If general lysosomal degradation is the mode of LDLR destruction the exact mechanisms are not therapeutically relevant. However, if there is another protein or protein complex that binds PCSK9 in the endosome to traffic the LDLR to the lysosome or to a specific degratory enzyme, it may be possible to block these interactions and cause recycling of the LDLR. To search for such proteins, several methods should be undertaken. First, a broad screening approach as described in Chapter 6 should be undertaken to search for either activators or inhibitors of PCSK9 function. Additionally, co-immunoprecipitation experiments coupled with mass spectrometry can be used. To look for interactions that might occur specifically in the endosome, cells can be treated with exogenous PCSK9 and chloroquine. Under these conditions, PCSK9 will be internalized into endosomes, but fusion of the endosome and lysosome will be prevented. A cell permeable crosslinker can then be applied to cells. PCSK9 can be immunoprecipitated and interacting proteins identified by mass spectrometry.

C-terminal uncertainties

Chapter 4 presents a co-crystal study of the EGF-A domain of the LDLR and PCSK. Of particular interest is the portion of the protein not involved in PCSK9:LDLR interaction, the C-terminal domain. The C-terminal domain is a nearly 250 AA heterotrimeric structure made up of three six-stranded β-sheet domains (28, 47, 91). So, what is the role of this domain in PCSK9 function? It is suggested that the domain has homology to the adipokine resistin and that the domain may mediate protein-protein interactions. Clearly the C-terminus is not involved in the binding of PCSK9 to the EGF-A region of the LDLR, but it does not exclude the possibility that in the context of the whole LDLR there may be other PCSK9:LDLR interaction sites. A structure of the entire LDLR-ECD complexed with PCSK9 will be required to determine if there are secondary PCSK9:LDLR contacts.

Recently, Zhang, *et al.* (128) suggested that the C-terminus is absolutely required for PCSK9 function, while Mayer, *et al.* (78) suggested that the C-terminus is responsible for inhibition of PCSK9. These studies hint at the possibility of a docking site in the C-terminus that can be occupied by either an activator or inhibitor of PCSK9. The C-terminal domain needs to be more carefully studied to determine its exact function. One line of study that needs to be pursued is purification of a PCSK9 lacking the C-terminal domain and a PCSK9 C-terminal domain alone. While Zhang *et al.* (128) made the former, they did not prove that they created a folded protein. With a C-terminal truncation, the affinity of the protein toward LDLR could be measured to determine if there are any secondary PCSK9:LDLR contact sites in the C-terminus. Additionally, the protein could be assessed for its ability to degrade the LDLR both *in vitro* and *in vivo*, as

it was for catalytically inactive PCSK9 in Chapter 3. This would really answer the question as to whether the C-terminal domain is necessary for PCSK9 to function. A purified C-terminal domain could be incubated with cell extracts and immunoprecipitated to identify interacting proteins. Along these lines, the C-terminal domain alone could be used as bait in a yeast two-hybrid screen for interacting proteins.

H306Y and hope for Familial Hypercholesterolemia

The co-crystal structure of PCSK9:LDLR in Chapter 5 gave insights in several Familial Hypercholesterolemia (FH) mutations. Based on the location of the binding interface of PCSK9:LDLR, it was clear that the Asp374Tyr mutation of PCSK9 observed in some patients with FH was likely due to an improved hydrogen bond with His306 of the EGF-A domain of LDLR. This agreed with the 10-fold increased binding of this mutation to LDLR seen previously (72). It also implied that the reciprocal mutation of His306Try in LDLR should have the same phenotype. This mutation had already been discovered in patients, but the mechanism had not been investigated (31, 37).

In Chapter 5, the His306Tyr mutation in *LDLR* was investigated. *LDLR* mutations have previously been classified into 5 categories based on their mechanism of dysfunction. They includee 1) null mutations, 2) receptors that do not reach the cell surface, 3) receptors that have diminished binding to LDL, 4) receptors that do not get endocytosed, and 5) receptors that do not recycle (55). The His306Tyr mutation represents a new sixth class of mutation that has increased susceptibility to degradation by PCSK9. The His306Tyr mutation has increased affinity for PCSK9, which leads to its

more rapid degradation. This is the first class of *LDLR* mutation that represents a gain-of-function in the LDLR protein.

The His306Tyr in *LDLR* will require further study *in vivo*. A knock-in mouse harboring the mutation is the next step in completely characterizing the mutation. The knock-in could be bred with *PCSK9* knockout mice. The LDL clearance in WT and *LDLR*(H306Y) mice could be compared with and without PCSK9 present. If the data in Chapter 5 are correct, it predicts that in the $PCSK9^{-/-}$ background, both WT and LDLR(H306Y) should have identical LDL clearance, whereas in the $PCSK9^{+/+}$ mice, LDLR(H306Y) would have markedly reduced function. PCSK9 clearance and effect on LDLR could also be measured in *LDLR*(H306Y) mice to show increased binding and effectiveness *in vivo*. These mice would also be useful for testing the efficacy of new therapeutics that disrupt the PCSK9:LDLR interaction in the context of increased PCSK9:LDLR binding affinity.

By exploiting the increased binding of the His306Tyr mutation, an EGF-AB fragment was created with the same mutation and used to compete PCSK9 away from the LDLR in cells. As shown in Chapter 5, this was effective in restoring the LDLR protein levels of cells overexpressing not only wild-type PCSK9, but also PCSK9 mutants that cause FH. This verifies the importance of disrupting PCSK9:LDLR interactions at the cell surface as a therapeutic intervention. Antibodies, peptides, peptoids, or small molecule inhibitors of PCSK9:LDLR interactions represent the first potential therapy for families suffering FH mutations in PCSK9 as well as those with *LDLR* mutations of the type described in Chapter 5. Additionally, these inhibitors combined with statins may increase LDLR enough to lower cholesterol in patients with type 3 *LDLR* mutations.

It is important that other *LDLR* mutations that affect susceptibility to PCSK9-mediated degradation be identified. The His306Tyr mutation was easily predicted from the co-crystal structure of PCSK9:LDLR, but many other uncharacterized *LDLR* mutations could fall into this new class of mutation. Because lymphocytes from patients are sensitive to PCSK9 (10), it should be routine to test FH mutations for increased susceptibility to PCSK9. Patients with increased susceptibility to PCSK9-mediated degradation of the LDLR would benefit the most from anti-PCSK9 therapies that are currently in development.

APPENDIX A
cDNAs Screened for PCSK9 Modulating Activity

cDNA ID	BLAST result
53-8-1	Matched to no genes. Matched region on chromosome 1
53-8-2	Glucose-6-phosphatase
53-8-3	Acidic ribosomal phosphoprotein P0
53-8-4	Serine incorporator 1
53-8-6	Matched to hypothetical RNA on chromosome 9
53-8-7	Serine incorporator 1
53-8-8	Brain protein I3
53-8-9	Ubiquitin B
53-8-11	Pituitary tumor transforming 1 interacting protein
53-8-12	Brain protein I3
53-15-1	hydroxy-Δ-5-steroid-dehydrogenase
53-15-2	Adenylate Kinase 3
53-15-3	Matched to a hypothetical RNA on chromosome 9
53-15-4	Glucose-6-phosphatase
53-15-5	ELOVL5
53-15-6	APO AI
53-15-7	Acidic ribosomal phosphoprotein P0
53-15-8	ELOVL5
53-15-9	Ornithine transcarbamylase
53-15-10	Albumin
53-15-11	Matches hypothetical gene on chromosome 4
53-15-12	APO AI
95-5-1	Serine peptidase inhibitor, clade A
95-5-2	Albumin
95-5-4	chromosome 13
95-5-5	Transthyretin
95-5-6	Transthyretin
95-5-7	amylase 1
95-5-8	Nucleobindin 1
95-5-9	isocitrate dehydrogenase 3
95-5-10	Leucyl-tRNA synthetase
95-5-11	Leucyl-tRNA synthetase
95-5-12	Tubulin, α 1c
95-9-1	Nucleobindin 1
95-9-2	Hyaluronoglucosaminidase 1
95-9-4	Hyaluronoglucosaminidase 1
95-9-7	Nucleobindin 1
95-9-8	Fibrinogen B
95-9-9	Major urinary protein 2
95-9-10	Cytochrome p450, family 2, subfamily c, polypeptide 39
95-9-12	Matched to no genes. Matches region of Chromosome 15

BIBLIOGRAPHY

1. Abifadel M, Varret M, Rabes JP, Allard D, Ouguerram K, et al. 2003. Mutations in *PCSK9* cause autosomal dominant hypercholesterolemia. *Nat. Genet.* 34: 154-6.

2. Allard D, Amsellem S, Abifadel M, Trillard M, Devillers M, et al. 2005. Novel mutations of the PCSK9 gene cause variable phenotype of autosomal dominant hypercholesterolemia. *Hum. Mutat.* 26: 497.

3. Anderson ED, Molloy SS, Jean F, Fei H, Shimamura S, Thomas G. 2002. The ordered and compartment-specfific autoproteolytic removal of the furin intramolecular chaperone is required for enzyme activation. *J. Biol. Chem.* 277: 12879-90.

4. Baker D, Shiau AK, Agard DA. 1993. The role of pro regions in protein folding. *Curr Opin Cell Biol* 5: 966-70

5. Basak A. 2005. Inhibitors of proprotein convertases. *J. Mol. Med.* 83: 844-55.

6. Beglova N, Blacklow SC. 2005. The LDL receptor: how acid pulls the trigger. *Trends Biochem Sci* 30: 309-17

7. Beglova N, Jeon H, Fisher C, Blacklow SC. 2004. Cooperation between fixed and low pH-inducible interfaces controls lipoprotein release by the LDL receptor. *Mol Cell* 16: 281-92

8. Beisiegel U, Kita T, Anderson RG, Schneider WJ, Brown MS, Goldstein JL. 1981. Immunologic cross-reactivity of the low density lipoprotein receptor from bovine adrenal cortex, human fibroblasts, canine liver and adrenal gland, and rat liver. *J. Biol. Chem.* 256: 4071-8

9. Beisiegel U, Schneider WJ, Brown MS, Goldstein JL. 1982. Immunoblot analysis of low density lipoprotein receptors in fibroblasts from subjects with familial hypercholesterolemia. *J. Biol. Chem.* 257: 13150-6

10. Benjannet S, Rhainds D, Essalmani R, Mayne J, Wickham L, et al. 2004. NARC-1/PCSK9 and its natural mutants: zymogen cleavage and effects on the low density lipoprotein (LDL) receptor and LDL cholesterol. *J. Biol. Chem.* 279: 48865-75.

11. Benjannet S, Rhainds D, Hamelin J, Nassoury N, Seidah NG. 2006. The proprotein convertase PCSK9 is inactivated by furin and/or PC5/6A: Functional consequences of natural mutations and post-translational modifications. *J. Biol. Chem.* 281: 30561-72.

12. Benjannet S, Rondeau N, Paquet L, Boudreault A, Lazure C, et al. 1993. Comparative biosynthesis, covalent post-translational modifications and efficiency of prosegment cleavage of the prohormone convertases PC1 and PC2: glycosylation, sulphation and identification of the intracellular site of prosegment cleavage of PC1 and PC2. *Biochem J* 294 (Pt 3): 735-43

13. Bergeron F, Leduc R, Day R. 2000. Subtilase-like pro-protein convertases: from molecular specificity to therapeutic applications. *J. Mol. Endocrinol.* 24: 1-22.

14. Boudreault A, Gauthier D, Lazure C. 1998. Proprotein convertase PC1/3-related peptides are potent slow tight-binding inhibitors of murine PC1/3 and Hfurin. *J Biol Chem* 273: 31574-80

15. Brown MS, Dana SE, Goldstein JL. 1974. Regulation of 3-hydroxy-3-methylglutaryl coenzyme A reductase activity in cultured human fibroblasts. Comparison of cells from a normal subject and from a patient with homozygous familial hypercholesterolemia. *J. Biol. Chem.* 249: 789-96

16. Brown MS, Goldstein JL. 1997. The SREBP pathway: regulation of cholesterol metabolism by proteolysis of a membrane-bound transcription factor. *Cell* 89: 331-40

17. Brown WJ, Goodhouse J, Farquhar MG. 1986. Mannose-6-phosphate receptors for lysosomal enzymes cycle between the Golgi complex and endosomes. *J. Cell Biol.* 103: 1235-47.

18. Brunger AT, Adams PD, Clore GM, DeLano WL, Gros P, et al. 1998. Crystallography & NMR system: A new software suite for macromolecular structure determination. *Acta Crystallogr D Biol Crystallogr* 54: 905-21

19. Cameron J, Holla OL, Ranheim T, Kulseth MA, Berge KE, Leren TP. 2006. Effect of mutations in the PCSK9 gene on the cell surface LDL receptors. *Hum. Mol. Genet.* 15: 1551-8.

20. Careskey HE, Davis RA, Alborn WE, Troutt JS, Cao G, Konrad RJ. 2008. Atorvastatin increases human serum levels of proprotein convertase subtilisin/kexin type 9. *J Lipid Res* 49: 394-8

21. Chen SN, Ballantyne CM, Gotto AM, Jr., Tan Y, Willerson JT, Marian AJ. 2005. A common PCSK9 haplotype, encompassing the E670G coding single nucleotide polymorphism, is a novel genetic marker for plasma low-density lipoprotein cholesterol levels and severity of coronary atherosclerosis. *J Am Coll Cardiol* 45: 1611-9

22. Chen WJ, Goldstein JL, Brown MS. 1990. NPXY, a sequence often found in cytoplasmic tails, is required for coated pit-mediated internalization of the low density lipoprotein receptor. *J. Biol. Chem.* 265: 3116-23

23. Cheng D, Espenshade PJ, Slaughter CA, Jaen JC, Brown MS, Goldstein JL. 1999. Secreted site-1 protease cleaves peptides corresponding to luminal loop of sterol regulatory element-binding proteins. *J. Biol. Chem.* 274: 22805-12

24. Cohen J, Pertsemlidis A, Kotowski IK, Graham R, Garcia CK, Hobbs HH. 2005. Low LDL cholesterol in individuals of African descent resulting from frequent nonsense mutations in PCSK9. *Nat. Genet.* 37: 161-5.

25. Cohen JC, Boerwinkle E, Mosley TH, Hobbs HH. 2006. Sequence variations in PCSK9, low LDL, and protection against coronary heart disease. *N. Engl. J. Med.* 354: 1264-72.

26. Collaborative Computational Project N. 1994. The CCP4 suite: programs for protein crystallography. *Acta Crystallogr D Biol Crystallogr* 50: 760-3

27. Crameri A, Whitehorn EA, Tate E, Stemmer WP. 1996. Improved green fluorescent protein by molecular evolution using DNA shuffling. *Nat Biotechnol* 14: 315-9

28. Cunningham D, Danley DE, Geoghegan KF, Griffor MC, Hawkins JL, et al. 2007. Structural and biophysical studies of PCSK9 and its mutants linked to familial hypercholesterolemia. *Nat. Struct. Mol. Biol.* 14: 413-9.

29. Daniel TO, Schneider WJ, Goldstein JL, Brown MS. 1983. Visualization of lipoprotein receptors by ligand blotting. *J. Biol. Chem.* 258: 4606-11

30. Davis CG, Goldstein JL, Sudhof TC, Anderson RG, Russell DW, Brown MS. 1987. Acid-dependent ligand dissociation and recycling of LDL receptor mediated by growth factor homology region. *Nature* 326: 760-5

31. Day IN, Whittall RA, O'Dell SD, Haddad L, Bolla MK, et al. 1997. Spectrum of LDL receptor gene mutations in heterozygous familial hypercholesterolemia. *Hum Mutat* 10: 116-27

32. DeSilva B, Smith W, Weiner R, Kelley M, Smolec J, et al. 2003. Recommendations for the bioanalytical method validation of ligand-binding assays to support pharmacokinetic assessments of macromolecules. *Pharm. Res.* 20: 1885-900.

33. Dubuc G, Chamberland A, Wassef H, Davignon J, Seidah NG, et al. 2004. Statins upregulate PCSK9, the gene encoding the proprotein convertase neural

apoptosis-regulated convertase-1 implicated in familial hypercholesterolemia. *Arterioscler. Thromb. Vasc. Biol.* 24: 1454-9.

34. Emsley P, Cowtan K. 2004. Coot: model-building tools for molecular graphics. *Acta Crystallogr D Biol Crystallogr* 60: 2126-32

35. Engelking LJ, Kuriyama H, Hammer RE, Horton JD, Brown MS, et al. 2004. Overexpression of Insig-1 in the livers of transgenic mice inhibits SREBP processing and reduces insulin-stimulated lipogenesis. *J. Clin. Invest.* 113: 1168-75

36. Fisher TS, Surdo PL, Pandit S, Mattu M, Santoro JC, et al. 2007. Effects of pH and low density lipoprotein (LDL) on PCSK9-dependent LDL receptor regulation. *J. Biol. Chem.* 282: 20502-12.

37. Fouchier SW, Defesche JC, Umans-Eckenhausen MW, Kastelein JP. 2001. The molecular basis of familial hypercholesterolemia in The Netherlands. *Hum Genet* 109: 602-15

38. Frank-Kamenetsky M, Grefhorst A, Anderson NN, Racie TS, Bramlage B, et al. 2008. Therapeutic RNAi targeting PCSK9 acutely lowers plasma cholesterol in rodents and LDL cholesterol in nonhuman primates. *Proc Natl Acad Sci U S A* 105: 11915-20

39. Fuller RS, Sterne RE, Thorner J. 1988. Enzymes Required for Yeast Prohormone Processing. *Annu. Rev. Physiol.* 50: 345-62.

40. Garcia CK, Wilund K, Arca M, Zuliani G, Fellin R, et al. 2001. Autosomal recessive hypercholesterolemia caused by mutations in a putative LDL receptor adaptor protein. *Science* 292: 1394-8

41. Gensberg K, Jan S, Matthews GM. 1998. Subtilisin-related serine proteases in the mammalian constitutive secretory pathway. *Semin Cell Dev Biol* 9: 11-7

42. Goldstein JL, Basu SK, Brown MS. 1983. Receptor-mediated endocytosis of low-density lipoprotein in cultured cells. *Meth. Enzymol.* 98: 241-60

43. Goldstein JL, Brown MS, Anderson RG, Russell DW, Schneider WJ. 1985. Receptor-mediated endocytosis: concepts emerging from the LDL receptor system. *Annu. Rev. Cell Biol.* 1: 1-39

44. Goldstein JL, Hobbs HH, Brown MS. 1995. Familial hypercholesterolemia. In *The Metabolic and Molecular Bases of Inherited Disease*, ed. CR Scriver, AL Beaudet, WS Sly, D Valle, pp. 1981. New York: McGraw-Hil

45. Grefhorst A, McNutt MC, Lagace TA, Horton JD. 2008. Plasma PCSK9 preferentially reduces liver LDL receptors in mice. *J Lipid Res* 49: 1303-11

46. Gregory LA, Thielens NM, Arlaud GJ, Fontecilla-Camps JC, Gaboriaud C. 2003. X-ray structure of the Ca2+-binding interaction domain of C1s. Insights into the assembly of the C1 complex of complement. *J Biol Chem* 278: 32157-64

47. Hampton EN, Knuth MW, Li J, Harris JL, Lesley SA, Spraggon G. 2007. The self-inhibited structure of full-length PCSK9 at 1.9 A reveals structural homology with resistin within the C-terminal domain. *Proc. Natl. Acad. Sci. U. S. A.* 104: 14604-9

48. Hanwell D, Ishikawa T, Saleki R, Rotin D. 2002. Trafficking and cell surface stability of the epithelial Na+ channel expressed in epithelial Madin-Darby canine kidney cells. *J. Biol. Chem.* 277: 9772-9.

49. He G, Gupta S, Yi M, Michaely P, Hobbs HH, Cohen JC. 2002. ARH is a modular adaptor protein that interacts with the LDL receptor, clathrin, and AP-2. *J. Biol. Chem.* 277: 44044-9.

50. Heller DA, de Faire U, Pedersen NL, Dahlen G, McClearn GE. 1993. Genetic and environmental influences on serum lipid levels in twins. *N Engl J Med* 328: 1150-6

51. Henrich S, Lindberg I, Bode W, Than ME. 2005. Proprotein convertase models based on the crystal structures of furin and kexin: explanation of their specificity. *J Mol Biol* 345: 211-27

52. Heron M. 2007. Deaths: leading causes for 2004. *Natl Vital Stat Rep* 56: 1-95

53. Herz J, Bock HH. 2002. Lipoprotein receptors in the nervous system. *Annu. Rev. Biochem.* 71: 405-34.

54. Herz J, Kowal RC, Ho YK, Brown MS, Goldstein JL. 1990. Low density lipoprotein receptor-related protein mediates endocytosis of monoclonal antibodies in cultured cells and rabbit liver. *J. Biol. Chem.* 265: 21355-62

55. Hobbs HH, Brown MS, Goldstein JL. 1992. Molecular genetics of the LDL receptor gene in familial hypercholesterolemia. *Hum. Mutat.* 1: 445-66

56. Hobbs HH, Russell DW, Brown MS, Goldstein JL. 1990. The LDL receptor locus in familial hypercholesterolemia: mutational analysis of a membrane protein. *Annu. Rev. Genet.* 24: 133-70

57. Homer VM, Marais AD, Charlton F, Laurie AD, Hurndell N, et al. 2008. Identification and characterization of two non-secreted PCSK9 mutants

associated with familial hypercholesterolemia in cohorts from New Zealand and South Africa. *Atherosclerosis* 196: 659-66.

58. Horton JD. 2002. Sterol regulatory element-binding proteins: transcriptional activators of lipid synthesis. *Biochem. Soc. Trans.* 30: 1091-5.

59. Horton JD, Goldstein JL, Brown MS. 2002. SREBPs:activators of the complete program of cholesterol and fatty acid synthesis in the liver. *J. Clin. Invest.* 109: 1125-31

60. Horton JD, Shah NA, Warrington JA, Anderson NN, Park SW, et al. 2003. Combined analysis of oligonucleotide microarray data from transgenic and knockout mice identifies direct SREBP target genes. *Proc. Natl. Acad. Sci. U. S. A.* 100: 12027-32

61. Hunt SC, Hopkins PN, Bulka K, McDermott MT, Thorne TL, et al. 2000. Genetic localization to chromosome 1p32 of the third locus for familial hypercholesterolemia in a Utah kindred. *Arterioscler. Thromb. Vasc. Biol.* 20: 1089-93

62. Innerarity TL, Mahley RW, Weisgraber KH, Bersot TP, Krauss RM, et al. 1990. Familial defective apolipoprotein B-100: a mutation of apolipoprotein B that causes hypercholesterolemia. *J. Lipid Res.* 31: 1337-49

63. Ishibashi S, Brown MS, Goldstein JL, Gerard RD, Hammer RE, Herz J. 1993. Hypercholesterolemia in low density lipoprotein receptor knockout mice and its reversal by adenovirus-mediated gene delivery. *J. Clin. Invest.* 92: 883-93.

64. Jeong Jeong H, Lee H-S, Kim K-S, Kim Y-K, Yoon D, Wook Park S. 2008. Sterol-dependent regulation of proprotein convertase subtilisin/kexin type 9 expression by sterol regulatory element-binding protein-2. *J. Lipid Res.* 49: 399-409.

65. Jonas MC, Costantini C, Puglielli L. 2008. PCSK9 is required for the disposal of non-acetylated intermediates of the nascent membrane protein BACE1. *EMBO Rep*

66. Jones C, Hammer RE, Li W-P, Cohen JC, Hobbs HH, Herz J. 2003. Normal sorting but defective endocytosis of the low density lipoprotein receptor in mice with autosomal recessive hypercholesterolemia. *J. Biol. Chem.* 278: 29024-30

67. Knouff C, Malloy S, Wilder J, Altenburg MK, Maeda N. 2001. Doubling expression of the low density lipoprotein receptor by truncation of the 3'-untranslated region sequence ameliorates type III hyperlipoproteinemia in mice expressing the human apoe2 isoform. *J Biol Chem* 276: 3856-62.

68. Koivisto UM, Hubbard AL, Mellman I. 2001. A novel cellular phenotype for familial hypercholesterolemia due to a defect in polarized targeting of LDL receptor. *Cell* 105: 575-85

69. Kotowski IK, Pertsemlidis A, Luke A, Cooper RS, Vega GL, et al. 2006. A spectrum of PCSK9 alleles contributes to plasma levels of low-density lipoprotein cholesterol. *Am. J. Hum. Genet.* 78: 410-22.

70. Kurniawan ND, Aliabadizadeh K, Brereton IM, Kroon PA, Smith R. 2001. NMR structure and backbone dynamics of a concatemer of epidermal growth factor homology modules of the human low-density lipoprotein receptor. *J Mol Biol* 311: 341-56

71. Kwon HJ, Lagace TA, McNutt MC, Horton JD, Deisenhofer J. 2008. Molecular basis for LDL receptor recognition by PCSK9. *Proc. Natl. Acad. Sci. U. S. A.* 105: 1820-5.

72. Lagace TA, Curtis DE, Garuti R, McNutt MC, Park SW, et al. 2006. Secreted PCSK9 decreases LDL receptors in hepatocytes and in livers of parabiotic mice. *J. Clin. Invest.* 116: 2995-3005.

73. Lalanne F, Lambert G, Amar MJA, Chetiveaux M, Zair Y, et al. 2005. Wild-type PCSK9 inhibits LDL clearance but does not affect apoB-containing lipoprotein production in mouse and cultured cells. *J. Lipid Res.* 46: 1312-9

74. Leren TP. 2004. Mutations in the PCSK9 gene in Norwegian subjects with autosomal dominant hypercholesterolemia. *Clin. Genet.* 65: 419-22.

75. Maxwell KN, Breslow JL. 2004. Adenoviral-mediated expression of Pcsk9 in mice results in a low-density lipoprotein receptor knockout phenotype. *Proc. Natl. Acad. Sci. U. S. A.* 101: 7100-5.

76. Maxwell KN, Fisher EA, Breslow JL. 2005. Overexpression of PCSK9 accelerates the degradation of the LDLR in a post-endoplasmic reticulum compartment. *Proc. Natl. Acad. Sci. U. S. A.* 102: 2069-74

77. Maxwell KN, Soccio RE, Duncan EM, Sehayek E, Breslow JL. 2003. Novel putative SREBP and LXR target genes identified by microarray analysis in liver of cholesterol-fed mice. *J. Lipid Res.* 44: 2109-19

78. Mayer G, Poirier S, Seidah NG. 2008. Annexin A2 is a C-terminal PCSK9 binding protein that regulates endogenous LDL receptor levels. *J Biol Chem*

79. Mayne J, Dewpura T, Raymond A, Cousins M, Chaplin A, et al. 2008. Plasma PCSK9 levels are significantly modified by statins and fibrates in humans. *Lipids Health Dis* 7: 22

80. McNutt MC, Lagace TA, Horton JD. 2007. Catalytic activity is not required for secreted PCSK9 to reduce low density lipoprotein receptors in HepG2 Cells. *J. Biol. Chem.* 282: 20799-803.

81. Molloy SS, Thomas L, VanSlyke JK, Stenberg PE, Thomas G. 1994. Intracellular trafficking and activation of the furin proprotein convertase: localization to the TGN and recycling from the cell surface. *EMBO J.* 13: 18-33

82. Murshudov GN, Vagin AA, Dodson EJ. 1997. Refinement of macromolecular structures by the maximum-likelihood method. *Acta Crystallogr D Biol Crystallogr* 53: 240-55

83. Nakayama K. 1997. Furin: a mammalian subtilisin/Kex2p-like endoprotease involved in processing of a wide variety of precursor proteins. *Biochem J* 327 (Pt 3): 625-35

84. Naoumova RP, Tosi I, Patel D, Neuwirth C, Horswell SD, et al. 2005. Severe hypercholesterolemia in four British families with the D374Y mutation in the PCSK9 gene: long-term follow-up and treatment response. *Arterioscler. Thromb. Vasc. Biol.* 25: 2654-60.

85. Nassoury N, Blasiole DA, Tebon Oler A, Benjannet S, Hamelin J, et al. 2007. The cellular trafficking of the secretory proprotein convertase PCSK9 and its dependence on the LDLR. *Traffic* 8: 718-32.

86. Naureckiene S, Ma L, Sreekumar K, Purandare U, Lo CF, et al. 2003. Functional characterization of Narc 1, a novel proteinase related to proteinase K. *Arch. Biochem. Biophys.* 420: 55-67.

87. Otwinowski Z, Minor W. 1997. Processing of X-ray Diffraction Data Collected in Oscillation Mode. *Methods in Enzymology* 276: 307-26

88. Ouguerrram K, Chetiveaux M, Zair Y, Costet P, Abifadel M, et al. 2004. Apolipoprotein B100 metabolism in autosomal-dominant hypercholesterolemia related to mutations in PCSK9. *Arterioscler. Thromb. Vasc. Biol.* 8: 1448-53.

89. Pandit S, Wisniewski D, Santoro JC, Ha S, Ramakrishnan V, et al. 2008. Functional analysis of sites within PCSK9 responsible for hypercholesterolemia. *J Lipid Res* 49: 1333-43

90. Park SW, Moon Y-A, Horton JD. 2004. Post-transcriptional regulation of low density lipoprotein receptor protein by proprotein convertase subtilisin/kexin type 9a in mouse liver. *J. Biol. Chem.* 279: 50630-8

91. Piper DE, Jackson S, Liu Q, Romanow WG, Shetterly S, et al. 2007. The crystal structure of PCSK9: A regulator of plasma LDL-cholesterol. *Structure* 15: 545-52.

92. Poirier S, Mayer G, Benjannet S, Bergeron E, Marcinkiewicz J, et al. 2008. The proprotein convertase PCSK9 induces the degradation of low density lipoprotein receptor (LDLR) and its closest family members VLDLR and ApoER2. *J. Biol. Chem.* 283: 2363-72.

93. Poirier S, Prat A, Marcinkiewicz E, Paquin J, Chitramuthu BP, et al. 2006. Implication of the proprotein convertase NARC-1/PCSK9 in the development of the nervous system. *J. Neurochem.* 98: 838-50.

94. Qian Y-W, Schmidt RJ, Zhang Y, Chu S, Lin A, et al. 2007. Secreted PCSK9 downregulates low density lipoprotein receptor through receptor-mediated endocytosis. *J. Lipid Res.* 48: 1488-98.

95. Rader DJ, Cohen J, Hobbs HH. 2003. Monogenic hypercholesterolemia:new insights in pathogenesis and treatment. *J. Clin. Invest.* 111: 1795-803

96. Rao Z, Handford P, Mayhew M, Knott V, Brownlee GG, Stuart D. 1995. The structure of a Ca(2+)-binding epidermal growth factor-like domain: its role in protein-protein interactions. *Cell* 82: 131-41

97. Rashid S, Curtis DE, Garuti R, Anderson NN, Bashmakov Y, et al. 2005. Decreased plasma cholesterol and hypersensitivity to statins in mice lacking Pcsk9. *Proc. Natl. Acad. Sci. U. S. A.* 102: 5374-9.

98. Reeves PJ, Thurmond RL, Khorana HG. 1996. Structure and function in rhodopsin: high level expression of a synthetic bovine opsin gene and its mutants in stable mammalian cell lines. *Proc. Natl. Acad. Sci. U. S. A.* 93: 11487-92.

99. Reynolds GD, St Clair RW. 1985. A comparative microscopic and biochemical study of the uptake of fluorescent and 125I-labeled lipoproteins by skin fibroblasts, smooth muscle cells, and peritoneal macrophages in culture. *Am J Pathol* 121: 200-11

100. Rudenko G, Deisenhofer J. 2003. The low-density lipoprotein receptor: ligands, debates and lore. *Curr Opin Struct Biol* 13: 683-9

101. Rudenko G, Henry L, Henderson K, Ichtchenko K, Brown MS, et al. 2002. Structure of the LDL receptor extracellular domain at endosomal pH. *Science* 298: 2353-8.

102. Russell DW, Brown MS, Goldstein JL. 1989. Different combinations of cysteine-rich repeats mediate binding of low density lipoprotein receptor to two different proteins. *Journal of Biological Chemistry* 264: 21682-8

103. Russell DW, Schneider WJ, Yamamoto T, Luskey KL, Brown MS, Goldstein JL. 1984. Domain map of the LDL receptor: sequence homology with the epidermal growth factor precursor. *Cell* 37: 577-85

104. Saha S, Boyd J, Werner JM, Knott V, Handford PA, et al. 2001. Solution structure of the LDL receptor EGF-AB pair: a paradigm for the assembly of tandem calcium binding EGF domains. *Structure* 9: 451-6

105. Sakai J, Nohturfft A, Cheng D, Ho YK, Brown MS, Goldstein JL. 1997. Identification of complexes between the COOH-terminal domains of sterol regulatory element-binding proteins (SREBPs) and SREBP cleavage-activating protein. *J. Biol. Chem.* 272: 20213-21

106. Sambrook J, Russell DW. 2001. *Molecular cloning: a laboratory manual*. New York: Cold Spring Harbor Laboratory Press

107. Schneider WJ, Beisiegel U, Goldstein JL, Brown MS. 1982. Purification of the low density lipoprotein receptor, an acidic glycoprotein of 164,000 molecular weight. *J. Biol. Chem.* 257: 2664-73

108. Seidah NG, Benjannet S, Wickham L, Marcinkiewicz J, Jasmin SB, et al. 2003. The secretory proprotein convertase neural apoptosis-regulated convertase 1 (NARC-1): liver regeneration and neuronal differentiation. *Proc. Natl. Acad. Sci. U. S. A.* 100: 928-33

109. Seidah NG, Chretien M. 1997. Eukaryotic protein processing: endoproteolysis of precursor proteins. *Curr. Opin. Biotechnol.* 8: 602-7.

110. Seidah NG, Chretien M. 1999. Proprotein and prohormone convertases: a family of subtilases generating diverse bioactive polypeptides. *Brain Res* 848: 45-62

111. Seidah NG, Prat A. 2007. The proprotein convertases are potential targets in the treatment of dyslipidemia. *J. Mol. Med.* 85: 685-96.

112. Shimano H, Horton JD, Hammer RE, Shimomura I, Brown MS, Goldstein JL. 1996. Overproduction of cholesterol and fatty acids causes massive liver enlargement in transgenic mice expressing truncated SREBP-1a. *J. Clin. Invest.* 98: 1575-84

113. Shioji K, Mannami T, Kokubo Y, Inamoto N, Takagi S, et al. 2004. Genetic variants in PCSK9 affect the cholesterol level in Japanese. *J. Hum. Genet.* 49: 109-14.

114. Simonet WS, Bucay N, Lauer SJ, Taylor JM. 1993. A far-downstream hepatocyte-specific control region directs expression of the linked human apolipoprotein E and C-I genes in transgenic mice. *J. Biol. Chem.* 268: 8221-9

115. Smeekens SP, Montag AG, Thomas G, Albiges-Rizo C, Carroll R, et al. 1992. Proinsulin processing by the subtilisin-related proprotein convertases furin, PC2, and PC3. *Proc Natl Acad Sci U S A* 89: 8822-6

116. Storoni LC, McCoy AJ, Read RJ. 2004. Likelihood-enhanced fast rotation functions. *Acta Crystallogr D Biol Crystallogr* 60: 432-8

117. Su AI, Cooke MP, Ching KA, Hakak Y, Walker JR, et al. 2002. Large-scale analysis of the human and mouse transcriptomes. *Proc Natl Acad Sci U S A* 99: 4465-70

118. Sun X-M, Eden ER, Tosi I, Neuwirth CK, Wile D, et al. 2005. Evidence for effect of mutant PCSK9 on apolipoprotein B secretion as the cause of unusually severe dominant hypercholesterolaemia. *Hum. Mol. Genet.* 14: 1161-9

119. Timms KM, Wagner S, Samuels ME, Forbey K, Goldfine H, et al. 2004. A mutation in PCSK9 causing autosomal-dominant hypercholesterolemia in a Utah pedigree. *Hum. Genet.* 114: 349-53.

120. van der Westhuyzen DR, Stein ML, Henderson HE, Marais AD, Fourie AM, Coetzee GA. 1991. Deletion of two growth-factor repeats from the low-density-lipoprotein receptor accelerates its degradation. *Biochem J* 277 (Pt 3): 677-82

121. van Driel IR, Goldstein JL, Sudhof TC, Brown MS. 1987. First cysteine-rich repeat in ligand-binding domain of low density lipoprotein receptor binds Ca2+ and monoclonal antibodies, but not lipoproteins. *J. Biol. Chem.* 262: 17443-9

122. Varret M, Rabes JP, Saint-Jore B, Cenarro A, Marinoni JC, et al. 1999. A third major locus for autosomal dominant hypercholesterolemia maps to 1p34.1-p32. *Am. J. Hum. Genet.* 64: 1378-87

123. Victor RG, Haley RW, Willett D, Peshock RM, Vaeth PC, et al. 2004. A population-based probability sample for the multidisciplinary study of ethnic disparities in cardiovascular disease: recruitment and validation in the Dallas Heart Study. *Am. J. Cardiol.* 93: 1473-80.

124. Willnow TE, Herz J. 1994. Genetic deficiency in low density lipoprotein receptor-related protein confers cellular resistance to Pseudomonas exotoxin A. Evidence that this protein is required for uptake and degradation of multiple ligands. *J. Cell Sci.* 107: 719-26.

125. Wright DE, Wagers AJ, Gulati AP, Johnson FL, Weissman IL. 2001. Physiological migration of hematopoietic stem and progenitor cells. *Science* 294: 1933-6.

126. Yang T, Espenshade PJ, Wright ME, Yabe D, Gong Y, et al. 2002. Crucial step in cholesterol homeostasis:sterols promote binding of SCAP to INSIG-1, a membrane protein that facilitates retention of SREBPs in ER. *Cell* 110: 489-500

127. Zhang D-W, Lagace TA, Garuti R, Zhao Z, McDonald M, et al. 2007. Binding of proprotein convertase subtilisin/kexin type 9 to epidermal growth factor-like repeat A of low density lipoprotein receptor decreases receptor recycling and increases degradation. *J. Biol. Chem.* 282: 18602-12

128. Zhang DW, Garuti R, Tang WJ, Cohen JC, Hobbs HH. 2008. Structural requirements for PCSK9-mediated degradation of the low-density lipoprotein receptor. *Proc Natl Acad Sci U S A* 105: 13045-50

129. Zhang Z, Schwartz S, Wagner L, Miller W. 2000. A greedy algorithm for aligning DNA sequences. *J Comput Biol* 7: 203-14

130. Zhao Z, Tuakli-Wosornu Y, Lagace TA, Kinch L, Grishin NV, et al. 2006. Molecular characterization of loss-of-function mutations in PCSK9 and identification of a compound heterozygote. *Am. J. Hum. Genet.* 79: 514-23.

131. Zhou A, Martin S, Lipkind G, LaMendola J, Steiner DF. 1998. Regulatory Roles of the P Domain of the Subtilisin-like Prohormone Convertases. *J. Biol. Chem.* 273: 11107-14